2013 Number 10

ISSN 2080-5187

Civil and Environmental Engineering Reports

Prace z Inżynierii Lądowej i Środowiska

University of Zielona Góra Press, Poland

CIVIL AND ENVIRONMENTAL ENGINEERING REPORTS

Civil and Environmental Engineering Reports (CEER) is a scientific journal published semi-annually by the University of Zielona Góra.

Kindly welcome are papers that are written in English and concerned with the research problems in civil and environmental engineering.

Papers are selected for publication through the review process. The authors will receive one copy of CEER.

Templates for manuscript preparation are available on the website: *www.ceer.uz.zgora.pl*

Address of the editorial office

CEER
University of Zielona Góra
Institute of Building Engineering
ul. Z. Szafrana 1
65-516 Zielona Góra, Poland

E-mail: ceer@uz.zgora.pl
Internet: www.ceer.uz.zgora.pl

ISSN 2080-5187

Nakład – 100 egz.
Druk – Oficyna Wydawnicza Uniwersytetu Zielonogórskiego, ul. Podgórna 50, 65-246 Zielona Góra
www.ow.uz.zgora.pl

Civil and Environmental Engineering Reports

2013
Number 10

University of
Zielona Góra
Press, Poland

CONTENTS

CIVIL AND ENVIRONMENTAL ENGINEERING REPORTS

No. 10 2013

IN MEMORIAM

KRZYSZTOF WILMAŃSKI
(1940 – 2012)

It is with deep regret and profound sadness that we inform the academic community of the death of Professor Krzysztof Wilmański on August 26, 2012. He passed away unexpectedly, after a brief illness. On behalf of his students, colleagues and friends, we wish to take this opportunity of acknowledging his enormous contribution to the field of mechanics. His genuine human warmth and generosity with his knowledge, determination and hard work will be vividly remembered by all of us.

We still have lively memories of the Special Jubilee International Conference *Continuous Media with Microstructure* held at the University of Zielona Góra on March 20, 2010, which was dedicated to him on the occasion of his 70^{th} birthday. A detailed description of the scientific life of Professor Krzysztof Wilmański is included in the book titled *Continuous Media with Microstructure* (Editor Bettina Albers, Springer-Verlag, Berlin 2010), which was also dedicated to him. This Journal also honoured him on that occasion by

publishing his biography (CEER, 2010 no. 5, pp. 3-5). Therefore, here we mention only some highlights of his very active and productive life.

Krzysztof Wilmański was born on March 1, 1940 in Łódź, Poland. At the Technical University of Łódź he completed his civil engineering studies (1962) and three years later was awarded the degree of doctor (1965). Since 1966 he worked at the Institute of Fundamental Technological Research of the Polish Academy of Sciences in Warsaw where he habilitated (1970), was Head of the Research Group "Continuum Thermodynamics", and was nominated full professor by the State Council (1979).

Professor Krzysztof Wilmański made his home at many places in the world. In 1969-1970 he spent one year at the Johns Hopkins University (USA); in 1972-1973 he taught for two years at the College of Engineering at the University of Baghdad; in 1978-1979 he spent a year and a half at the University of Paderborn and the Technical University of Berlin; in 1984 he worked on thermodynamics at the Institute for Advanced Study “Wissenschaftskolleg zu Berlin”. He researched and taught at the Technical University of Berlin, the University of Paderborn, the Technical University of Hamburg-Harburg, and the University of Essen. In 1996 he became Head of the Research Group of Continuum Mechanics at the Weierstrass Institute for Applied Analysis and Stochastics in Berlin, where he retired in 2005. In 2006 he spent one semester at Technion in Haifa. In 2005-2010 he was professor at the University of Zielona Góra and a staff member of the Rose School in Pavia.

Professor Wilmański taught undergraduate, graduate, and postgraduate courses on Strength of Materials, Mechanics of Structures, Linear and Nonlinear Mechanics of Continua, Thermodynamics of Multicomponent Systems, to cite a few. For students of many universities in Poland, Germany, Italy, Austria, and Israel he will be remembered as a brilliant teacher of great knowledge and understanding. His scientific activities and great accomplishments are mainly concentrated in the area of linear and nonlinear thermodynamics, including in particular such research topics as non-newtonian fluids, phase transformations, porous and granular materials. He published 14 books and some 140 scientific papers (www.mech-wilmanski.de), and inter alia he served as Editorial Board member of this Journal. He organized and co-organized many colloquia and conferences, in particular, together we chaired the International Conference on Computer Methods in Mechanics, CMM 2009 in Zielona Góra.

Professor Krzysztof Wilmański will be remembered not only for his scientific accomplishments and passion for research, but also as an extremely rare individual who was brilliant, kind, and gentle. We join in our thoughts and condolences for his wife Anna and their children. We will all miss him.

Mieczysław Kuczma
Editor

CIVIL AND ENVIRONMENTAL ENGINEERING REPORTS

No. 10 2013

FLOOD RISK OF LOWER SILESIA VOIVODSHIP

Mariusz ADYNKIEWICZ-PIRAGAS*, Iwona LEJCUŚ
Institute of Meteorology and Water Mangement – National Resarch Instytute
Wrocław Branch, Regional Research Department,
Parkowa St. 30, 51-616 Wrocław, Poland

Floods are natural events of a random nature that cause damage in property, agriculture, and industry. Floods in the upper and middle Odra basin, particularly on a large scale, are characterized by their specificity of arising and shaping. Analyses of historical material prove that the largest floods are during the summer season, especially in July and August. Those events are caused by wide and intensive precipitation lasting 2-3 days. Moreover spatial ranges in the Odra basin and runoff sequence are also the important reasons. Other important factors for the flood risk scale in a region is knowledge of the flood risk index established on the basis of observed floods or that of Maximum Probability Flood. In this paper flood risk in the territory of Lower Silesia Province was evaluated on the basis of chosen indices of flood risk.

Keywords: Odra catchment, flood risk zones

1. INTRODUCTION

Flood is a natural disaster that threatens the safety of people and animals, and cause damage to human property, and losses in the national economy. It is natural and random phenomenon. It can cause torrential rains, short thunderstorms, rapid melting of snow, strong winds on the coast from the sea towards the land and the freezing of rivers. Flood is a high water, during which water overflows the level of embankment crown and flood river valleys or depressed areas, thereby causing damage and financial and non-economic (social, moral, etc.) losses [Dubicki, Malinowska-Małek 1999].

However, high water level is a raise in water level in streams, reservoirs, at sea, which does not cause damage or loss in the adjacent areas. Spate acquires the character of flood after exceeding the boundary level, when flooding river valleys and areas of depression, causing losses. Level of risk of flooding

* Corresponding author. E-mail: mariusz.adynkiewicz@imgw.pl

depends on the state of development of the river valley and is conditioned by two factors: the size of spate and the size of the losses caused by the flood.

High water is not formed at the same time along the entire length of the watercourse, but usually moves along its course, creating a freshet wave. This primarily applies to larger rivers, which have their origin in the mountains or highlands. As the wave moves along the course of the river, the wave front is reduced, and the length is extended and, at the same time, the wave height is decreased. In addition, freshets can occur depending on the origin of formation at different times of the year. On a national scale high water most often occur in March, April and July, and less frequently in February and June. In the basin of Odra River, 59% of the annual climax falls on the winter half-year (including 27% in March), and 41% on the summer half-year (including 14% in July) [Byczkowski 1996].

2. CAUSES OF FLOODING

Floods on the Odra River, especially those of large size, have specific sources of origin and the process of forming. Analysis of historical floods on the Odra revealed that the greatest high water occur mostly in the summer months, with particular intensity in July and August. These freshets are caused by the presence of extensive and intensive rainfalls lasting for at least 2-3 days. In addition, analysis of the summer floods showed that the cause of their formation is not only a high rainfall, but also the time of its occurrence in different areas of the river basin, and the order of runoff from individual sub-basins and their functions in the formation of the wave. Summer floods may occur in the mountains, foothills and lowlands areas. The most difficult to predict are precipitation floods, derived from torrential rains usually of thermal origin. Occur locally on a small mountain and lowland streams, and cause the most damage. The largest share of the outflow formation is the size and shape of the basin, orography, slopes inclination, the permeability of the ground and land cover. Widespread floods, which are associated with frontal rains, have much wider range. They occur both in mountainous and lowlands areas, and may cover the entire river basin. Amount of rainfall within a few days, recorded during the floods, may exceed the monthly norm.

Conditions conducive to the occurrence of snowmelt flooding is the rapid melting of snow due to the sudden increase in air temperature and heavy rain accelerating the melting of snow, which, with a high degree of frozen ground increases surface runoff. The period of the formation of these floods are the winter and early spring months, with particular intensity in March.

Winter floods differ in cause of formation, course, location, range, time of occurrence and associated conditions. Divided into: jam floods and frazil-ice

floods. Water rises are caused by jams during ice flow in rivers, in places predisposed, such as the narrowings, sandbars, islands, in places with sudden changes in flow direction, in bridge profiles, in the upper sections of the damming barriers (reservoirs) are the causes of ice–jam floods. Occur in lowland and mountain rivers. However, frazil-ice floods are formed by great intensity of formed anchor and frazil ice. Then the whole river profile is jammed, the water piles up, causing local severe flooding. Most often floods of this type occur in December and January at low water levels.

The source of the formation of the Odra floods is the area of upper Odra. The interaction of water outflow from this area with other outflows determines flood sizes. Another cause of high water is an outflow of significant amounts of water from the basin of Nysa Kłodzka. Freshets in the upper Odra and Nysa Kłodzka cause substantial floods on Odra River in its upper and middle part. The formation of the flood wave, which entails a risk of flooding, can also occur during high water in the upper part of the Odra River and its right-bank tributaries, to Barycz inclusive. Substantial flood may also occur on Bóbr and Lusatian Neisse during high spate. In this case, high waters in Nysa Kłodzka and middle Odra tributaries can be moderate. In addition, the overflow of Odra River may occur as a result of high water in middle Odra tributaries, with moderate high waters in upper Odra [Dubicki, Słota, Zieliński 1999, Dubicki 2005].

3. THE BIGGEST FLOODS IN THE ODRA RIVER AND ITS TRIBUTARIES IN THE NINETEENTH AND TWENTIETH CENTURY

Started in the early nineteenth century, systematic observations of water levels allowed collecting more accurate information about the size of the flood on the Odra River and its tributaries. The floods, which were the result of high water on the upper Odra, Nysa Kłodzka, Beaver and Lusatian Neisse, occurred in the years 1813-1855. The largest flood in the middle of the nineteenth century Europe, on the Odra River occurred in 1813. Other major floods occurred between 1854 and 1855 with the highest maximum from Wroclaw to Slubice. They caused numerous broke of levees and significant overflows. Local very severe floods occurred in 1879 in the basin of Nysa Kłodzka, Bóbr, Kwisa and Lusatian Neisse. Major spates on the Odra also occurred in 1888 and 1889.

In the twentieth century, large summer floods occurred in 1903, 1926, 1940,1977, 1985, 1997, 2009 and 2010, snowmelt floods in March 1909 and 1922, and in February 1946, in the autumn in October 1910 and 1915, and in November of 1930. By the time of the most disastrous flood in the Odra River in July of 1997, for the largest, was considered a flood of July 1903, which was

only slightly lower (in the middle and lower reach of Odra) than the flood of 1854 [Maciejewski, Ostojski, Tokarczyk 2011, Rast, Obrdlik, Nieznański 2000, Dubicki, Malinowska-Małek 1999].

4. MEASURES OF FLOOD RISKS IN ODRA RIVER AND ITS TRIBUTARIES

Started in the An important element of knowledge about the scale of flood risks is the knowledge of the basin flood measures, established on the basis of the observed flood flows or on the basis of expected probable maximum flow. Measures of flood risk include: flood potential (*Pq / Fp*), flood risk index (*WZP / FRI*) and complementary floodgenerativity index (*WKP / CFI*).

Flood potential (*Pq / Fp*) is one of flood measures used so far, proposed by Balcerski [Lambor 1971]:

$$P_q(F_p) = \frac{WWQ - Q_{brzeg}}{Q_{brzeg}} \sqrt{A} \tag{1}$$

where:
WWQ – the highest observed flow in multi-year,
Q_{brzeg} – flow according to the bankfull waters level,
A – basin area in km^2

This index provides a flood measure in relation to the basin area. It gives the opportunity to compare the risk in different regions, but only when the length of the observation sequences is comparable, and when historical episodes of flooding cover compared areas at the same time. Otherwise there can be no assurance that the maximum observed freshets, in the compared basins, had the same rank. Flood risk increases with the size of the flood potential. Flood potential in Lower Silesia (Fig. 1) varies widely from about 761 (Oława) to 1355 (Głogów) for the Odra River and from about 10 (Bukówka) to 480 (Żelazno) for the tributaries. In general it can be stated that the flood potential for the Odra increases with basin growth. Also tributaries of the Odra River, with larger basin areas have greater flood potential (Fig. 1).

Flood risk index (*WZP / FRI*) is a measure that describes floodgenerativity in terms of flood risk.

$$WZP(FRI) = \frac{MWW - Q_{dozw}}{MWW} \tag{2}$$

where:
Q_{dozw} – nondamaging flow (Qgr - boundary flow of safety = $Q_{max50\%}$) [Ozga-Zielińska 2003]

MWW – maximum probable spate (Q_p = 0,01%) [BERGA 1992].

WZP (FRI) defines the actual level of flood risk, recognizing that the threat occur only after exceeding the boundary flow, determined by local conditions. *WZP* (FRI) succinctly describes the scale of local flood risk.

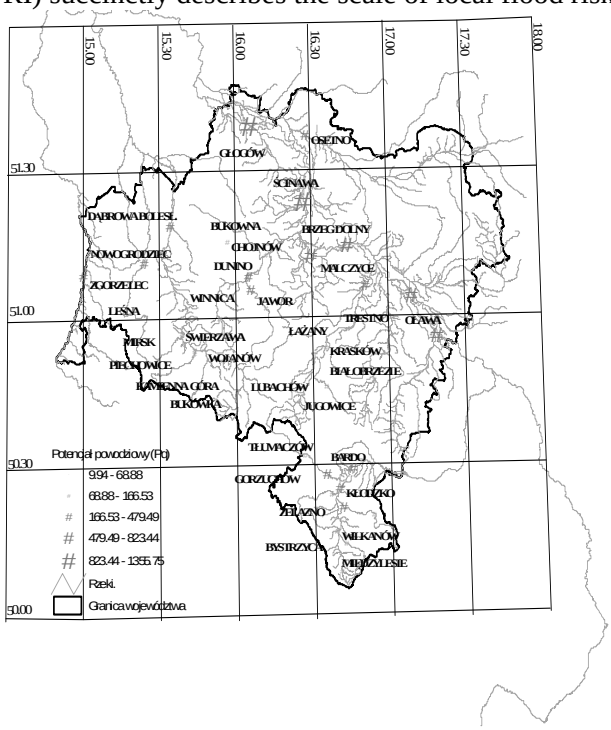

Fig. 1. Variability of flood potential in gauging cross-sections within the Lower Silesia Province

Designation of this measure allowed for the identification of areas with the greatest flood risk potential for the Lower Silesia province. Indicator of flood risk should be considered as high. It is in range from 0.7903 on Widawa in Zbytowa section to 0.9887 on Bystrzyca in Lubachów. For the middle Odra, it is in range from 0,8486 (Oława) to 0,9118 (Ścinawa) (Fig. 2.).

Complementary floodgenerativity index (*WKP*/CFI) is a measure that describes floodgenerativity in terms of the largest flow so far observed.

$$WKP(CFI) = \frac{MWW - WWQ}{MWW} \tag{3}$$

gdzie:
MWW – maximum probable spate (Q_p = 0,01%) [Berga 1992]
WWQ – the highest observed flow in multi-year,

WPK/CFI rate, determines the level of current "non-attainment" of maximum floodgenerativity, which is a measure of MWW. It is therefore complementary (supplemental) part of floodgenerativity, which can be expected in a situation of occurrence of flows that are larger than the largest previously observed, i.e. from WWQ. In other words, it determines the level of potential possibility of exceeding the highest flow observed previously [Ozga-Zielińska 2003].

Value of complementary floodgenerativity indicator, which provide the degree of non-attainment of MWW, in the province of Lower Silesia for the Odra basin ranges from 0.0 to 0.947. For Odra within Lower Silesia province this indicator is relatively low, ranging from 0.0 in Trestno to 0.3 in Scinawa. This indicator has very high values for some of the tributaries of Odra River. For most of them it reaches values above 0.4, and for Ślęza, Bystrzyca Widawa and Kwisa it exceeds 0.9 (Fig. 2).

5. FLOOD RISK ZONES

According to the Water Law (Article 79, paragraph 2) for the purpose of flood protection planning, the Regional Water Management Boards are required to determine the borders of flood waters range, of a certain probability of occurrence. These areas [D.U. 115 z 2001 r] are considered i.a. in the preparation of development plans of the province and in the study of conditions and directions, and they are called the flood risk zones. These areas include littoral zones of rivers, which at the time of the flood are flooded by an overflowing river. The extent of these zones is determined by the flow adopted as dependable for the zone. Flood risk zones are associated with flood protection zones, and in fact they are determined to establish protection zones [Ozga-Zielińska 2003].

5.1 Flood risk zones for water of Q1% probability

Floodplains for Lower Silesia region were determined on the basis of existing maps that identify areas of potential flooding for Q1% flows, and by interpolation of probable water table elevations calculated for gauging cross-sections. Interpolation between gauging sections was performed with the use of cross-sections of the river bed and valley. Water table elevations in individual sections were calculated using the computer program "HYKOR" developed by R. Dąbrowski and R. Eliasiewicz of Agricultural University.

The analysis of the areas flooded by waters likely to surpass Q = 1%, shows that the areas potentially at risk in Lower Silesia covers the adjacent areas along the following sections of rivers:

- River Odra within the province of Lower Silesia,

- River Nysa Kłodzka from Międzylesie gage the border of province,
- River Oława from Henryków to the estuary,
- River Ślęza from Marcinkowice to the estuary,
- River Bystrzyca from the reservoir Lubachów to the estuary,
- River Widawa from the voivodship border to the estuary,
- River Kaczawa from Świerzawa gage to estuary,
- River Barycz from Łąki gage to the estuary to River Odra,
- River Bóbr from the reservoir Bukówka to the estuary.

These areas were prepared on the basis of „Development of range of controlled flooding of rivers in the RZGW area, taking into account Q1%, and the maximum states of the observation period" [Tokarczyk 2002].

5.2 Flood risk zones of 1997

Floodplains Danger zones for historical floods were determined on the basis of flooded areas during the flood of July 1997 in the Lower Silesia province, and prepared on the basis of "General protection strategy against flood of the upper and middle Odra basin after the great flood of July 1997". During this flood areas along the following rivers have been flood:

- Odra River within the Voivodeship of Lower Silesia,
- River Oława from Kazanów, to the estuary to Odra River, with estuary sections of tributaries: Podgorka, Krynka, tributary in Biskupice and Gnojna,
- River Ślęza from Sienice to the estuary, along with estuary sections of tributaries: Krzywula and Księginka and rivers Oleszna and Mała Ślęza,
- River Bystrzyca from the reservoir Mietków, along with the River Strzegomka from Pyszczyn, and Czarna Woda from Garncarsko,
- River Widawa from the province border to the estuary,
- River Barycz from Milicz to Sułów Milicki, and from Bartków, including the estuary section of tributary Łacha.

It is estimated that during the food in 2010 the maximum flow in Wroclaw Floodway System amounted about 2200 m^3/s (compared to 3600 m^3/s in 1997) and was the limit for the flow of the water system. Without limiting the flow on the reservoirs of Nysa Kłodzka cascade, losses in the region of Lower Silesia would be incomparably higher, including Wroclaw itself [Kosierb 2011]. Probability of flood discharge waters in July 1997, is much higher than the likelihood of potential floods of Q = 1%. In addition, during the flood of 1997 there were numerous damaged embankments and hydraulic devices, which have contributed to the growth of the flooded area [Tokarczyk 2002] Hence the flood of 1997 can still be considered as the biggest and most catastrophic [Kitowski, Lubacz 2010].

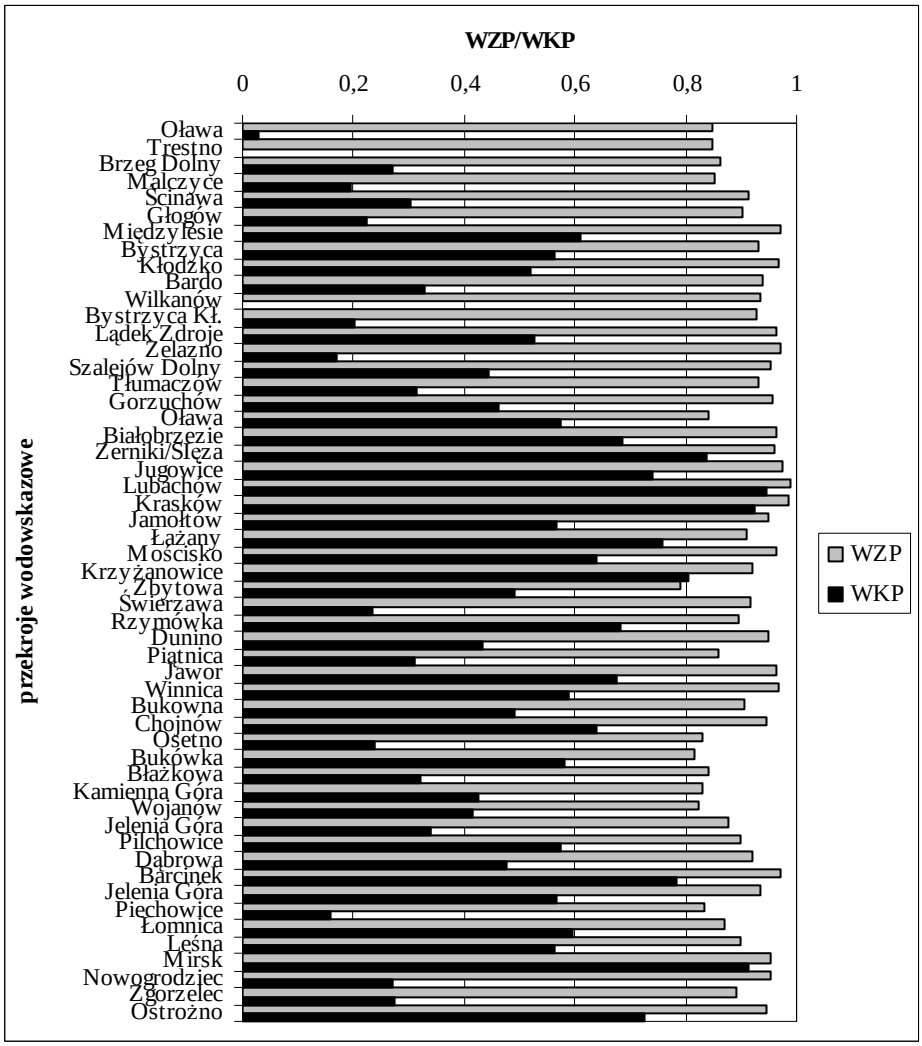

Fig. 2. Variability of WZP (FRI) and WKP (CFI) coefficients in gauging sections in the province of Lower Silesia

5.3 Flood risk zones prepared in the project ISOK

Currently Directive 2007/60/EC on the assessment and management of flood risks requires all EU Member States to develop flood hazard maps and flood risk maps (in accordance with Article. 6 – until end of 2013) and then develop flood risk management plans on their basis (in accordance with Article. 7 and 8 – until end of 2015). Currently, preliminary flood risk assessment is created in the project "Global Monitoring for Environment and Security" (ISOK) financed

by the European Regional Development Fund under the Innovative Economy Operational Programme. The project is implemented by the Institute of Meteorology and Water Management - National Research Institute (IMGW – PIB Flood and Drought Modelling Centers) in consortium with the National Water Management Board (KZGW), Head Office of Geodesy and Cartography (GUGiK), the Government Security Centre (RCB) and the Institute of Communications. Created maps are based mainly on a combination of data from laser scanning of high accuracy and hydraulic modeling, and are aimed to provide a diagnosis of intensity of the flooding and the level of its potential adverse effects. Therby maps of areas of direct and potential flood risk after opinion of the council of municipalities, districts and provincial assemblies are the basis for the verification of land use planning [Kitowski 2011].

6. SUMMARY

Flood risk assessment of Lower Silesia was based on the analysis of the process of formation and the causes of flood, its size, character of the course, time of movement, period of occurrence and the location and territorial extent. Flood risk size was determined on the basis of an analysis of the floodgenerativity status indicators and based on maps of historical potential flooding. The article uses the existing elaborations and observation and measurement materials of IMGW.

The source of the floods occurring in Lower Silesia are mostly summer freshets especially in July and August, caused by high precipitation, especially in the mountain areas of Odra River and its tributaries, especially Nysa Kłodzka and Bóbr.

The greatest flood potential (*Pq / Fp*), in the Lower Silesia region, occurs in the pravalley of Odra River and basin of Nysa Kłodzka, Bóbr and Kaczawa, as evidenced by the designated zones of historical (July 1997) and potential floods (Q = 1%). However, the greatest flood risk (*WZP / FRI*) is concentrated in a few regions of Odra River basin ie basins of Bystrzyca, Nysa Kłodzka, Kwisa, Ślęza and Nysa Szalona. In addition, attention should be paid to the reduction of flood risk by reservoirs, which is especially visible in Bystrzyca - Mietków reservoir (*WZP / FRI* = 0.9887 in Kraskow and *WZP / FRI* = 0.9498 in Jarnołtowie) and in Kwisa, Złotniki and Leśna reservoirs (*WZP / FRI* = 0.9533 in Mirsk and *WZP / FRI* = 0.8986 in Leśna). Flood risk in the section below the reservoirs is much smaller than in the upper part of the basin. Areas with a high ratio of the *WZP / FRI* are the areas where people should not live, nor should not be located any permanent economic facilities without flood protection.

Complementary floodgenerativity index (*WKP / CFI*) of Lower Silesia province shows that the largest possible flood risks in relation to those already

observed, may occur in the basins of Kwisa and Bystrzyca as well as Widawa and Ślęza. However, this index is significantly lower for the basin of the upper Nysa Kłodzka. This may suggest that in the case of Nysa Kłodzka as well as the Oder the catastrophic floods that would be expected may slightly exceed the largest observed so far.

REFERENCES

1. Berga L., *New trends in design flood assesment*. International Symposium on Dams and Extreme Floods T.III., Spain, Granada 1992
2. Byczkowski A., *Hydrologia*. Warszawa, SGGW 1996
3. Dubicki A. i inni, *Zagrożenie powodziowe*. Opracowanie ekofizjograficzne dla województwa dolnośląskiego. Wrocław, Wojewódzkie Biuro Urbanistyczne we Wrocławiu 2005
4. Dubicki A., Malinowska-Małek J., *Wielkie powodzie w dorzeczu Odry w ostatnim stuleciu*, Wrocław, IMGW (maszynopis), 1999
5. Dubicki A., Słota H., Zieliński J. (red.), 1999: Dorzecze Odry. Monografia powodzi lipiec 1997. Seria Atlasy i Monografie. Instytut Meteorologii i Gospodarki Wodnej, Warszawa
6. Kitowski K. *Planowanie przestrzenne i jego rola w ochronie przeciwpowodziowej*. W: Przyszłe wymagania w zakresie zarządzania ryzykiem powodziowym oraz zrównoważonego gospodarowania wodami w dorzeczu Odry. Wrocław, mater. konf. MKOO 2011
7. Kitowski K., Lubacz E. *Powódź w czerwcu i lipcu 2009 r. w dorzeczu środkowej Odry ze szczególnym uwzględnieniem Dolnego Śląska*. W: Konferencja Dolny Śląsk: Powódź a Śropdowisko – dobre praktyki. Polanica Zdrój. mater. konf. 2010
8. Kosierb R. *Gospodarka wodna na zbiornikach retencyjnych rzeki Nysy Kłodzkiej podczas wezbrania w maju 2010 roku.* W: Przyszłe wymagania w zakresie zarządzania ryzykiem powodziowym oraz zrównoważonego gospodarowania wodami w dorzeczu Odry. Wrocław, mater. konf. MKOO 2011
9. Lambor J., *Hydrologia inżynierska*. Warszawa, ARKADY 1971
10. Maciejewski M., Ostojski M.S., Tokarczyk T. (red.), 2011: Dorzecze Odry monografia powodzi 2010. Seria Monografie, Instytut Meteorologii i Gospodarki Wodnej – Państwowy Instytut Badawczy, Warszawa
11. Ozga-Zielińska M. i inni, *Powodziogenność rzek pod kątem bezpieczeństwa budowli hydrotechnicznych i zagrożenia powodziowego.* Materiały Badawcze IMGW Nr 29, Seria Hydrologia i Oceanologia. Warszawa, IMGW 2003
12. Prawo Wodne, Dziennik Ustaw nr 115 z 2001 r.

13. Rast G., Obrdlik P., Nieznański P. (red.), 2000: Atlas obszarów zalewowych Odry, WWf Deutschland
14. Tokarczyk T. i inni, *Opracowanie zasięgów zalewów rzek kontrolowanych na obszarze RZGW przy uwzględnieniu Q1% i maksymalnych stanów z okresu obserwacyjnego*, Wrocław, IMGW 2002

ZAGROŻENIE POWODZIOWE WOJEWÓDZTWA DOLNOŚLĄSKIEGO

S t r e s z c z e n i e

Powodzie to naturalne i losowe wydarzenia powodujące liczne szkody w rolnictwie, przemyśle i mieniu ludzkim. Analiza materiałów historycznych wskazuje, że największe powodzie w województwie dolnośląskim wystąpiły w sezonie letnim, najczęściej w lipcu i sierpniu. Wydarzenia te są najczęściej spowodowane przez rozległe i intensywne opady w obszarze górnego biegu Odry i jej lewostronnych dopływów (Nysa Kłodzka, Bóbr). W skali określania zagrożenia powodziowego w regionie ważna jest znajomość wskaźnika potencjału powodziowego, wskaźnika zagrożenia powodziowego i wskaźnika potencjalnej powodziogenności. W artykule podano informacje o tworzeniu stref zagrożenia powodziowego, w tym tworzonych w ramach projektu ISOK.

CIVIL AND ENVIRONMENTAL ENGINEERING REPORTS

No. 10 2013

THE DIRECTIONS OF PROTECTION AND DEVELOPMENT OF NATURAL ENVIRONMENT OF A METROPOLIS ON THE EXAMPLE OF THE POZNAŃ METROPOLITAN AREA

Hanna BORUCIŃSKA –BIEŃKOWSKA*
University of Zielona Góra, Faculty of Civil and Environmental Engineering
Division of Architecture and Urban Planning
Szafrana st 1, 65-516 Zielona Góra, Poland

The aim of this study is a presentation of issues related to directions of changes which take place in natural environment in heavily urbanized areas, in a metropolis and the interaction of the central city and municipalities of the metropolitan area in the issue of natural environment. It shows natural environment as an important factor influencing functional and spatial conditionings of a metropolitan area.

Keywords: natural environment, metropolitan area, metropolis

1. INTRODUCTION

The spatial planning and development act of 27 March 2003 introduced the term 'metropolitan area'. According to the act, it is the area of a city and its functionally related surroundings. For a metropolitan area, a land development plan of the metropolitan area is prepared as part of the land development plan of the voivodeship.

To specify a metropolitan area, the primary importance is the delimitation of its borders based on adopted assumptions and a wide spectrum of delimitation criteria. The aim of delimitation of metropolitan areas is designation of settlement schemes which, in terms of functional and spatial relations and advancement of urbanization processes, will provide integrity and will differ only in the administrative status of included territorial units (Z. Gontarski, „Obszary metropolitalne w Polsce". Polska Akademia Nauk, Komitet Przestrzennego Zagospodarowania Kraju, Warszawa 1980 r.).

* Corresponding author. E-mail: h.borucinska-bienkowska@ib.uz.zgora.pl

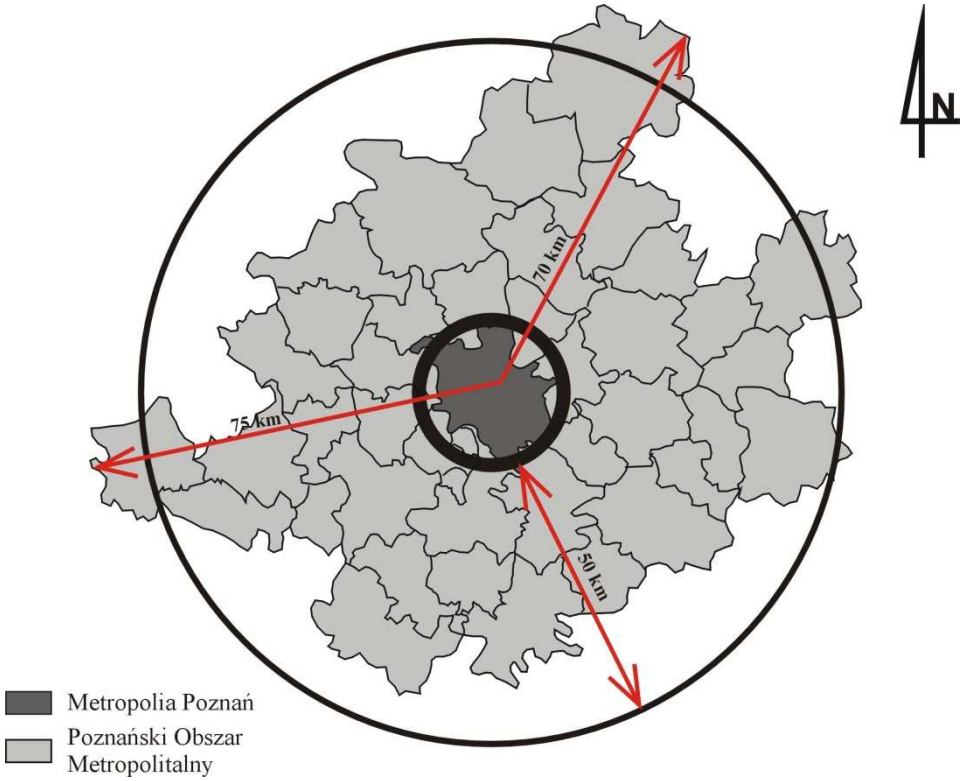

Fig.1. Area – central view –diagram Source: author's study – based on "the Poznań Metropolitan Area" Wielkopolskie Biuro Planowania Przestrzennego w Poznaniu (regional spatial planning office in Poznań), Poznań 2006

The delimitation of the Poznań Metropolitan Area was conducted on the basis of studies and analyses of urbanization processes in relation to the area surrounding the city of Poznań in the following research aspects.

Poznań Metropolitan Socio-economic environment expressed inter alia by demographic changes such as population density and dynamics of population growth;

1. Accessibility of public transport expressed by 30 min isochrone of a journey by public transport in relation to the distance of 10, 30 and 50 kilometres to the centre of the metropolis and 60 min isochrone of a journey by public transport in relation to the distance of 10, 30 and 50 kilometres to the centre of the metropolis;
2. Natural environment expressed inter alia by valorization of agricultural production area, index of forest coverage, area percentage of nature conservation units in municipalities;

3. The delimited Poznań Metropolitan Area covers 45 municipalities including Poznań. The area includes 10 poviat towns and 15 other towns. The acreage of the area equals 6205 km^2 (20.8% of the area of the voivodeship). The Poznań Metropolitan Area is inhabited by 1326.9 thousand people, which constitutes 39% of the inhabitants of the voivodeship. The population density is 214 people per 1 km^2, whereas the average population density in the voivodeship equals 112 people per 1 km^2.
   After: Poznań Metropolitan Area, Wielkopolskie Biuro Planowania Przestrzennego w Poznaniu (regional planning office in Poznań), Poznań 2006.

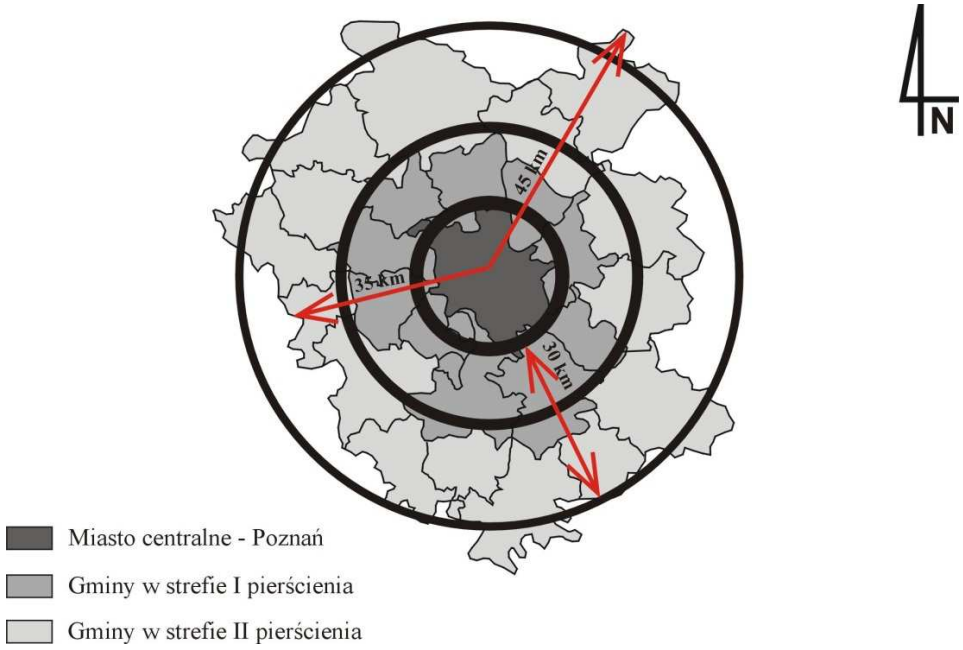

Fig. 2. Poznań Metropolitan Area – central view – diagram. Source: author's study based on the spatial development plan of the Greater Poland Voivodeship – the Poznań Metropolitan Area, wielkopolskie Biuro Planowania Przestrzennego in Poznań (regional spatial planning office in Poznań), 2003

The delimitation of the Poznań Metropolitan Area was conducted on the basis of studies and analyses od of urbanization processes in relation to the area surrounding the city of Poznań in the following research aspects:

– socio-economic environment and spatial development expressed by demographic changes and changes in the socio-economic structure of the population;

– transportation accessibility and distance expressed by a 30 min. isochrone of time accessibility of means of public transportation and a 30 km isochrone of distance; natural environment.

2. RESOURCES OF NATURAL ENVIRONMENT

The quality of natural environment is directly dependent on the condition of biotic elements of nature. The problem of anthropopression on natural environment exists in highly urbanized areas, agglomerations and metropolises. The anthropopression occurs where it is characterized by superior assets, where geodiversity and biodiversity occur. Apart from inadequate level of knowledge related to this issue in society as well as in local governments, there is the lack of systematic solutions, including inter alia a system of sufficient compensations for individuals who accomplish pro-ecological actions connected with optimizing energy consumption in households and in entire residential and farming areas.

The questions of ecology are better and better recognized and implemented on the local level and beyond. The role of education in local governments and local communities increases. Pro-ecological actions are undertaken in all fields and at all levels beginning from the increase of awareness in scientific circles by the introduction of pro-ecological issues to schools at every level of education. This increasingly better ecological awareness contributes to numerous actions in all fields of economic and social existence. A sustainable development has become the aim of actions of local communities as well as local authorities at the ecological, economic and social level.

Climatic and hydrologic conditionings contribute to water shortages, especially for farming purposes, but also to deterioration of water purity in lakes used for recreational and touristic purposes within the Poznań Metropolitan Area. The problem is the deficiency of water retention in reservoirs, little ground retention and lack of storage reservoirs regulating water flow in the catchment area.

There is a slight danger of flooding for the Poznań Metropolitan Area from the Warta river, but it is possible only in extreme cases. It is influenced by the river control conducted over the years and urbanization of flood plains, which causes low accumulation of overflowing water. The share of flood plains in the Poznań Metropolitan Area constitutes only around 5% in relation to endangered areas in the Greater Poland voivodeship. The status quo is assured by the storage reservoir 'Jeziorsko' located near the upper catchment area of the Warta river between Sieradz and Uniejów.

During the flood (also called the flood of the century) in 1997, the flooded areas covered the Mosina-Śrem part (especially the area of Rogalinek) of the

Poznań agglomeration, fragments of oxbows, meanders near Luboń and flood plains to the north of the water intake 'Dębina', causing health risks. The natural polders of the Warta river played an important role in the reduction of the risk of flood; they included the part devoid of dikes from Nowa Wieś Podgórna to Śrem and from Śrem to Rogalinek.

Small storage reservoirs are important for the local environments. They are: Kowalskie Lake, Śródka, Iwno, and Malta Lake, and ponds: Olszak, Browarny, Młyński, Antoninek, and Radzyny. The protection against floods from the Warta river and its tributaries are embankments, which protect cubature objects. The length of embankments of river valleys in communes on the Warta river equals 38.1 km, including 10.0 km of girdle embankments within the borders of Śrem.

The directions of natural environment protection and development cover actions within the range of energy, underground and surface water protection and rational water management. Inadequate amounts of drinking water, its high consumption and overuse of underground waters in highly urbanized areas enforce actions to modernize water intakes, water conditioning plants and power transmission grids in order to minimize the loss during the transfer. It is necessary to build local intakes and maximally reduce underground water use for industry by the introduction of new technological developments.

The problem conditioning the development of a metropolis is provision of adequate high, rule abiding standard of living of inhabitants, but above all, access to drinking water in sufficient amounts and rationalization of energy consumption by the use of alternative sources.

The conditions for having access to proper quality drinking water are:

1. Maintenance of balance in natural environment and its maximal protection against uncontrolled urbanization;
2. Protection of existing drinking water resources by rigorous application of protective zones around water intakes;
3. Reservation of area for new water infrastructure facilities in spatial planning
4. Building water mains;
5. Modernization and automatization of water supply plants and pumping stations;
6. Building missing fragments and modernization of the existing water-pipe networks;
7. Constant monitoring of facilities and water intakes.

For environment protection, apart from water-pipe networks, an efficient sewerage system including the sanitary and rain system, is also important.

For reliable wastewater collection and its proper neutralization, necessary are:

1. protection against uncontrolled urbanization;
2. Efficient sewage treatment plants;

3. Modernization and development of pumping mains to already existing sewage treatment plants;
4. Reservation of an area for new sewerage infrastructure facilities in spatial planning;
5. Building sewage systems in new housing estates;
6. Building storage reservoirs;
7. Use of alternative ways of rainwaters disposal and application;
8. Development of rainwater sewage systems with cleaning facilities as well as building and development of facilities storing rainwaters in water catchment area.

Reasonable waste management is yet another factor influencing the quality of urbanized environment, especially areas heavily adapted, such as metropolises. It should be based on waste sorting, recycling and introduction of technologies reducing detrimental effects and amounts of industrial waste. There is a need for application of standards in hierarchies of waste management. Currently working waste dumping grounds in the ,Poznań Metropolitan Area which have long forecast operating life, as well as waste dumping grounds designed in land development plans, all assure proper and non-colliding waste management.

It is vital to introduce systematic solutions to problems of industrial waste management and issues related to pesticide burial areas and medical or veterinary waste.

Nature conservation, development of technical infrastructure, rational management of water, sewage and waste as well as application of pro-ecological sources of heat energy will directly contribute to the protection and development of natural environment of an agglomeration.

The directions of protection and development of the Poznań Metropolitan Area, apart from essential actions connected with technical infrastructure within the scope of environmental protection, should assume the continuation of the concept of wedge-shaped / ring-shaped system of greenery for the city of Poznań devised by prof. WładysławCzarnecki and Adam Wodziczko in the 1920s and 1930s. The wedge-shaped / ring-shaped system of greenery was the basis of the structure of land development plans in the city and distinguished it in the country.

The role of green areas in the structure of the city is irreplaceable, so it is important to aim at the preservation of existing resources and change and develop them in a creative way. The function of social and pro-health functions of these areas increases. They decide about the quality and comfort of life, well-being and health of inhabitants of an agglomeration. Parks and gardens have always distinguished precious architectural objects and enhanced the social status of their owners.

In an urbanized agglomeration with dense street network and tight built-up area, greenery was pushed aside. The increase of pro-ecological awareness and social needs of living in healthy environment forced actions which favoured preservation of precious green areas, as well as their modernization and development.

The legal act of 16.04.2004 on nature preservation[1] and the legal act of 03.02.1995 on farming and forest areas[2] obliged communes to proper care of greenery and trees. The character of greenery in cities is very diverse and depends on buildings. Greenery is different in areas of housing estates, where gardens have utilitarian, decorative and recreational functions; in city centres; and in housing estates, where greenery forms a garden-park for all inhabitants and has a function of public space. Greenery incorporated into building areas is diversified with small architectural elements, playgrounds, and has the recreational-rest function.

Plants along routes, which play the role of isolation, soothe noise, stop a part of exhaust fumes and dust, are subject to heavy degradation. Parks, lawns and city gardens create larger enclaves of greenery and should be thoroughly protected. In the suburbs, in communes of metropolitan areas this role is fulfilled by manorial, church and cloister parks with a wide range of trees and bushes, diversified by ponds that make attractive enclaves and ecosystems.

The main roles of greenery in cities are:

1. Creation of landscape and enhancing esthetical architectural and spatial compositions;
2. Neutralizing pollution and diminishing noise;
3. Creation of microclimate;
4. Giving inhabitants an opportunity to contact nature on everyday basis, enabling recreation and rest;
5. Creating social spheres in parks.

Green areas are devised in physical management plans and the owner of the area is responsible. Greenery, especially in heavily urbanized areas, has become even more valued element of the functional-spatial structure in existing town-planning systems and designed housing, service and farming facilities.

Greenery in metropolis should be embraced by:

1. Protection of existing green areas;
2. Renewal, modernization, protection and development of existing green areas;
3. Saving old trees which are naturally and socially precious;
4. Work related to the improvement of safety for users of green areas, including proper lighting and paving park paths, safety of passages and bridges;

[1] Dz. U. Nr 92, poz. 880
[2] Dz. U. Nr 16, poz. 78

5. Tidying of existing forest areas, including the ones beside the road;
6. Proper condition of little architecture and playgrounds for children.

These actions enable proper functioning of green areas of a metropolis, create friendly environment and influence the improvement of social relationships among users of common space, and they are an element creating healthy living environment. Another form of greenery is made by monumental cemeteries often placed in the centres of metropolises. Their function, apart from the fundamental one, is also extended by diverse old trees and fine tomb sculptures.

The role of greenery is not only limited to the ecological aspect, but also has social, esthetic and functional-spatial aspects.

The Poznań agglomeration is composed of the central city and communes of zone I and II of the ring. The Poznań Metropolitan Area is composed of the central city – metropolis and communes from the zone I, II and III.

The communes adjacent to the central city, which are under its functional-spatial and socio-economic influence, belong to zone I. The communes in zone III are significantly less connected by factors, conditionings and economic or social relations than communes in zone I and II. However, factors, conditionings and ecological relations play an important part in urbanization processes of a metropolis.

Natural bonds of the central city and communes create a common system and in many aspects introduce social development of the whole metropolis.

3. DIAGNOSIS OF NATURAL ENVIRONMENT RESOURCES

One of the most important problems in the Poznań Metropolitan Area is uneven location of natural areas, which form 'ecological islands'. Many of them are beyond protected areas, which causes their further degradation.

The development of building industry and the constant lack of investment areas cause that numerous natural areas are becoming developers' target. Natural environment of adjacent communes is more and more endangered due to increasing anthropopression. However, the process of urbanization will not diminish, so a deep analysis of all location decisions and local plans of spatial development made according to the rule of sustainable development and investments will reduce their negative effects.

The dynamically developing city of Poznań claims further farming areas, especially in adjacent communes in zone I of the ring. Road and technical infrastructure construction tightly connected with the development of the Poznań Metropolitan Area cause further reduction of green areas and farmlands.

Also, degradation of the Poznań Metropolitan Area is caused by external factors, such as improper agricultural actions, irrational energy management, global warming and reduction of the amount of drinking water.

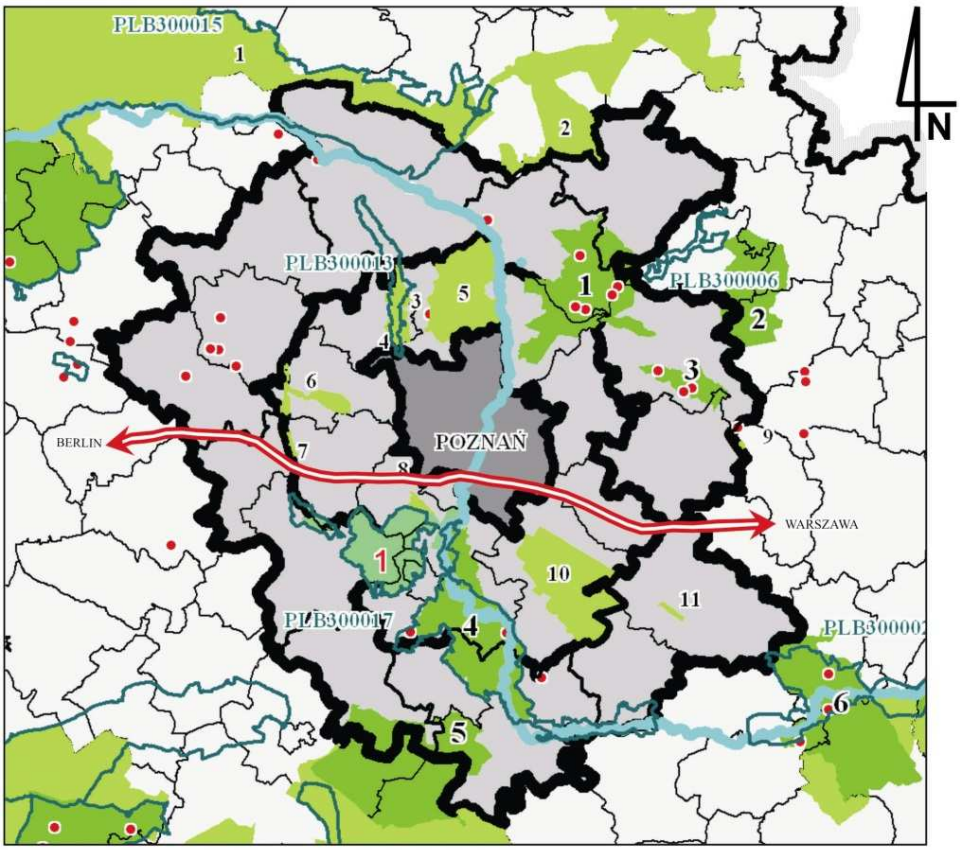

1 National parks

Wielkopolski National Park

Natural landscape parks

1 Zielonka Forest Landscape Park
2 Lednica Landscape Park
3 Promno Landscape Park
4 Rogalin Landscape Park
5 Dezydery Chłapowski Landscape Park
6 Żerkowsko-Czeszewski Landscape Park

Areas of protected landscape

1 Notecka Forest
2 Wełna River Valley and Gołaniecko-Wagrowiecka Trough
3 Samica Kierska River Valley in Suchy Las commune
4 Pawłowicko-Sobocki area
5 Biedrusko area
6 Trough of Lusowskie Lake and Sama River Valley
7 Area of Niepruszewskie Lake in Dopiewo commune
8 Wirynka River Valley
9 Cybina River Valley in Nekielka
10 Area of Reception Basin of Kórnicko-Zaniemyskie lakes in Kórnik commune
11 Średzkie Marshes

Special protection areas for birds

PLB300015 Notecka Forest
PLB300013 Samica River Valley
PLB300006 Zgierzynieckie Lake
PLB300017 Rogalińska Nature Refuge
PLB300002 Middle Warta River Valley

Nature reserves

Border of the Greater Poland (Wielkopolskie) Voivodeship

Border of Poznań Metropolitan Area, zone II of the ring

Border of Poznań Metropolitan Area, zone I of the ring

Border of the City of Poznań

Fig. 3. Protected enwironmental areat of Poznań Metropolita Area.

After recognition of the state of natural environment resources of the Poznań Metropolitan Area, it may be ascertained that they possess a significant value thanks to the existence of:

- Diverse farming-forest-meadow environment with large quantities of surface water;
- Compact complex of agricultural production areas with high quality classification;
- Favourable ground-water conditions for the development of building industry;
- The Warta river being the main ecological axis;
- Good forest coverage – 21.3% of the Poznań Metropolitan Area (10% of the Greater Poland voivodeship);
- Good amount of natural resources, gas deposits, thermal waters with industrial signification for local purposes.

It may be assumed that the most serious threat for the environment in the process of changes and development occurs in adjacent communes, in zone I of the ring.

The diagnosis of the state of the environment in adjacent communes in zone I revealed that negative factors influencing changes in environment may include:

1. Reduction of valuable farming and natural areas by:
   a. development and creation of road and railway networks
   b. development and creation of linear technical infrastructure
   c. development and creation of housing estates within communes
   d. development of area-consuming fields of economy
   e. creation of large shopping centres in the commune of Tarnowo Podgórne and Komorniki
   f. creation of large waste deposits
2. Pollution of water and atmosphere by:
   a. lack of sewage systems and rainwater drainage in all urbanized areas
   b. emission of harmful exhaust fumes resulting from different emission sources
   c. improper agricultural actions
3. Degradation of greenery by:
   a. treating green areas as a reserve for building industry
   b. excessive emission of harmful exhaust fumes in city centres
   c. inappropriate way of winter road maintenance due to excessive use of chemical compounds destroying trees
   d. no planting of greenery as replacement in green areas
   e. inappropriate maintenance of existing greenery

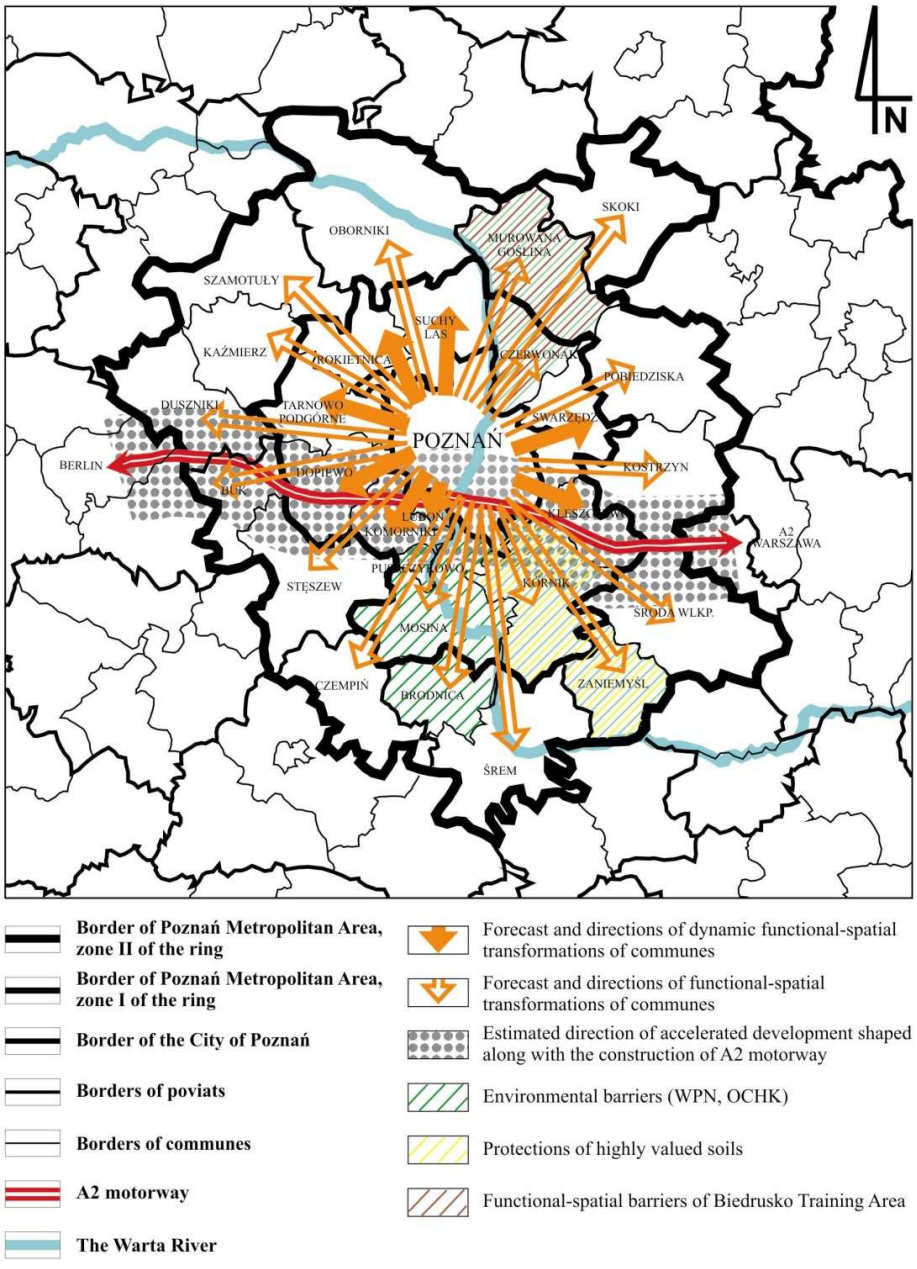

Fig. 4. Forecast of directions-spatial transformations of communes within the impact zone of the central city, impact of the socio-economic potential and predispositions of local communities, and impact of local authorities on transformation and development

4. CONCLUSIONS

One of the most basic problems of the Poznań Metropolitan Area is uneven distribution of natural areas. They form 'ecological islands', which under anthropopression, are being diminished. The development of building industry and constant lack of areas for investments cause that many naturally valuable areas of metropolis become the target of developers' actions. The developing central city, Poznań, takes over further farmlands, especially in the adjacent communes. Road constructions and technical infrastructure tightly connected with the development of the Poznań Metropolitan Area causes reduction of natural areas and areas for agricultural industry.

Such further actions will lead to significant degradation of natural environment, especially in the adjacent communes in zone I. In zone II and III of the ring, communes remain more agricultural. Dense complexes of soils of high quality classification form areas of intensive farming industry, which makes it impossible to change their purpose. Agricultural production areas of metropolitan area with a high rate of soils with high quality classification forms a certain barrier for further intensive urbanization. Rational management of area by sensible, sustainable functional-spatial and social-economical development may stop the chaotic urbanization of areas in communes forming a metropolitan area.

Protection of environmental values of agglomerations and metropolitan areas can be achieved through implementation of rules of eco-development, such as (inter alia):

- systemic approach to areas of high environmental value, treated as an element of functional-spatial structurization;
- prevention of intensification of real estate development, inter alia through execution of investment absorption capacity of a given area in compliance with ecological priorities;
- introduction of a compulsory system of analyses of construction (housing) market capacity to prevent overinvestment of the land.

REFERENCES

1. Borucińska-Bieńkowska H.: *Wpływ transformacji społeczno-gospodarczej kraju na mechanizmy rozwoju aglomeracji i gmin. Rozwój aglomeracji poznańskiej i gmin Wielkopolski.* PAN oddział w Lublinie, TEKA KOMISJI ARCHITEKTURY, URBANISTYKI I STUDIÓW KRAJOBRAZOWYCH, Tom IV B, Lublin 2008.
2. Gorzelak G., and Smętkowski M. : *Metropolia i jej region w gospodarce informacyjnej*. University of Warsaw. Warsaw: Wydawnictwo naukowe SCHOLAR, 2005.

3. Gorzelak G.: *Polska regionalna i lokalna w świetle badań EUROREG-u.* The Centre for European Regional and Local Studies at University of Warsaw. Warsaw: Wydawnictwo naukowe SCHOLAR, 2007.
4. Schneider - Skalska G.: *Kształtowanie zdrowego środowiska mieszkaniowego.* Architektura. Krakow University of Technology. 2004.
5. Skibniewska H., Bożkowska D. and Goryńska A.: Tereny otwarte w miejskim środowisku mieszkaniowym. Warszawa :PWN, 1968.
6. *Plan Zagospodarowania Przestrzennego Województwa Wielkopolskiego – 2001*. Poznań: WBPP, 2001.
7. *Studium Rozwoju Przestrzennego Województwa Wielkopolskiego-Aglomeracja Poznańska 2003.* Poznań: WBPP, 2003.
8. *Studium Uwarunkowań i Kierunków Zagospodarowania Przestrzennego Miasta Poznania - 2008.* Poznań: MPU, 2008.
9. *Studium Rozwoju Przestrzennego. Uwarunkowania Rozwoju.* Poznań: WBPP, 2003.

KIERUNKI OCHRONY I ROZWOJU ŚRODOWISKA PRZYRODNICZEGO METROPOLII NA PRZYKŁADZIE POZNAŃSKIEGO OBSZARU METROPOLITALNEGO

S t r e s z c z e n i e

Celem opracowania jest przedstawienie zagadnień związanych z kierunkami zmian jakie zachodzą w środowisku przyrodniczym na terenach silnie zurbanizowanych, w metropolii oraz analiza wzajemnych relacji miasta centralnego i gmin obszaru metropolitalnego na płaszczyźnie środowiska przyrodniczego. Pokazanie środowiska przyrodniczego jako istotnego czynnika wpływającego na uwarunkowania funkcjonalno-przestrzenne obszaru metropolitalnego. Jednym z ważniejszych problemów Poznańskiego Obszaru Metropolitalnego jest nierównomierne rozłożenie obszarów przyrodniczych. Tworzą one, „wyspy ekologiczne", które pod wpływem antropopresji ulegają ciągłemu zmniejszaniu. Rozwój budownictwa i ciągły brak terenów pod tego typu inwestycje powoduje, że wiele obszarów cennych przyrodniczo metropolii staje się celem działań deweloperów. Rozwijające się coraz bardziej dynamicznie miasto centralne Poznań pochłania kolejne tereny rolnicze, szczególnie gmin stykowych. Budowa dróg i infrastruktury technicznej ściśle powiązana z rozwojem Poznańskiego Obszaru Metropolitalnego powoduje kurczenie się terenów przyrodniczych i rolniczej przestrzeni produkcyjnej.

Dalsze postępowanie tego typu doprowadzi do znacznej degradacji środowiska przyrodniczego, szczególnie gmin stykowych strefy I pierścienia. W strefie II i III pierścienia, gminy w większym stopniu zachowują swoja rolniczą funkcję. Zwarte kompleksy gleb o wysokiej bonitacji tworzą rejony intensywnej gospodarki rolnej, co uniemożliwia zmiany ich przeznaczenia. Rolnicza przestrzeń produkcyjna gmin obszaru

metropolitalnego o dużym wskaźniku gruntów rolniczych o wysokim stopniu bonitacji stanowi pewnego rodzaju barierę dla dalszej intensywnej urbanizacji. Racjonalna gospodarka przestrzenią poprzez świadomy, równoważony rozwój funkcjonalno-przestrzenny i społeczno-gospodarczy może powstrzymać chaotyczną urbanizację terenów gmin tworzących obszar metropolitalny

CIVIL AND ENVIRONMENTAL ENGINEERING REPORTS

No. 10 2013

MINERAL COMPOSITION OF MELAPHYRE ROCKS AND DURABLITY OF A MOTORWAY SURFACE

Tadeusz CHRZAN*, Justyna ZAWORSKA†
University of Zielona Góra, Faculty of Civil and Envirnomental Engeenering
ul. prof. Z. Szafrana 1, 65-615 Zielona Góra, Poland

The article presents the mineral composition of melaphyre and discusses durability of minerals contained in the rock for the impact of weather conditions on stability and strength of mineral rocks. The analysis showed that the tested melafir contained too many minerals not resistant to weathering. This fact had a significant impact on the exploitatnion of the new done motorway surface. The surface layer of the motorway was made between June and November 2001 and at the beginning of 2003 there started its renovation. The resulting rapid wear of the upper surface of the motorway may be explained by an excessive content of minerals that have gone rapid transformations (weathering and oxidation) in the conditions of the top surface layer of the motorway.

Keywords: melaphyre rocks, motorway, surface layer

1. INTRODUCTION

The surface layer of the Konin-Września motorway section was made during the period from July to November 2001. The layer was made from granulated aggregate 0-20 mm in diameter derived from Borówko and Grzędy melaphyre quarry, bounded with modified bituminous mass. The tests of melaphyre aggregates against grade and class requirements had confirmed that those grits were the first class and grade [1,2,3] according to the Polish Standards [11,12, 14].

The binding layer of asphaltic concrete made and tested on samples that were taken from the completed motorway also conformed to the standard requirements according to Polish Standards [4,15,16]. Also, the adhesion of asphalt to the melaphyre grit conformed to the standard [6,13].

* Corresponding author. E-mail: t.chrzan@iis.uz.zgora.pl
† Doctoral student

After the wintertime, in spring 2002, on the surface of the roadway, distinct signs of scaling and weathering were observed on the surface of larger melaphyre grit grains. In August 2002, it was found that the number of weathered grains had increased and some of them lost their compactness and disintegrated [10,7]. Between September and November of 2003, due to the above reason, which threatened the safety of moving vehicles, partial repairs were carried out covering 1600 square meters. The surface of motorway has been excessively worn and looks as if it were used for at least 5 years. In this paper, it is explained why the motorway has been worn so quickly.

2. ANALYSIS OF DECREASE OF ASPHALTIC CONCRETE STRENGTH ON MOTORWAY BINDING LAYER IN RESPECT TO MINERAL COMPOSITION OF ROCKS

2.1. Description of melaphyre deposit

The melaphyre used for road construction come from deposit that was formed from basalt-type volcanic rocks in the Permian period around 350 million years ago. The volcanic rocks created trachyte-basalt, trachyte and tuff-type rocks. The melaphyre deposit is mined in the quarries of Borówno, Grzędy and Rybnica Leśna.

There are two types of trachyte basalts. The first one includes rocks coloured cherry-brown, cherry-brick and grey-violet. They have chaotic structure and aphanitic texture. Cracks are filled with the ferruginous and carbonate substance. The second type is the rock ranging from grey-brown through grey-greenish to nearly black in colour. The structure is aphanitic and the texture is dense. Coursegrained breccia of chaotic texture is also found. Volcanic spalls are cemented with the ferruginous and carbonate binder. The rock spalls are grey-brown and are of various size and aphanitic structure. The sedimentary rocks are cherry-brown in colour and have fine-grained structure with directional texture. They disintegrate into irregular small blocks. Rocks of lava mudstone fraction are found in the deposit which may have been the result of lava flooding during volcano eruption of weathered layers from the previous outflow.

The exploited rock is melaphyre-type aphanite lava ranging from dark grey to black in colour; solid but intensely cracked rock. The cracks make it vulnerable to weathering and 0-10 mm sized rock is dumped as waste [5] in amount of 21% at Borówno quarry, and 15% at Grzędy quarry.

This gives evidence that melaphyre in the Borówno quarry is built from minerals that are subject of stronger weathering than that in the Grzędy quarry. The melaphyre in both quarries is built from minerals that disintegrate under the influence of temperature, air and water.

2.2. Petrographic analysis of melaphyre

The petrographic analysis of Grzędy deposit shows that plagioclases are found in the form of small phenocrysts. Feldspars undergo the process of sericitization and carbonization, and weathering processes lead to kaolinization. The ferruginous substance infiltrates the strips of plagioclases. Dark minerals were completely transformed. They were replaced with hydrated iron oxides accompanied by concentrations of carbonates, and in place of olivine there is a substance that is difficult to identify. Chlorite is rarely found. Pores are refilled with calcite accompanied by ferruginous pigment. In the pores there are concentrations of chalcedony. Concentrations of limonite are often found. Apatite, limonite and magnetite are accessory minerals. Volcanic glass, brown or orange in colour is also found. The rock groundmass consists of heavily carbonatizated glass, perches of plagioclases, ash fraction and iron oxides.

3. MINERALOGICAL TESTS

The testing of samples collected from the Borówno quarry was carried out both on fresh solid, not weathered samples, and on weathered, low-cohesion samples in a laboratory in Austria [9]. The petrographic study determined, as it is specified in the Polish geological documentation of Borówno melaphyre deposit [8] that in the melaphyre there are clay minerals and plagioclases which undergo weathering into quartz and clay minerals.

The contents of plagioclases in both cases were very high in samples from Borówno (58% to 76% according to Austrian study and from 45%, 75% according to the Polish study).

Samples were collected from the Borówno quarry and were designated as:

- BO–2 - brittle grains taken from key aggregate 16/22, brown, able to be ground with fingers,
- BO–3 - sample taken from fresh gram,
- BO–4 - sample able to be ground with fingers,
- BO–5 - sample from 2nd production level,
- BO–6 - sample from 2nd level at the road.

3.1. Clay minerals

Clay minerals is kaolinite ranging from white to red or greenish in colour. It is commonly found as a product of feldspar and aluminosilicates weathering. It becomes plastic under the influence of water.

Clay minerals include kaolinite, which is a product of weathering of feldspars and plagioclases that make up 60% of the deposit illite products of feldspar and kaolin weathering. Commonly found components of clay rocks such as kaolin, clay, silt, and rocks that are formed in sea environment. These

minerals are chemically related and do not differ in macroscopic properties. Their colour depend on iron admixture.

Montmorillonites are a dense concentrated wax. Their colour depend on iron admixture and ranges from white to black-brown. They swell when flooded with water. They discolour methylene blue solution. Components of sedimentary rocks and hydrothermal formations of low temperature. Montmorillonites are created as the products of magma glaze weathering in alkaline and heavily salted environment.

3.2. Quartz SiO_2

Rock forming mineral, very durable and weatherproof. It may also be found as tridymite and cristobalite. Its colourless form is called mountain crystal, other forms are yellow, violet, black, pink, green. It does not reduce the strength of grits in the motorway surface. A small content of quartz in the rocks causes that the rocks are not resistant.

3.3. Plagioclases

According to the mineralogical testing of the deposit, there is from 58% to 76% of plagioclases in melaphyre. These minerals are sodium-calcium feldspars, which with increasing calcium content due to the weathering process, disintegrate into kaolin, which is a clay mineral. It may not be ruled out that the weathering process in melaphyre grits, which has begun in the deposit, will continue on the surface of the motorway.

3.4. Carbonates

Carbonate minerals such as calcite, aragonite, dolomite and magnesite are products of hydrothermal formations and are found in melaphyre. They do not undergo oxidation or weathering process. Howeyer, syderyte ($FeCO_3$) is a product of hydrothermal waters, and under the influence of water and oxygen, that is possible on the motorway surface, transforms into iron hydroxides. It can also contains admixtures of clay minerals and calcite. That carbonate mineral may have a great impact on the strength of grits in the motorway surface, assuming goethite's colour.

3.5. Oxides and hydroxides

These kinds of minerals occur in melaphyre with the content ranging from 6 to 39%. They may be iron compounds, which are components of magma rocks. Goethite (FeOOH), a product of iron mineral oxidation, may be also found, which is also a product of low temperature hydrothermal activity. The minerals undergo considerable oxidation during one-year period (visible change in aggregate colour in the storage yard). The impact of their content on grit strength

in the motorway surface is difficult to determine. However, the iron oxidation process certainly reduces the strength of rock components in asphaltic concrete.

3.6. Amphiboles

Amphiboles are important rock-forming ribbon silicates and aluminosilicates minerals. Four groups of amphiboles are distinguished: 1) Fe-Mg-Mn, 2) Ca, 3) Na-Ca, and 4) Na. Amphiboles also include the hornblende group usually containing Na, Ca, K, Fe, Si, AI, SiO_2 ranging from light green to dark green in colour, with density 2.9-3.4 Mg/m^3. Hornblende usually occurs in magma rocks of any type from neutral, acid to alkaline.

3.7. Pyroxenes

Pyroxenes belong to aliphatic silicates and aluminosilicates. Group I consists of Mg-Fe, Mn-Mg, Ca, Ca-Na, Na-type pyroxenes. Pyroxenes are an important group of rock forming minerals, which are created at high temperatures and at low water pressure. They are components of magma rocks and metamorphic rocks. They are not resistive to climatic factors, therefore are rarely found in sedimentary rocks. The colour of pyroxenes depends on iron and titanium content. At small content, it ranges from white to greenish, with larger content, it is olive, brown or dark green. Orthorhombic pyroxenes form the isomorphous series from Mg to Fe, with distinguished enstatite, bronzes, hypersthenes, ferrohyperstene, eulite. Monoclinic pyroxenes include four minerals creating a diopsyde-hedenbergite series built from Ca, Mg, Fe, SiO_2. Pyroxene minerals are not weatherproof. It is visible in table 1.

Table 1. Content of minerals in samples taken for the Borówno quarry [9]

	Weathered samples		Fresh samples	
	BO-4	BO-2	BO-3	BO-5
Clay minerals, montmorillonites	60	50	32	13
Qartz	7	3	-	-
Plagioclases	13	45	58	76
Calcite	15	-	-	-
Geothite	5	-	-	-
Amphiboles	-	2	-	-
Pyroxenes	-	-	10	11

Table 1. shows that montmorillonite and quartz are formed from plagioclases. In alkaline environment montmorillonite is formed, and kaolinite is formed in the acidic environment. In the weathering process, iron hydroxides are formed (such as goethite), which is not present in samples taken from the fresh rocks. The study shows that pyroxenes also disintegrate into iron hydroxides and calcite, which were not present in the fresh samples. On the basis of tests and analysis, it may be stated that melaphyre and its minerals, used for the top layer

have undergone oxidation and weathering processes that cause rapid disintegration of melaphyre and compactness of the motorway top layer.

4. SUMMARY AND CONCLUSIONS

The petrographic analysis shows that melaphyre is built from the minerals, which undergo weathering and oxidation under the influence of water, temperature, air and therefore it should not be used for top layers of roads and motorways.

In the melaphyre deposit of Borówno quarry, the intense and developed processes of weathering and oxidation take place, which is obvious, considering 21% of waste being dumped. This 21% of waste confirms the petrographic appearance of the rock in which there are minerals not resistant to weathering and oxidation processes. The rock is not weatherproof, and this is a reason of rapid disintegration of melaphyre grits contained in asphalt. The mineralogical analysis of the rock applied to asphalt mass makes it possible to explain the reason of rapid deterioration of the new motorway surface:

1. Rocks containing more than 45% of minerals that are not resistant to oxidation and weathering processes despite conforming to all standard requirements should not be used for the top layers of motorways.
2. This type of rock includes melaphyre and gabbros.

REFERENCES

1. Bolewski A., Manecki A.: *Mineralogia szczegółowa*, Wydawnictwo PAE, Warszawa 1993.
2. Bolewski A.: *Rozpoznawanie minerałów*, Wydawnictwa Geologiczne, Warszawa 1972.
3. Chrzan T.: *Autostrady i surowce do ich budowy*, Politechnika Wrocławska, Wrocław 1997.
4. Kancler M.: *Operat ewidencyjny zasobów złoża melafiru 'Borówno"* Kopalnia Melafiru „Borów" Wałbrzych, 2002.
5. Kancler M.: *Operat ewidencyjny zasobów złoża melafiru „Grzędy*" Kopalnia Melafiru „Grzędy" Wałbrzych, 2002.
6. Radziszewska-Jagosz E.: *Opracowanie petrograficzne skał ze złoża Grzędy*, Przedsiębiorstwo Geologiczne, Wrocław, 1982.
7. Ruttmar I.: *Degradacja grysów melafirowych na nawierzchni autostrady A-2* Raport nr. O2/A2/EW/SW/IR/05 Instytut Badań Technicznych TPA, Poznań, 2002.
8. Szuszkiewicz K., Król J.: *Dokumentacja geologiczna złoża melafiru Borówno*, Przedsiębiorstwo Geologiczne. Wrocław, 1988.

9. Strasser M.: *Badania petrograficzne melafiru Czarny Bór*, Laboratorium TP, sprawozdanie nr. 5, 7/02,Wiedeń, Austria, 2002.
10. Wysokowski A.: *Orzeczenie o jakości kruszywa.* Instytut Badawczy Dróg i Mostów, Filia Wrocław, 2001.
11. PN-B- 11112: 1996r. Kruszywa łamane do nawierzchni drogowych.
12. PN-B-A 1110 Surowce skalne lite dla produkcji i kruszyw łamanych, stosowanych w budownictwie drogowym.
13. PN-84 / B-067 14 / 22 Oznaczanie przyczepności do bituminów.
14. PN-EN 1097-2 Badanie mechanicznych właściwości kruszyw.
15. PN-S / 96025 Badanie mieszanek mineralnych i betonów asfaltowych.
16. PN-74 / S-96022 Badanie masy z betonu asfaltowego przy układaniu i wykonaniu.

SKŁAD MINERALNY SKAŁ MELAFIROWYCH A TRWAŁOŚĆ AUTOSTRADY

S t r e s z c z e n i e

W artykule poddano analizie skład mineralny melafiru użytego do budowy nawierzchni autostrady oraz omówiono trwałość poszczególnych minerałów pod kątem ich odporności na czynniki atmosferyczne i ogólnej wytrzymałości skały. W wyniku analizy stwierdzono, że zbadany melafir zawierał zbyt dużą ilość minerałów nieodpornych na czynniki atmosferyczne, co miało znaczący wpływ na eksploatację nawierzchni autostrady; powierzchniowa warstwa autostrady powstała pomiędzy czerwcem i listopadem 2001 r., a już na początku 2003 r. przystąpiono do jej remontu. Szybkie zużycie górnej warstwy autostrady wytłumaczono nadmierną zawartością tych minerałów, które pod wpływem czynników atmosferycznych stosunkowo szybko uległy przemianom.

CIVIL AND ENVIRONMENTAL ENGINEERING REPORTS

No. 10 2013

TWO-SCALE MODELLING OF REACTIVE POWDER CONCRETE. PART I: REPRESENTATIVE VOLUME ELEMENT AND SOLUTION OF THE CORRESPONDING BOUNDARY VALUE PROBLEM

Arkadiusz DENISIEWICZ*, Mieczysław KUCZMA
University of Zielona Góra,Department of Structural Mechanics,
Institute of Building Engineering
Szafrana st 1, 65-516 Zielona Góra, Poland

The article is the first part of a series concerned with the modelling of reactive powder concrete by using a numerical homogenization technique. This technique is a multi-scale modelling approach. Specifically, in this paper a two scale modelling concept was applied. A model of reactive powder concrete (RPC) is considered whose behaviour on the macro scale is described on the basis of the phenomena occurring in the microstructure of the material. This approach provides the ability to take into account some complex phenomena occurring in the microstructure and their influence on the macroscopic physical and mechanical properties of the material. The method does not require knowledge of the constitutive equation parameters at the macro level. These are determined implicitly for each load increment on the basis of numerical model of a representative volume element (RVE), which reflects the geometrical layout of particular material phases, their constitutive relations and mutual interactions. In this paper the linearly elastic behaviour of each constituent material is assumed within the small strain range. In solving the boundary value problems formulated on the RVE for RPC, the finite element method was utilized. A number of numerical test examples were solved which illustrate the influence of inhomogeneities on the overall response.

Keywords: multiscale modelling, RPC, micro-scale, macro-scale, RVE, computational homogenization, FEM

1. INTRODUCTION

Reactive powder concrete (RPC) is currently one of the most modern building materials created on the basis of cement [2]. RPC is included in the class of

* Corresponding author. E-mail: a.denisiewicz@ib.uz.zgora.pl

ultrahigh value concretes with the resistance to compression compared to steel. They are also classified as composites with cement matrix of ultrahigh resistance properties, and are often called the low-temperature ceramics. Thanks to the high resistance and ductility of RPC concrete, we can significantly reduce the weight and cross-sectional dimensions of structures built from it, while simultaneously the designer is given a larger freedom in providing the structure with the fine architectural expression and in overcoming significant spans. By virtue of the good physical and mechanical properties of reactive powder concrete, it finds a wide interest not only as the construction material, but also as the cladding material for houses and other buildings, and even as a material for furniture making (Fig.1).

Fig. 1. Examples of applications of reactive powder concrete [9]: a) elevation of the Bus Centre in Thiais France, b) roofing at the railway station in Calgary, c) a table

As an effective compuatational tool for determing and testing the material properties of RPC concrete and for the needs of the static-strength analysis of building and engineering constructions made of RPC, we have developed a two-scale model of reactive powder concrete. The modelling approach used is based upon the concept of representative volume element (RVE) and numerical homogenization and leads to a complex computational procedure, so we decided

to divide its presentation into two parts. In this first part, we shall discuss the fundamental features of the microstructure of reactive powder concrete (Sect. 3) and shall present the algorithm of numerical homogenization in the context of solving the boundary value problem formulated for the RVE of RPC. Here all the constituents of RVE are assumed to behave linearly elastic.

In Section 2 we skatch out the idea of computational homogenization. In Sections 3 and 4 the characteristic properties of the RPC microstructure and the corresponding RVE are outlined. The FEM approximation and the BVP posed on the RVE are defined in Sections 5 and 6, and numerical results in Section 7.

2. COMPUTATIONAL HOMOGENIZATION

The concept of computational homogenization is diagrammatically illustrated in Fig. 2. In the method of two-scale numerical homogenization, one determines the response of a material at the macro-scale through an analysis of the material's micro-structure. On the micro-scale level the distributions of micro-stresses and micro-strains are calculated, which via homogenization provide information on the distributions of overaged macroscopic quantities. The whole micro-analysis is carried out on the so-called representative volume element. This is the volume assigned to a material point that is representative for a small surrounding of the point. When the characteristic microscopic length is one order smaller than the characteristic macroscopic length, we can take into consideration only effects of the first order. In case of the RPC concrete, this condition is fulfilled. We can assume that the characteristic dimension in micro-scale is that of the fraction of ground quartz of 0.2 mm. While in the macro-scale it is the dimension of the cross-section of the construction element, e.g. 0.2 x 0.2 m. The numerical homogenization procedure is multistage and computationally complicated [3,4].

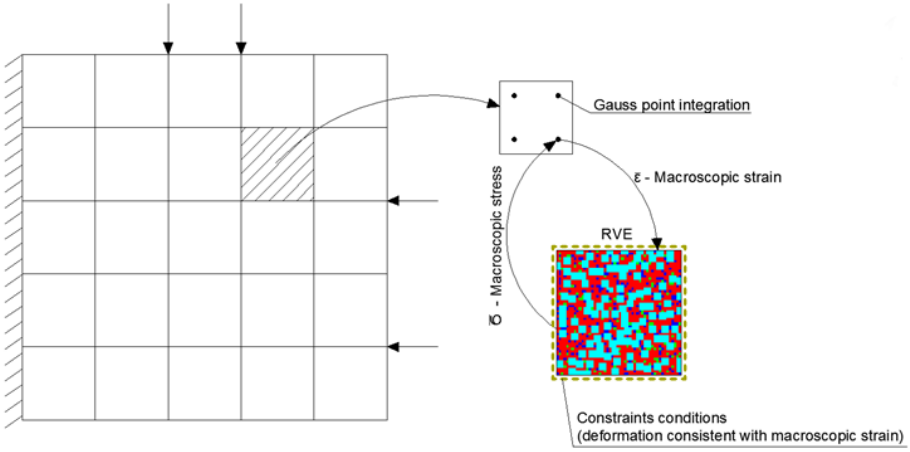

Fig. 2. Idea of two-scale numerical homogenization

3. MICROSTRUCTURE OF REACTIVE POWDER CONCRETE

Reactive powder concrete is invented with the aim of eliminating the faults of the traditional concrete, which is especially achieved by minimizing its porosity to the level of about 4%, by:

- using aggregates with granulation enabling the maximal packaging of components,
- potentially maximal reduction of the water-cement index, with simultaneous application of super-plasticizers,
- applying treatments of pressing in the initial period of the adhesive bonding process.

The improvement of physical and mechanical properties is also obtained by modifying the microstructure of the adhesive matrix by using the proper heat treatment and thanks to using fillers of very small grains, e.g., ground quartz and silica dust. Contrary to the traditional concrete, where the aggregate is the reinforcing element but usually a chemically passive component, the micro-aggregate in RPC concrete, which are usually quartz powders, exhibits the pozzolanic activity. Two characteristic features of the RPC microstructure should be mentioned [6]:

- very compact microstructure of the C-S-H phase
- very good adhesion of the C-S-H phase to mineral inclusions in the form of powder grains and quartz sand and fibers

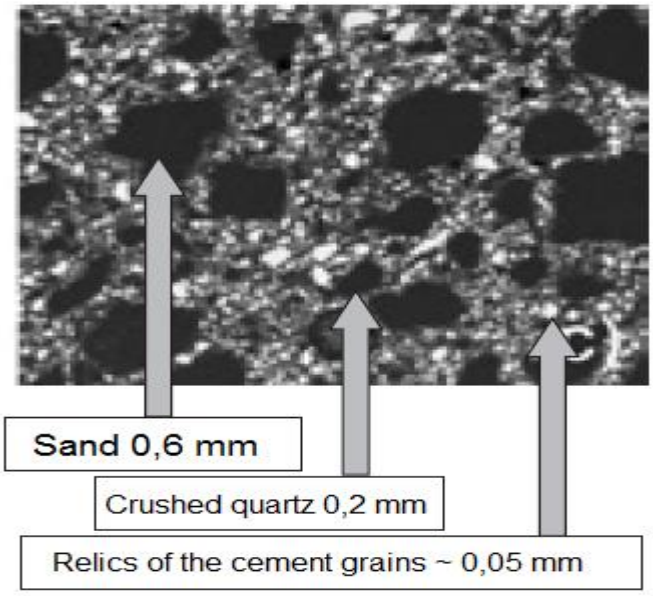

Fig. 3. Microstructure of reavtive powder concrete zoom 200x [6]

4. REPRESENTATIVE VOLUME ELEMENT

In order to model the microstructure of RPC concrete with the composition as in Table 1, in the first approximation step a two-dimensional representative volume element (RVE) was assumed. RVE is modelled with the help of the finite element method. In the calculations we have divided a square RVE into 2500 finite elements, each with the size of 0.2 x 0.2 mm, i.e. each side of RVE of the length of 10 mm is split into 50 equal finite intervals. A representative composition of reactive powder concrete is listed in Tab. 1.

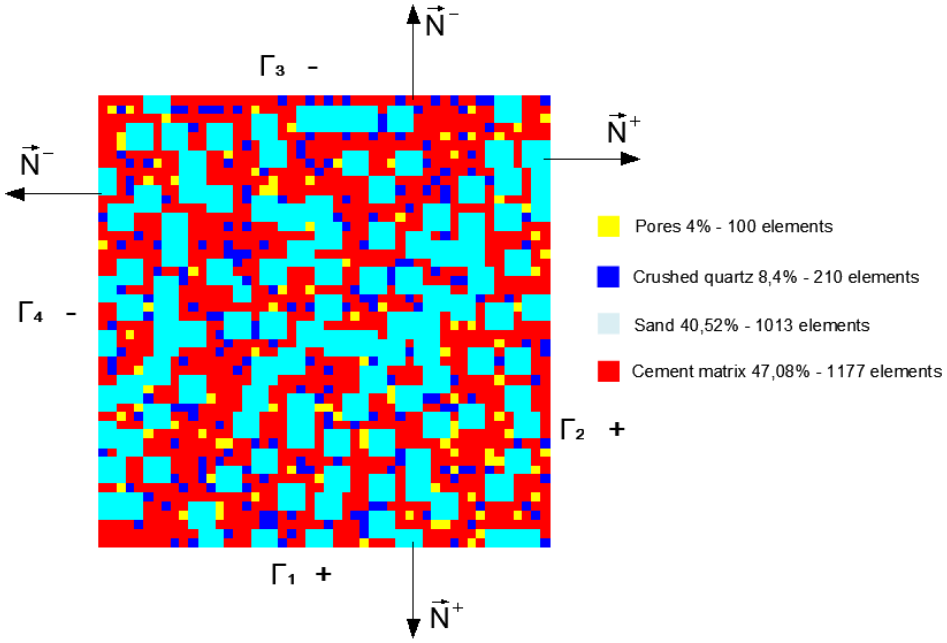

Fig. 4. Representative Volume Element (2D): cement matrix (red colour), sand of grain size to 0.6 mm (cyan colour), crushed quartz of grain size to 0.2 mm (blue colour), pores (yellow green colour)

Table 1. Representative composition of RPC concrete

Component	Volume [kg/m3]	Mass percentage [%]
Cement	705	28,20
Silica fume	230	9,20
Crushed quartz	210	8,40
Sand	1013	40,52
Superplasticizer	17	0,68
Steel fibers	140	5,60
Water	185	7,40

Because of the random character of the arrangement of concrete's components, a stochastic approach to generating the RVE structure was applied (Fig. 4). Building the structure consists of the random selection of an element (from the 50x50 grid) and then also of the random assignment of a component (pores, crushed quartz, sand, cement matrix) to the selected position. The basic size of the RVE component was assumed to be equal of 0.2 mm. In case of drawing the sand component, the process of arranging elements of the grid takes place according to the scheme shown in Fig. 5, which takes into account the maximal size of the grain of 0.6 mm. The extreme locations correspond to the smaller grains of the same component.

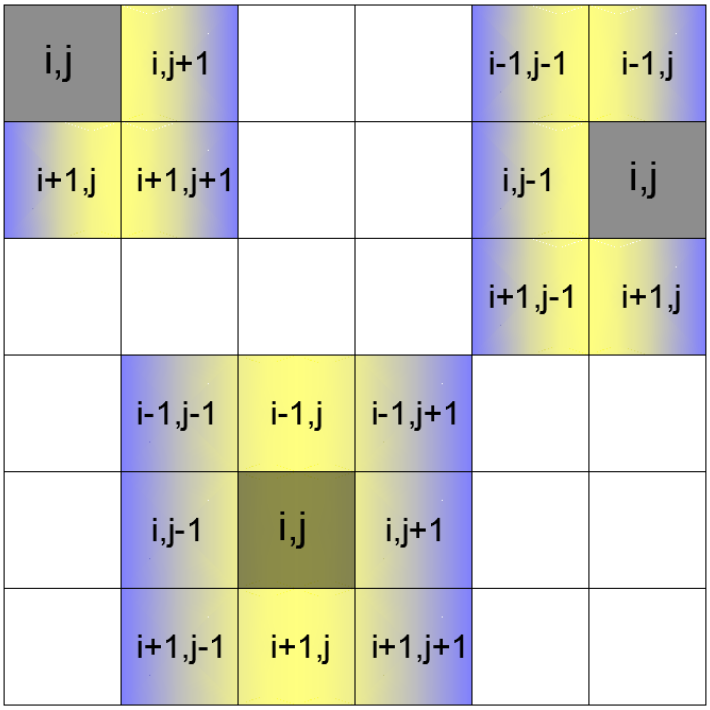

Fig. 5. Principle of generating a RVE structure

For generating the total pseudo-random integer number γ_{n+1} from the intervals of <1,4> (number of component) and of <1,50> (position of component) there was applied a generator

$$\gamma_{n+1} = \text{int}\,(x + (y - x + 1) \cdot X_{n+1}) \tag{4.1}$$

where x is the left endpoint of the range of drawing and y is the right endpoint of the range of drawing, and

$$
\begin{aligned}
&X_{n+1} = (aX_n + b) \bmod c \\
&a = 7^5 = 16807 \quad b = 0 \\
&c = 2^{31} - 1 = 2147483647
\end{aligned}
\tag{4.2}
$$

It is the affine generator of pseudo-random numbers from the range of <0,1>. The whole procedure of building the structure of the represented volume element is performed by a computer programme written in the FORTRAN 90 language in which the libraries [7,8] were used.

5. FINITE ELEMENT METHOD IN COMPUTATIONAL HOMOGENIZATION

For solving the boundary value problems at the macro and micro scales, the classical displacement version of the finite element method was applied. The 2D domain under consideration Ω was discretized by means of the four node finite element Q4 with two degrees of freedom at each node. The horizontal $u = u(\xi,\eta)$ and vertical $v = v(\xi,\eta)$ components of displacement field $\mathbf{u}$ are approximated with the bilinear shape functions

$$
\begin{aligned}
&N_1(\xi,\eta) = \frac{1}{4}(1-\xi-\eta+\xi\eta) \quad N_2(\xi,\eta) = \frac{1}{4}(1+\xi-\eta-\xi\eta) \\
&N_3(\xi,\eta) = \frac{1}{4}(1+\xi+\eta+\xi\eta) \quad N_4(\xi,\eta) = \frac{1}{4}(1-\xi+\eta-\xi\eta)
\end{aligned}
\tag{5.1}
$$

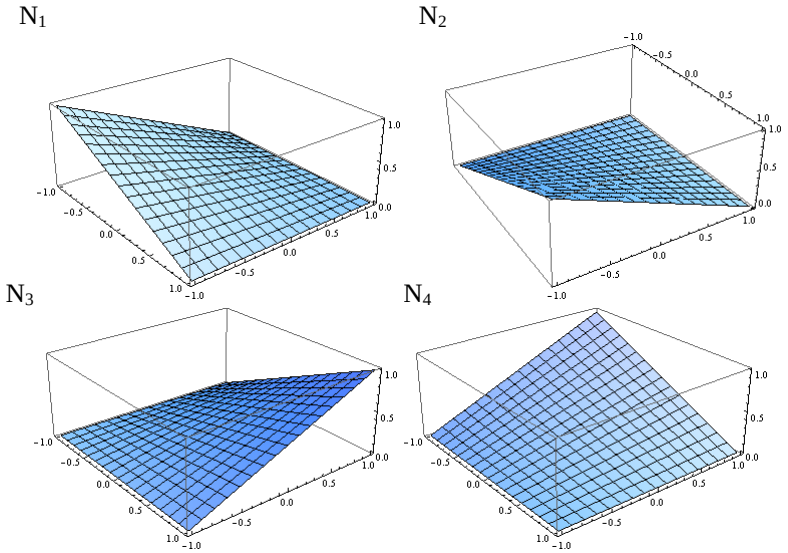

Fig. 6. Bilinear shape functions

The relation between the components of deformation within a finite element and its nodal displacements is described by the formula

$$\boldsymbol{\varepsilon} = \begin{bmatrix} \varepsilon_{11} \\ \varepsilon_{22} \\ 2\varepsilon_{12} \end{bmatrix} = \partial \mathbf{N}\mathbf{q} = \mathbf{B}\mathbf{q} \tag{5.2}$$

in which ∂ is the matrix operator of partial derivatives, $\mathbf{B}$ is the matrix of deformation compatibility consisting of the derivatives of shape functions N_i, and $\mathbf{q}^T = \left[u_1, v_1, u_2, v_2, u_3, v_3, u_4, v_4\right]$ is a vector of nodal displacements of the finite element. The displacement field within an element $\Omega_e \subset \Omega$ is expressed as

$$\mathbf{u} = \mathbf{N}\mathbf{q} \tag{5.3}$$

wherein

$$\mathbf{N} = \begin{bmatrix} N_1 & 0 & N_2 & 0 & N_3 & 0 & N_4 & 0 \\ 0 & N_1 & 0 & N_2 & 0 & N_3 & 0 & N_4 \end{bmatrix} \tag{5.4}$$

In modelling the components of microstructure, the linear elastic model of isotropic material was applied. For the isotropic elastic material being in the plain state of stress, the element stiffness matrix is defined by the formula

$$\mathbf{K}^e = \int_{\Omega_e} \mathbf{B}^T \mathbf{D}_i \mathbf{B} d\Omega \tag{5.5}$$

where

$$\mathbf{D}_i = \frac{E_i}{1-\nu_i^2} \begin{bmatrix} 1 & \nu_i & 0 \\ \nu_i & 1 & 0 \\ 0 & 0 & \dfrac{1-\nu_i}{2} \end{bmatrix} \tag{5.6}$$

and i = 1,2,3 is the number of the particular component of microstructure assigned to the finite element Ω_e.

The element stiffness matrix $\overline{\mathbf{D}}_E$ of the material on the macro scale is calculated by Eq. (5.5), in which a matrix $\overline{\mathbf{D}}$ is used instead of $\mathbf{D}_i$. The elasticity matrix $\overline{\mathbf{D}}$ of the homogenized material on the macro scale are determined by solving the boundary value problem on the micro scale for imposed components

of macro strain $\bar{\boldsymbol{\varepsilon}}$. A finite element formulation of the boundary value problem on the micro scale is considered next.

6. BOUNDARY VALUE PROBLEM

The boundary value problem of mechanics for the specified RVE after the FEM discretization is solved by the minimization of the elastic strain energy function with additional constraints

$$\min_{\mathbf{u}} \varphi(\mathbf{u}) = \frac{1}{2}\mathbf{u}^{\mathrm{T}}\mathbf{K}\mathbf{u} - \mathbf{u}^{\mathrm{T}}\mathbf{f} \qquad s.t. \quad \mathbf{C}\mathbf{u} - \mathbf{g} = \mathbf{0} \tag{6.1}$$

The minimization problem (6.1) can be solved by using the Lagrange multiplier method. However, due to a large computational complexity of the numerical homogenization method the approach based on Lagrange multipliers is too time consuming. Hence we follow an alternative approach [1, 3] that brings down to the solution of the equations:

$$\tilde{\mathbf{K}}\mathbf{u} = \tilde{\mathbf{F}} \tag{6.2}$$

where

$$\tilde{\mathbf{K}} = \mathop{\mathrm{A}}_{e}\left[(\mathbf{C}_u^e)^T\mathbf{C}_u^e + (\mathbf{Q}_u^e)^T\mathbf{K}^e\mathbf{Q}_u^e\right] \tag{6.3}$$

$$\tilde{\mathbf{F}} = \mathop{\mathrm{A}}_{e}\left[\mathbf{D}_u^e\bar{\boldsymbol{\varepsilon}}[(\mathbf{C}_u^e)^T - (\mathbf{Q}_u^e)^T\mathbf{K}^e\mathbf{R}_u^e]\right] \tag{6.4}$$

$$\mathbf{Q}_u^e = \mathbf{I} - \mathbf{R}_u^e\mathbf{C}_u^e \tag{6.5}$$

$$\mathbf{R}_u^e = (\mathbf{C}_u^e)^T[\mathbf{C}_u^e(\mathbf{C}_u^e)^T]^{-1} \tag{6.6}$$

In Eqns. (6.3) and (6.4) the symbol $\mathop{\mathrm{A}}_{e}$ means the finite element aggregation of matrices. To enforce deformations of RVE in accordance with the macro-deformations $\bar{\boldsymbol{\varepsilon}}$ there were applied the displacement boundary conditions of the first type

$$\mathbf{C}_u^e\mathbf{u} = \mathbf{D}_u^e\bar{\boldsymbol{\varepsilon}} = \mathbf{g}_u^e \tag{6.7}$$

where

$$\mathbf{C}_u^e = \int_{\Gamma}\mathbf{H}_u\mathbf{N}^T\mathbf{N}d\Gamma \tag{6.8}$$

$$\mathbf{D}_u^e = \int_\Gamma \mathbf{H}_u \mathbf{N}^T \mathbf{X} d\Gamma \tag{6.9}$$

The matrices $\mathbf{C}_u^e$, $\mathbf{D}_u^e$ and others involved in Eqns. (6.8) and (6.9) are given in explicit form in the Appendix. The master finite element $\Omega_e = (-1,1)\times(-1,1)$ together with definition of its boundary Γ used in analysis is presented in Fig. 7, whereas the way of integrating along the boundary in Eqn. (6.10).

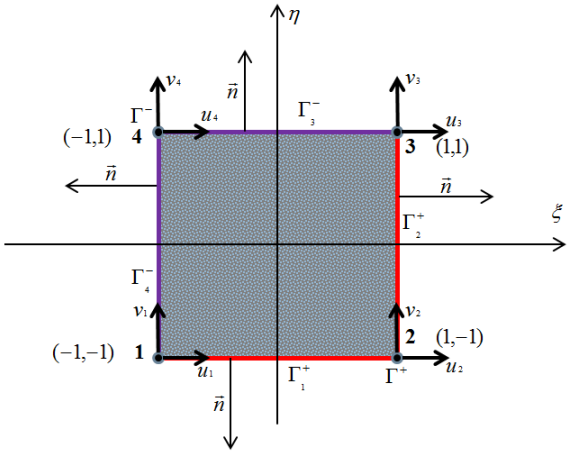

Fig. 7. Master finite element Q4

$$\begin{aligned}\int_\Gamma (\bullet)(\xi,\eta)d\Gamma = &\int_{-1}^{1} (\bullet)(\xi,-1)d\xi + \int_{-1}^{1} (\bullet)(1,\eta)d\eta \\ &+ \int_{-1}^{1} (\bullet)(\xi,1)d\xi + \int_{-1}^{1} (\bullet)(-1,\eta)d\eta\end{aligned} \tag{6.10}$$

7. NUMERICAL EXAMPLES

In this section we present the results of numerical tests we obtained as the solution of the boundary value problem on micro-scale for the RVE shown in Fig. 14. However, let us begin with tests checking the response of homogeneous isotropic material to some imposed macro-strains. The forms of deformation (lighter line) of one homogeneous element due to the enforced macro-deformations $\overline{\boldsymbol{\varepsilon}}$, with

values given therein, are displayed in Fig. 8. Test results for a homogenous isotropic material and 5x5 finite element mesh are shown in Figs. 9 – 12 (deformed grids in darker line). As can be seen the obtained results confirm the expected deformation modes of RVE. Figure 13 shows the distribution of micro-stresses induced by sheering $\bar{\boldsymbol{\varepsilon}}^{\mathrm{T}} = [0 \quad 0 \quad 1]$ for three microstructures of two-component material with isotropic components of parameters E_1=20 GPa, ν_1=0.4, E_2=200 GPa, ν_2=0.4, and the 10x10 grid RVE.

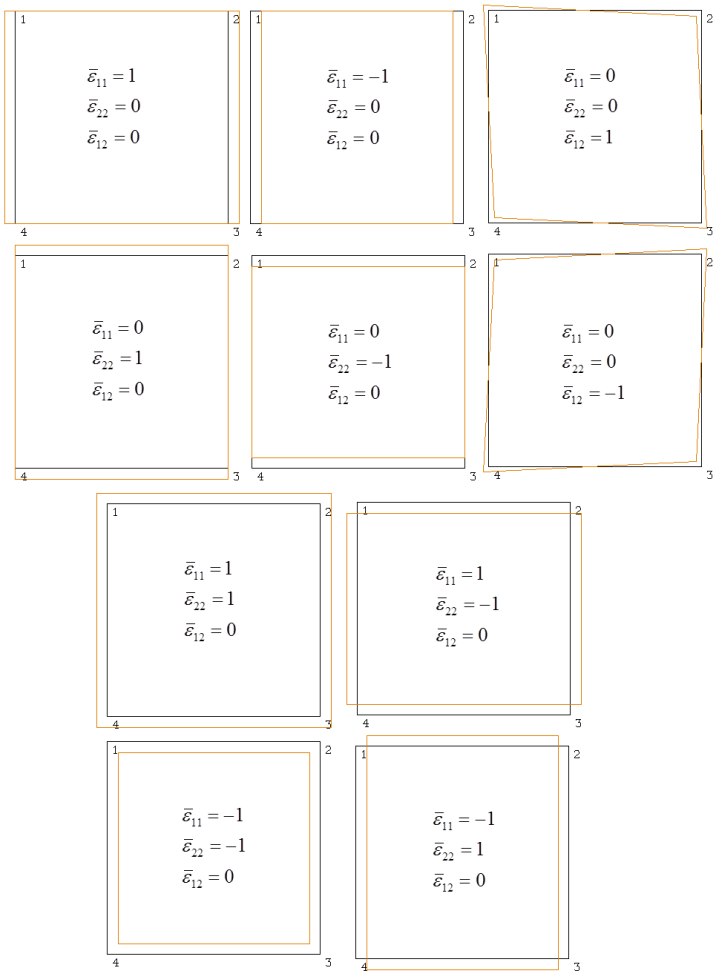

Fig. 8. Deformation tests on single-element homogeneous cell

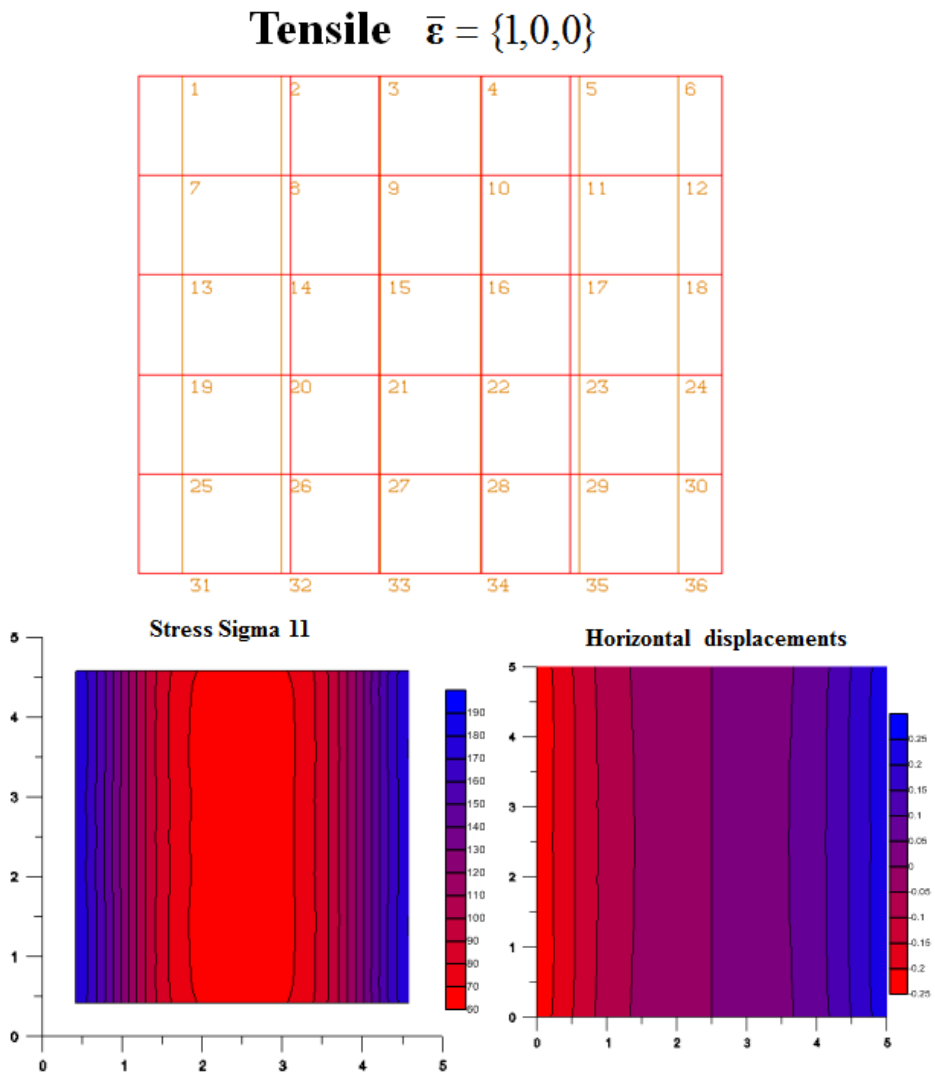

Fig. 9. Tensile test for a homogenous material, deformed finite element mesh in dark line

Finally, Fig. 14 shows the distribution of stresses in a randomly generated microstructure of RPC composed of cement matrix (47.08%), crushed quartz (8.4%), sand (40.52%) and pores (4%). The used values of material parameters: cement matrix E=30 GPa, ν=0.16, crushed quartz and sand E=75 GPa, ν=0.3. The RVE was divided into 50x50 finite elements. The macro-strain imposed on the boundary of RVE was $\bar{\varepsilon} = \{-1,0.2,0\}$.

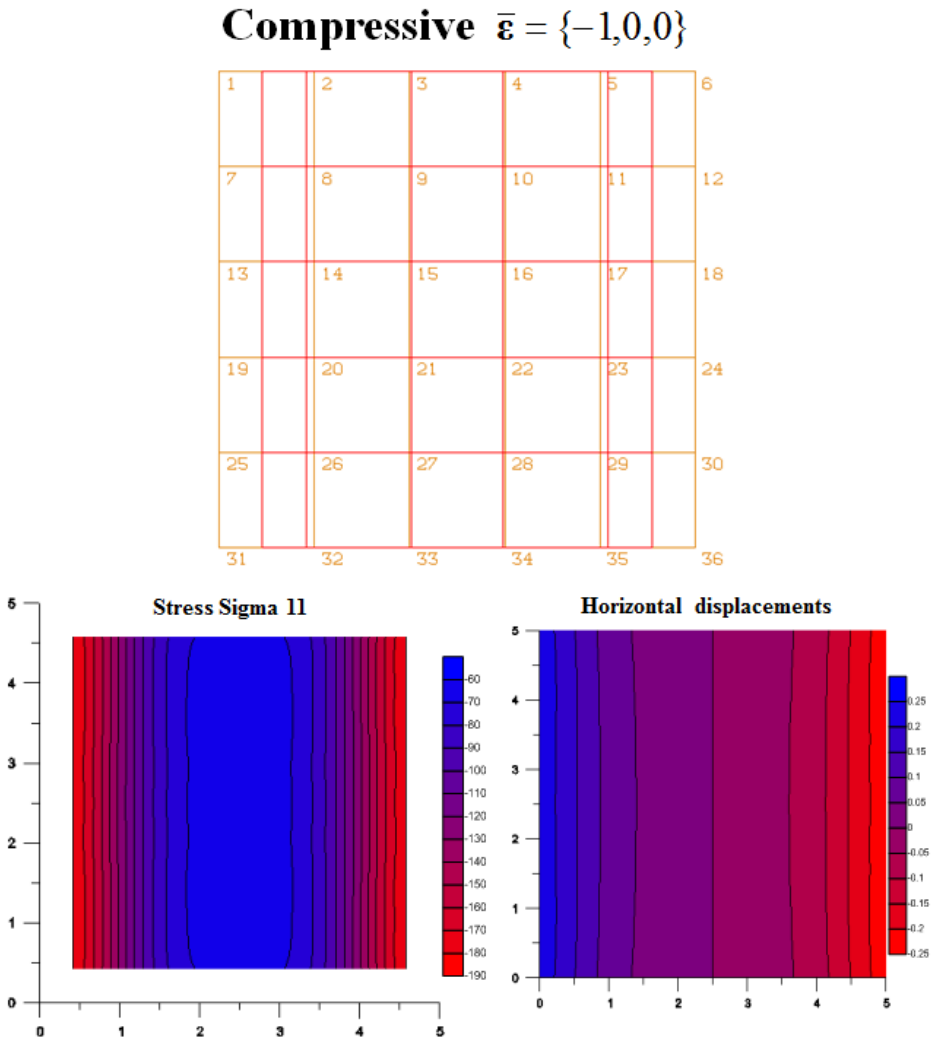

Fig. 10. Compressive test for a homogenous material, deformed finite element mesh in dark line

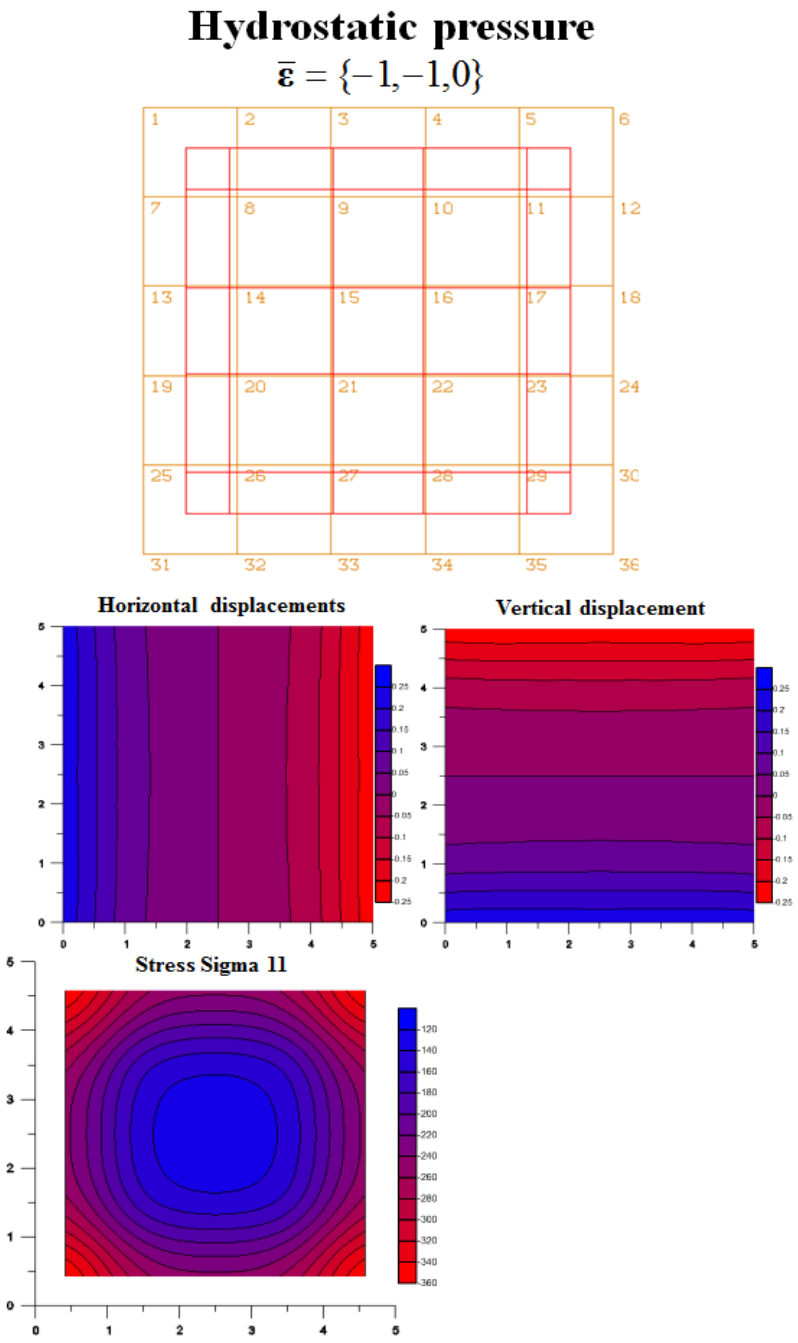

Fig. 11. Hydrostatic pressure test for a homogenous material, deformed finite element mesh in dark line

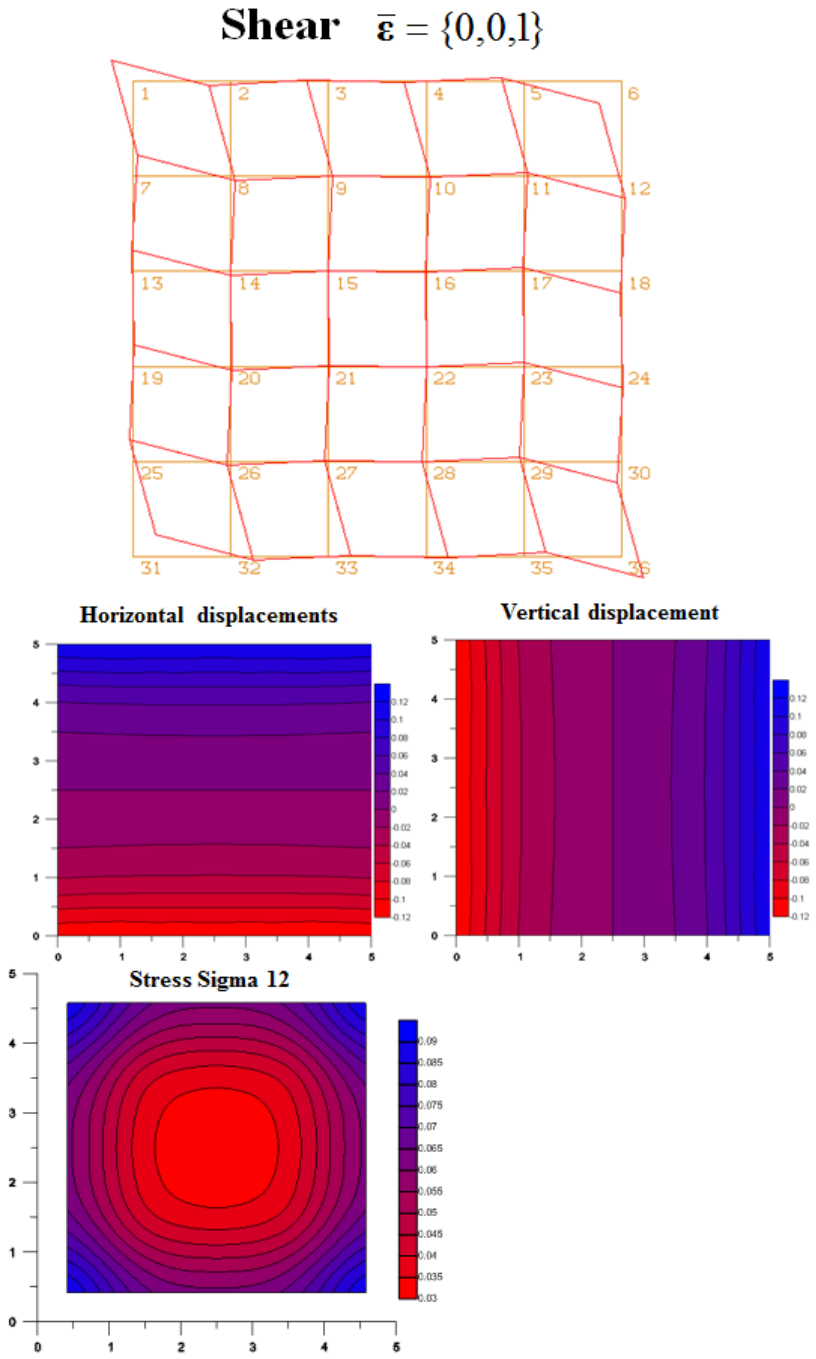

Fig. 12. Shear test for a homogenous material

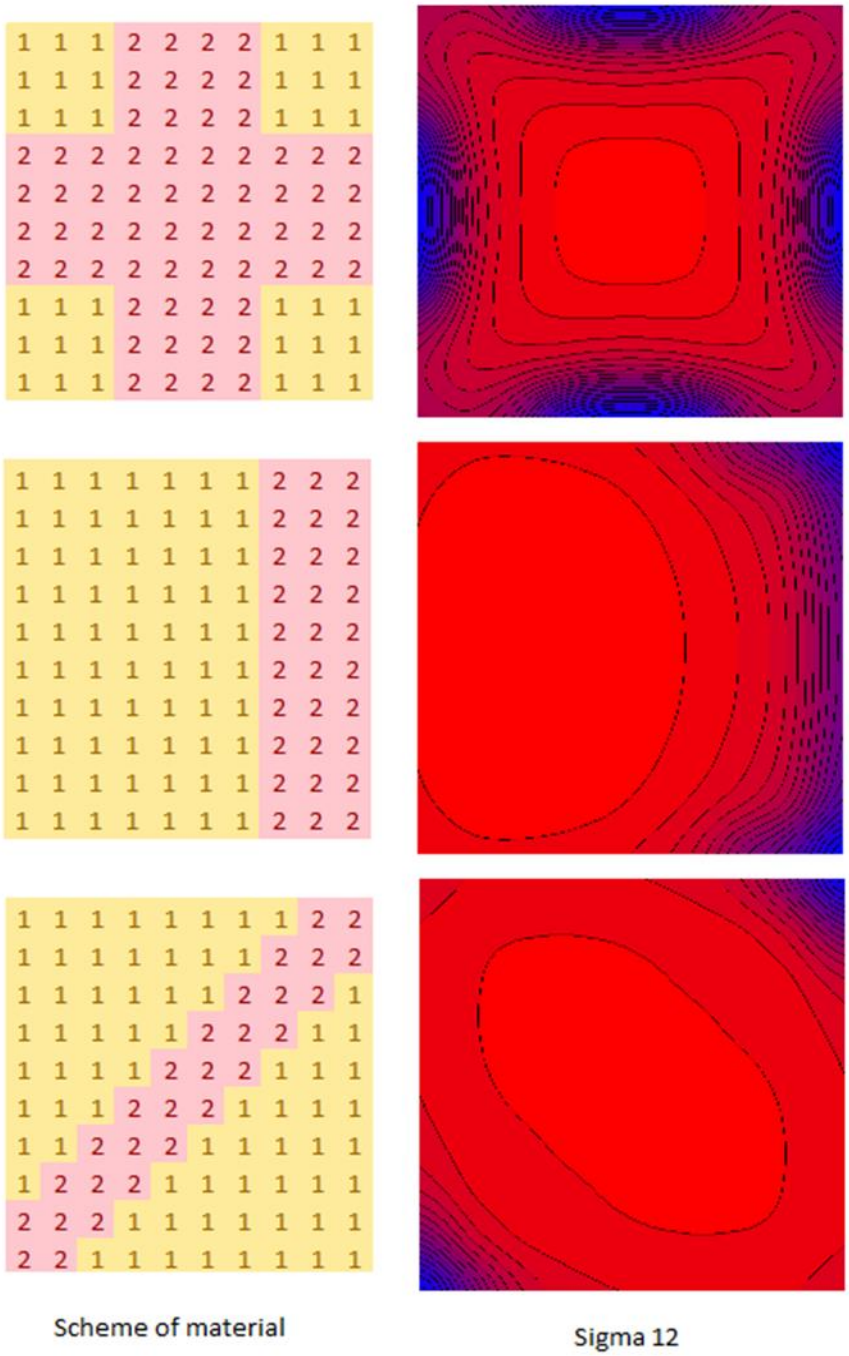

Fig. 13. Shear test for a heterogeneous material

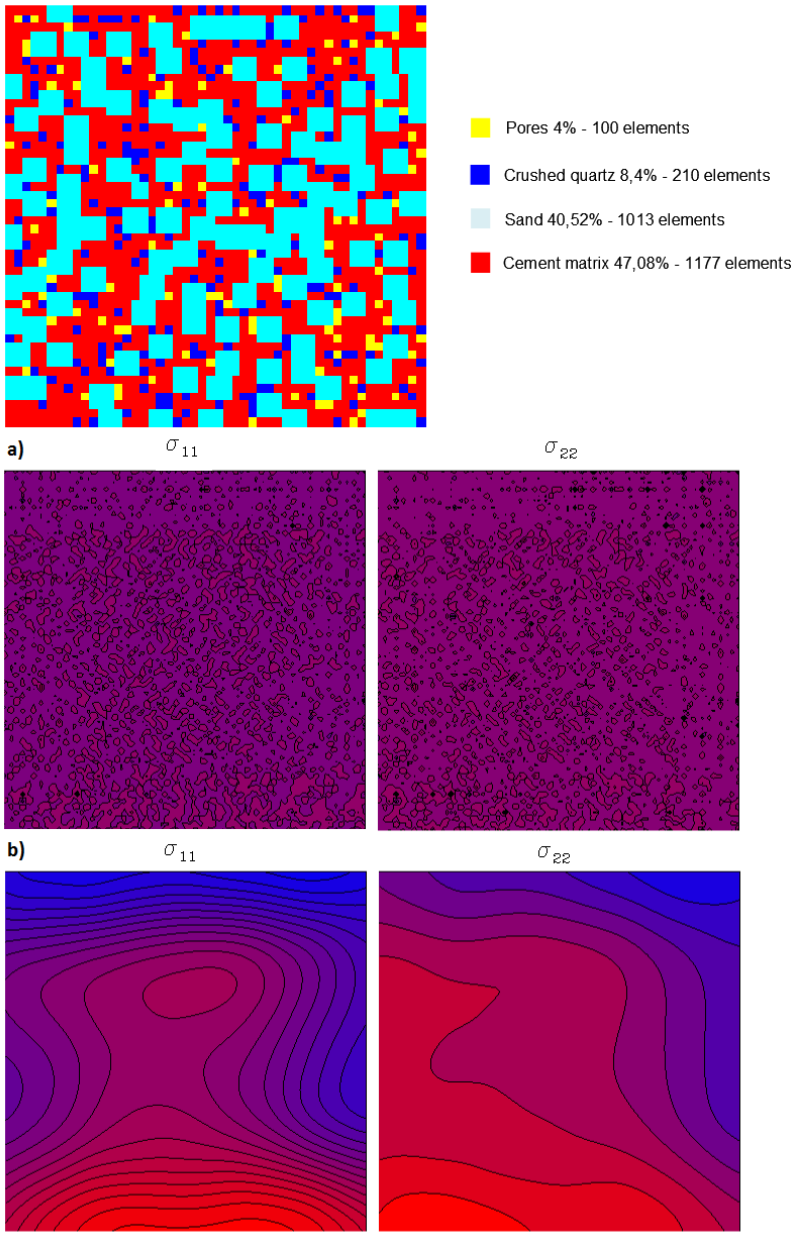

Fig. 14. Microstructure of the RVE, a) micro-stress distribution and b) smoothed micro-stress distribution induced by macro-strain $\bar{\boldsymbol{\varepsilon}} = \{-1{,}0.2{,}0\}$

8. CLOSING REMARK

A two-scale numerical approach to the modelling of reactive powder concrete (RPC) was presented, in which the layout of microstructure (2D case) is generated randomly for a given composition of RPC. The boundary value problem on representative volume element (RVE) was solved for the case of imposed (given) macro-strains on the boundary of RVE. A computer program was developed and herein results of some numerical tests are included. In the next part of the work, results of a fully two-scale analysis will be presented as well as results of our own laboratory tests curried out on cubes and beams made of RPC.

ACKNOWLEDGEMENTS

The first author is a scholar within Sub-measure 8.2.2 Regional Innovation Strategies, Measure 8.2 Transfer of knowledge, Priority VIII Regional human resources for the economy Human Capital Operational Programme co-financed by European Social Fund and state budget.

REFERENCES

1. Ainsworth M.: Essential boundary conditions and multi-point constraints in finite element analysis, *Comput. Methods Appl. Mech. Engrg*. 190 (2001) 6323 - 6339.
2. Jasiczak J., Wdowska A., Rudnicki T.: *Betony ultrawysokowartościowe. Właściwości, technologie, zastosowania*, Stowarzyszenie Producentów Cementu, Kraków 2008.
3. Kaczmarczyk Ł.: *Numeryczna analiza wybranych problemów mechaniki ośrodków niejednorodnych*, PhD thesis, Cracow University of Technology 2006.
4. Kouznetsova V.G., Geers M.G.D., Brekelmans W.A.M.: Multi-scale second-order computational homogenization of multi-phase materials: a nested finite element solution strategy, *Comput. Methods Appl. Mech. Engrg*. 193 (2004) 5525 - 5550.
5. Miehe C.: Computational micro-to-macro transitions for discretized micro-structures of heterogeneous materials at finite strains based on the minimization of averaged incremental energy, *Comput. Methods Appl. Mech. Engrg*. 192 (2003) 559 - 591.
6. Zdeb T., Śliwiński J.: Beton z proszków reaktywnych – właściwości mechaniczne i mikrostruktura, *Budownictwo Technologie Architektura* 51 (2010) 51 - 55.
7. DISLIN Scientific Plotting Software http://www.mps.mpg.de/dislin/
8. SLATEC A Mathematical Library http://www.netlib.org/slatec/index.html
9. http://www.ductal-lafarge.com/

DWUSKALOWY MODEL BETONU Z PROSZKÓW REAKTYWNYCH.
CZĘŚĆ I: REPREZENTATYWNY ELEMENT OBJĘTOŚCIOWY (RVE)
I ROZWIĄZANIE ZAGADNIENIA BRZEGOWEGO NA RVE

S t r e s z c z e n i e

Artykuł jest pierwszą częścią pracy dotyczącej modelowaniu betonów z proszków reaktywnych przy zastosowaniu numerycznej homogenizacji. Technika ta jest podejściem wielkoskalowego modelowania. W tym konkretnym przypadku modelowania dwuskalowego. Zachowanie modelu betonu typu RPC w skali makro (skala punktu materialnego, poziom opisu fenomenologicznego) opisywane jest na podstawie zjawisk zachodzących w mikrostrukturze materiału (mikroskala). Takie podejście daje możliwość uwzględnienia szeregu zjawisk zachodzących w mikrostrukturze na właściwości fizyczne i mechaniczne materiału. Na przykład wpływ mikropęknięć na wytrzymałość betonu. Nie bez znaczenia jest fakt, że metoda nie wymaga znajomości równań konstytutywnych w skali makro, związki te są wyznaczane w sposób niejawny dla każdego przyrostu obciążenia na podstawie numerycznego modelu reprezentatywnego elementu objętościowego RVE. Do wyznaczenia niejawnych związków fizycznych w makroskali niezbędna jest znajomość geometrii mikrostruktury, równań konstytutywnych na poziomie skali mikro oraz ich parametrów. W tej pierwszej części pracy ograniczono się do sformułowania i rozwiązania zagadnienia brzegowego na poziomie mikroskali dla zadanych makronaprężeń na brzegu RVE. Opracowano własny program komputerowy, który generuje w sposób losowy mikrostrukturę RPC i rozwiązuje problem brzegowy zdyskretyzowany metodą elementów skończonych. Praca zawiera wyniki obliczeń zadań testowych.

APPENDIX

Matrix $\mathbf{C}_u^e$, $\mathbf{D}_u^e$ for displacement boundary conditions where x_i and y_i i = 1,2,3,4 are coordinates of nodes in the global coordinate system.

$$\mathbf{H}_u = \operatorname{diag}\begin{bmatrix}1 & 1 & 1 & 1 & 1 & 1 & 1 & 1\end{bmatrix} \qquad \mathbf{X} = \frac{1}{2}\begin{bmatrix}2\xi & 0 & \eta \\ 0 & 2\eta & \xi\end{bmatrix}$$

$$\mathbf{J} = \begin{bmatrix} \frac{1}{4}\left[(\eta-1)x_1 - (\eta-1)x_2 + (\eta+1)(x_3 - x_4)\right] & \frac{1}{4}\left[(\eta-1)y_1 - (\eta-1)y_2 + (\eta+1)(y_3 - y_4)\right] \\ \frac{1}{4}\left[(\xi-1)x_1 - (\xi+1)x_2 + \xi x_3 - \xi x_4 + x_3 + x_4\right] & \frac{1}{4}\left[(\xi-1)y_1 - (\xi+1)y_2 + \xi y_3 - \xi y_4 + y_3 + y_4\right] \end{bmatrix}$$

$$\mathbf{C}_u^e = \int_\Gamma \mathbf{H}_u \mathbf{N}^{\mathrm{T}} \mathbf{N} \cdot \det|\mathbf{J}| d\Gamma = \int_{-1}^{1} \mathbf{H}_u \mathbf{N}^{\mathrm{T}}(\xi,-1)\mathbf{N}(\xi,-1) \cdot \det|\mathbf{J}| d\xi +$$
$$\int_{-1}^{1} \mathbf{H}_u \mathbf{N}^{\mathrm{T}}(1,\eta)\mathbf{N}(1,\eta) \cdot \det|\mathbf{J}| d\eta + \int_{-1}^{1} \mathbf{H}_u \mathbf{N}^{\mathrm{T}}(\xi,1)\mathbf{N}(\xi,1) \cdot \det|\mathbf{J}| d\xi +$$
$$\int_{-1}^{1} \mathbf{H}_u \mathbf{N}^{\mathrm{T}}(-1,\eta)\mathbf{N}(-1,\eta) \cdot \det|\mathbf{J}| d\eta$$

$$\mathbf{C}_u^e = \begin{bmatrix} C_1 & 0 & C_2 & 0 & 0 & 0 & C_3 & 0 \\ & C_1 & 0 & C_2 & 0 & 0 & 0 & C_3 \\ & & C_4 & 0 & C_5 & 0 & 0 & 0 \\ & & & C_4 & 0 & C_5 & 0 & 0 \\ & & & & C_6 & 0 & C_7 & 0 \\ & & \textit{sym.} & & & C_6 & 0 & C_7 \\ & & & & & & C_8 & 0 \\ & & & & & & & C_8 \end{bmatrix}$$

$$C_1 = \frac{1}{24}\left(x_4(7y_1 - 6y_2 - y_3) + (7x_1 - x_3)(y_2 - y_4) + x_2(-7y_1 + y_3 + 6y_4)\right)$$

$$C_2 = \frac{1}{24}(x_4y_1 + x_3(y_1 - y_2) + 2x_1y_2 - x_4y_2 - x_1y_3 - x_1y_4 + x_2(-2y_1 + y_3 + y_4))$$

$$C_3 = \frac{1}{24}(2x_4y_1 + x_1y_2 - x_4y_2 + x_1y_3 - x_4y_3 - 2x_1y_4 + x_2(y_4 - y_1) + x_3(y_4 - y_1))$$

$$C_4 = \frac{1}{24}(x_4y_1 + 7x_1y_2 - 7x_2(y_1 - y_3) - 6x_1y_3 - x_4y_3 - x_1y_4 + x_3(6y_1 - 7y_2 + y_4))$$

$$C_5 = \frac{1}{24}((x_1 + x_4)(y_2 - y_3) + x_3(y_1 - 2y_2 + y_4) - x_2(y_1 - 2y_3 + y_4))$$

$$C_6 = \frac{1}{24}(x_4(y_1 + 6y_2 - 7y_3) + (x_1 - 7x_3)(y_2 - y_4) - x_2(y_1 - 7y_3 + 6y_4))$$

$$C_7 = \frac{1}{24}(x_4(y_1 + y_2 - 2y_3) + (x_1 + x_2)(y_3 - y_4) - x_3(y_1 + y_2 - 2y_4))$$

$$C_8 = \frac{1}{24}(7x_4y_1 + x_1y_2 + 6x_1y_3 - 7x_4y_3 + x_2(y_3 - y_1) - 7x_1y_4 - x_3(6y_1 + y_2 - 7y_4))$$

$$\mathbf{D}_u^e = \int_\Gamma \mathbf{H}_u \mathbf{N}^T \mathbf{X} \cdot \det|\mathbf{J}| d\Gamma = \int_{-1}^{1} \mathbf{H}_u \mathbf{N}^T(\xi,-1)\mathbf{X}(\xi,-1) \cdot \det|\mathbf{J}| d\xi +$$
$$\int_{-1}^{1} \mathbf{H}_u \mathbf{N}^T(1,\eta)\mathbf{X}(1,\eta) \cdot \det|\mathbf{J}| d\eta + \int_{-1}^{1} \mathbf{H}_u \mathbf{N}^T(\xi,1)\mathbf{X}(\xi,1) \cdot \det|\mathbf{J}| d\xi +$$
$$\int_{-1}^{1} \mathbf{H}_u \mathbf{N}^T(-1,\eta)\mathbf{X}(-1,\eta) \cdot \det|\mathbf{J}| d\eta$$

$$\mathbf{D}_u^e = \begin{bmatrix} D_1 & 0 & D_5 \\ 0 & D_5 & D_1 \\ D_2 & 0 & D_6 \\ 0 & D_6 & D_2 \\ D_3 & 0 & D_7 \\ 0 & D_7 & D_3 \\ D_4 & 0 & D_8 \\ 0 & D_8 & D_4 \end{bmatrix}$$

$$D_1 = \frac{1}{12}(-4x_4y_1 - 3x_1y_2 + 3x_4y_2 - x_1y_3 + x_4y_3 + 3x_2(y_1 - y_4) + x_3(y_1 - y_4) + 4x_1y_4)$$

$$D_2 = \frac{1}{12}((3x_1 + x_4)(y_2 - y_3) + x_3(3y_1 - 4y_2 + y_4) - x_2(3y_1 - 4y_3 + y_4))$$

$$D_3 = \frac{1}{12}((x_1 + 3x_4)(y_2 - y_3) + x_3(y_1 - 4y_2 + 3y_4) - x_2(y_1 - 4y_3 + 3y_4))$$

$$D_4 = \frac{1}{12}(-4x_4y_1 - x_1y_2 + x_4y_2 - 3x_1y_3 + 3x_4y_3 + x_2(y_1 - y_4) + 3x_3(y_1 - y_4) + 4x_1y_4)$$

$$D_5 = \frac{1}{12}\big(-3x_4y_1 - 4x_1y_2 + 3x_4y_2 + x_3(y_2 - y_1) + x_1y_3 + 3x_1y_4 + x_2(4y_1 - y_3 - 3y_4)\big)$$

$$D_6 = \frac{1}{12}(-x_4y_1 - 3x_3(y_1 - y_2) - 4x_1y_2 + x_4y_2 + 3x_1y_3 + x_2(4y_1 - 3y_3 - y_4) + x_1y_4)$$

$$D_7 = \frac{1}{12}\big(x_4(y_1 + 3y_2 - 4y_3) + (x_1 + 3x_2)(y_3 - y_4) - x_3(y_1 + 3y_2 - 4y_4)\big)$$

$$D_8 = \frac{1}{12}\big(x_4(3y_1 + y_2 - 4y_3) + (3x_1 + x_2)(y_3 - y_4) - x_3(3y_1 + y_2 - 4y_4)\big)$$

CIVIL AND ENVIRONMENTAL ENGINEERING REPORTS

No. 10 2013

INCINERATION OF TANNERY WASTE IN A TUNNEL FURNACE SYSTEM

Stanisław FAMIELEC*, Krystyna WIECZOREK-CIUROWA
Politechnika Krakowska, Wydział Inżynierii i Technologii Chemicznej

The leather industry generates significant amounts of waste for which there is not comprehensive treatment method. Such waste is mainly landfilled, which is an environmental threat. However, solid tannery waste could be incinerated since it contains organic matter. This paper describes research on the incineration of solid tannery waste which was conducted on an experimental installation with a tunnel furnace as the main component. The paper includes brief characteristics of tannery waste and the experimental installation overview. Further on, the experimental conditions as well as measurements and residue analysis results are presented.

Keywords: tannery waste, tunnel furnace, waste incineration, waste treatment

1. INTRODUCTION

Production of leather is one of the oldest industrial processes in mankind's history. It is based in the conversion of raw hide or skin, a highly putrescible material, into leather, a stable material, which can be used in the manufacture of a wide range of products. The whole process involves a sequence of complex chemical reactions and mechanical processes. Among these, tanning is the fundamental stage, which gives leather its stability and essential character [1].

Processing hides into leather requires a substantial input of energy and water. It generates significant amounts of waste, wastewater and odors. Thus, the leather industry is considered to have a negative impact on the environment and is a burden on the tanneries' immediate neighborhood [2].

Depending on the technology, from ca. 450 to ca. 730 kg solid waste is produced per 1 Mg of input material processed [3]. Its treatment is a huge problem for tanneries since there is no comprehensive method applicable for all types of solid waste. In most situations the only economically efficient method

* Corresponding author. E-mail: famielec@chemia.pk.edu.pl

is landfilling which, according to the European Waste Hierarchy, is the least favored waste treatment method [4].

Worth noting is the fact that most types of tannery solid waste consist of organic matter and therefore their heating values are high enough for combustion processes. The research on a comprehensive thermal method of solid tannery waste treatment is currently being developed at the Cracow University of Technology. The aim of the research is to develop the technology for solid tannery waste combustion which, on the one hand, utilizes waste in an economically efficient manner and, on the other hand, meets all the standards for waste incineration. For this purpose an experimental installation has been designed and manufactured. In this paper the first measurements conducted on a new type of installation as well as brief thermal characteristics of tannery waste are presented.

2. CHARACTERISTICS OF TANNERY WASTE

Leather processing involves a series of operations. It can be broadly classified into pretanning (known as beamhouse operations), tanning, post-tanning, and finishing. The crucial operation is tanning during which tanning agent compounds crosslink collagen fibers of the hides. As a result the leather gains its biological stability. The most commonly used tanning agents are chromium(III) compounds. The content of chromium in finished leather amounts to approximately 4-5 %w/w [1].

The waste generated prior to and after tanning differs significantly. Untanned waste includes hide trimmings (or unusable pieces of raw hides) and fleshing (or mechanically scrapped out tissues adjacent to the hide). Tanned wastes containing trivalent chromium are leather trimmings, splits (obtained during splitting operation), shavings and buffing dust. These wastes are biologically stable. Solid waste also comes from wastewater sludge [2], [5]. The input/output overview for a conventional tanning process including the quantities of solid waste generated is shown in Fig. 1.

All major types of solid tannery waste were characterized for their suitability for disposal in a combustion process. Total organic content, water content, combustion residue, as well as lower heating value were analyzed [6]–[8]. The characteristics are presented in Table I.

Heating values of all types of waste (with the exception of sludge) are relatively high, which indicates that combustion of the waste is feasible. The problem is the high water content in some types of waste – up to 60 %w/w. This implies the necessity of preliminary drying prior to actual incineration. The combustion residue consists of ash in relatively small amounts – 4-8 %w/w

(apart from sludge, which contains significantly more inorganic incombustible matter). Ash created during combustion of tanned waste contains mainly chromium(III) oxide and therefore it can be used as a substitute for chromium ore in chromate(VI) production [8].

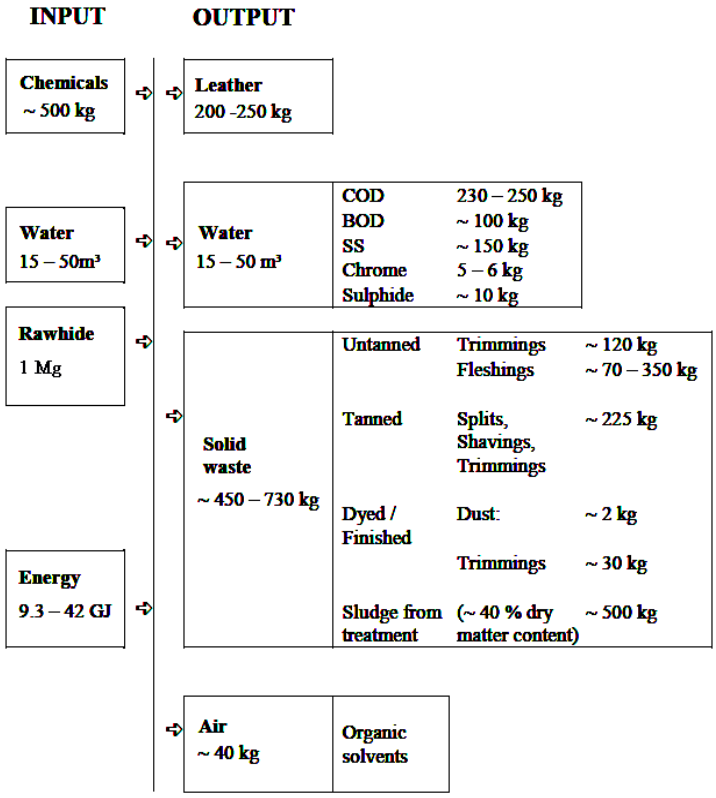

Fig. 1. Input/output overview for a conventional chrome-tanning process for bovine salted hides per 1 Mg of raw hide processed [3]

Table 1. Characteristics of Tannery Waste [6]–[8]

Type of waste	Total organic substances content in dry matter (% w/w)	Water content (%w/w)	Combustion residue – ash (%w/w)	Lower heating value (kJ/kg)
Shavings	87.5	53.6	7.8	6 663
Sludge	65.5	54.7	24.3	716
Buffing dust	87.4	14.3	6.2	16 953
Leather trimmings	87.7	10.2	4.7	19 772
Hide trimmings	86.9	59.9	4.7	7 753
Fleshings	91.4	59.5	4.6	8 952

3. THE EXPERIMENTAL INSTALLATION

In order to carry out research on tannery waste incineration an experimental installation was designed and built [4], [8], [9]. The contractor for the construction was Firma CZYLOK, Poland. The installation is located at the site of Krakowskie Zakłady Garbarskie S.A. (Cracow Tannery Works S.A., Cracow, Poland), who participate in the research and enable direct access to the waste. The main component of the installation is a tunnel furnace. As mentioned, tannery waste contains a significant amount of moisture, which needs to be evaporated prior to combustion. In a tunnel furnace it is possible to maintain thermal conditions which continuously change along the length of the tunnel. Thus, the tunnel can be virtually divided in a few sections corresponding to the following processes: waste drying, volatilization of organic matter, and combustion.

The scheme of the installation is presented in Fig. 2. The tunnel is approx. 7 m long. The waste is put into containers which can be transmitted along the tunnel by a roller system. The bottoms of the containers are perforated to enable air penetration. The nominal efficiency of the installation is 50 kg of waste per hour, but it can be changed in a wide range by 1) regulating the amount of waste in each container, 2) by regulating the velocity of the rollers. In order to preheat the furnace and to maintain the set temperatures three sections of electric heaters were installed. Technical reasons excluded the application of gas burners which had been preferable. The nominal power of the total system is 78 kW. Pressure, temperature and oxygen sensors give information about: temperature at several points of the system, pressure at the entrance and in the combustion section, as well as oxygen concentration in the flue gas. The flue gas which leaves the tunnel passes through a heat exchanger system with water and air as cooling media. The heated water is used by the tannery, the air is the intake air for the process. The air can be subsequently heated electrically and its flow can be regulated. The heat exchange enables the reuse of energy input to the system as well as waste energy recovery. The cooled flue gas passes next through the filter chamber where flue-ash is partially deposited, and leaves the system through a chimney. In the chimney there are measurement points which enable the mounting of gas sensors.

4. EXPERIMENTS

In one experimental series 81 kg of waste was incinerated. The tanned wastes incinerated were: leather trimmings, shavings, and buffing dust, in a weight ratio of 2:2:1. The average lower heating value of the mixture is ca. 13 900 kJ/kg, the average water content – ca. 28 %w/w. Each container consisted 3 kg (+/- 0.1 kg) of the mixture.

The temperature of the preheated combustion air was 350 °C. The air is introduced right after the entrance door of the tunnel. The temperature in the combustion section was set at 875°C in order to exceed 850 °C – the minimum temperature of waste incineration allowed by EU regulations. The introduction of containers started when the temperature in the combustion section approached 650 °C. The time interval between the introduction of containers was 12 min. This gives 5 containers (or 15 kg of waste) per hour. The total time of container transmission through the tunnel was 1 h 45 min. The temperatures, pressures, and oxygen content in the flue gas were recorded.

A AWE-PW analyzer was used for analysis of the volatile organic compounds (VOC) present in the flue gas (producer: ZAM Kęty sp z o.o., Poland).

The residue ash was weighted and analyzed using powder X-ray diffraction (XRD). XRD measurements were performed on an X'pert Phillips diffractometer using a CuKα radiation (λ = 1.54178 Å) in 2 Theta range from 10^o to 60^o. A Perkin Elmer 2400 CHN Elemental Analyzer was used for carbon, hydrogen, and nitrogen (CHN) elemental analysis.

5. RESULTS

As a result of the process the waste was incinerated, leaving residues of ash and flue gas. The variation of temperature during the process at several measurement points of the installation is presented in Fig. 3. The time 0:00 refers to the introduction of the first container. Noticeable is the periodicity corresponding to the introduction of following containers. The highest temperature amplitude is observed in the first section. Immediately after the introduction of waste, drying and subsequently volatilization takes place. It lasts app. 3-4 min. and then ignition occurs which manifests itself through the rapid increase of the temperature. After the burning waste moves further into the tunnel and leaves the first sensor range, the temperature in the first section decreases. In subsequent sections the temperature is higher due to preheating and the fact that hot flue gas from the first section passes through them and raises the temperature. The temperature in the final combustion section rises to 850 °C after about 4.5 h and is stable during the rest of the experiment. The amount of electrical energy required to maintain the temperature decreases significantly at this stage of the experiment, but some electrical input is still required.

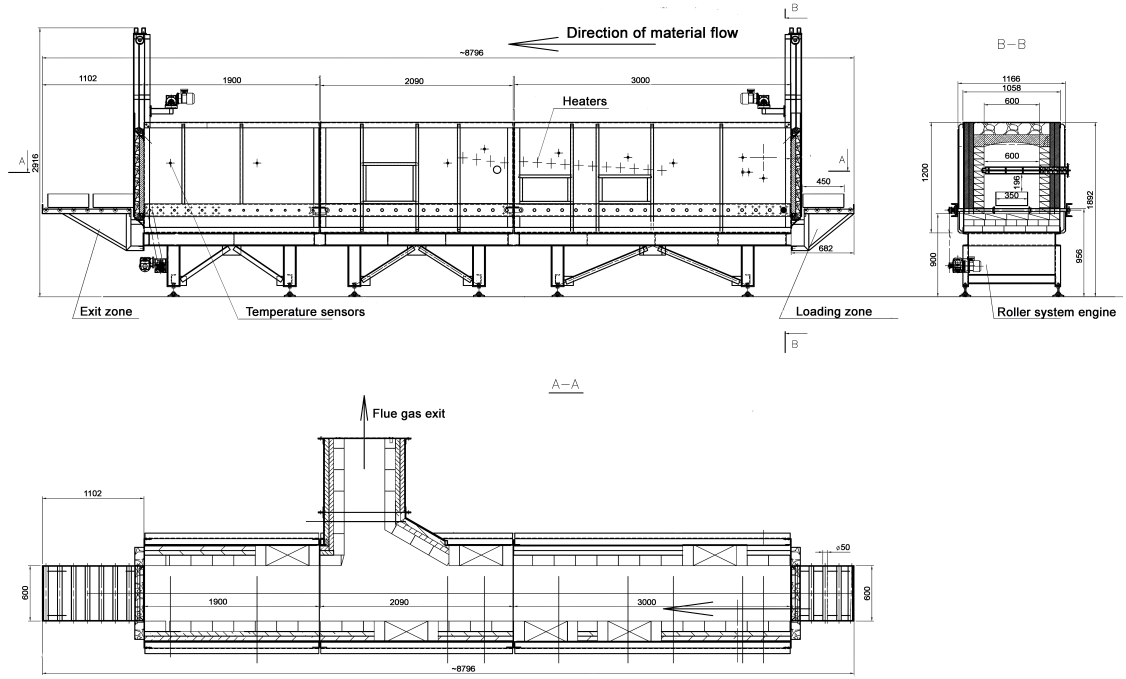

Fig. 2. Scheme of the tannery waste incinerating installation

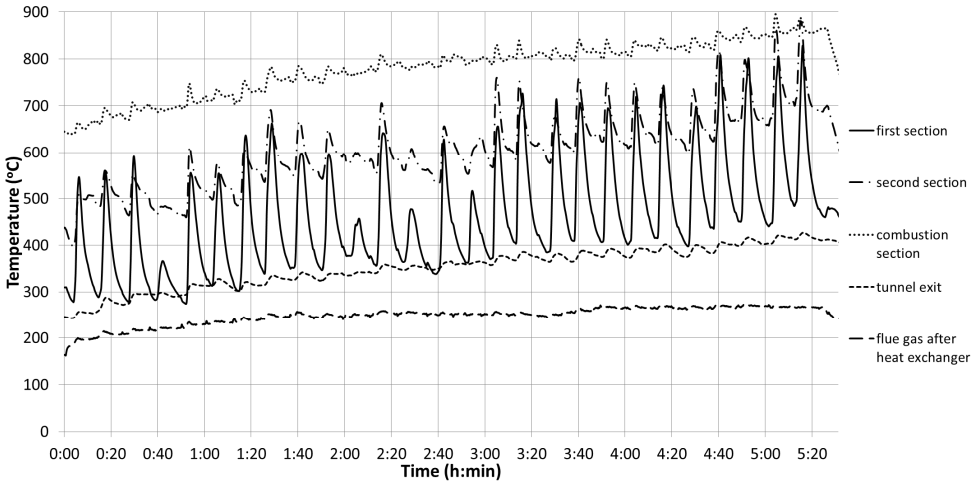

Fig. 3. Furnace temperature vs. time diagram

From 4:40 after the start to the end of the experiment the concentration of VOC was measured and recorded. The results were converted for the standard oxygen concentration of 11 %. The diagram of VOC concentration, oxygen concentration and the temperature variation in the first section of the tunnel are shown in Fig 4. The average oxygen concentration is relatively high, and it decreases significantly (to 11-14 %) only when the ignition and rapid combustion of the new portion of waste takes place. After ca. 3 min the oxygen concentration rises again to ca. 18 %. Keeping the oxygen concentration at a high level is not particularly efficient (more preheated combustion air is needed) but it is necessary to not allow oxygen concentration to drop too much during the ignition of each portion of waste. Unfortunately, the air flow cannot be regulated dynamically.

Noticeable in Fig. 4 is the fact that immediately after the introduction of a new portion of waste (which took place at 4:48, 5:00, and 5:12) and before the ignition (demonstrated by the sudden drop of the oxygen concentration) the VOC concentration rises. Then, during ignition, it decreases for a short time and rises again. The explanation of such a trend lies in the process of volatilization of organic matter. Shortly after the input of waste into the furnace the volatilization starts. The concentration of VOC rises (first of two peaks in the diagram) but soon it reaches the level when in the given thermal conditions ignition occurs (VOC concentration and oxygen concentration both drop). The combustion is at first rapid and some incomplete combustion may occur, which results in another rise in the VOC concentration. After ca. 2 min. the combustion calms and the VOC concentration decreases again.

The fluctuations of curves at 4:46, 4:58, and 5:11result from the disturbances caused by opening the exit door and allowing the container to exit the tunnel. The average VOC concentration during the measurement was 18.84 mg/m^3 and it did not exceed the emission standard (20 mg/m^3).

The total amount of ash after the experiment was 6.3 kg, which gives 10 % of the weight of waste incinerated. The ash was analyzed using XRD. The resulting diagram is presented in Fig. 5. The only visible peaks correspond to the structure of chromium(III) oxide. The CHN analysis shows that concentration of elemental carbon in the ash amounts to 0.21 %w/w, hydrogen and nitrogen were not found (meaning their concentrations are below 0.1 %w/w). These results indicate that the obtained ash contains mostly chromium(III) oxide and could be perfectly used as a chromium ore substitute in chemical industry.

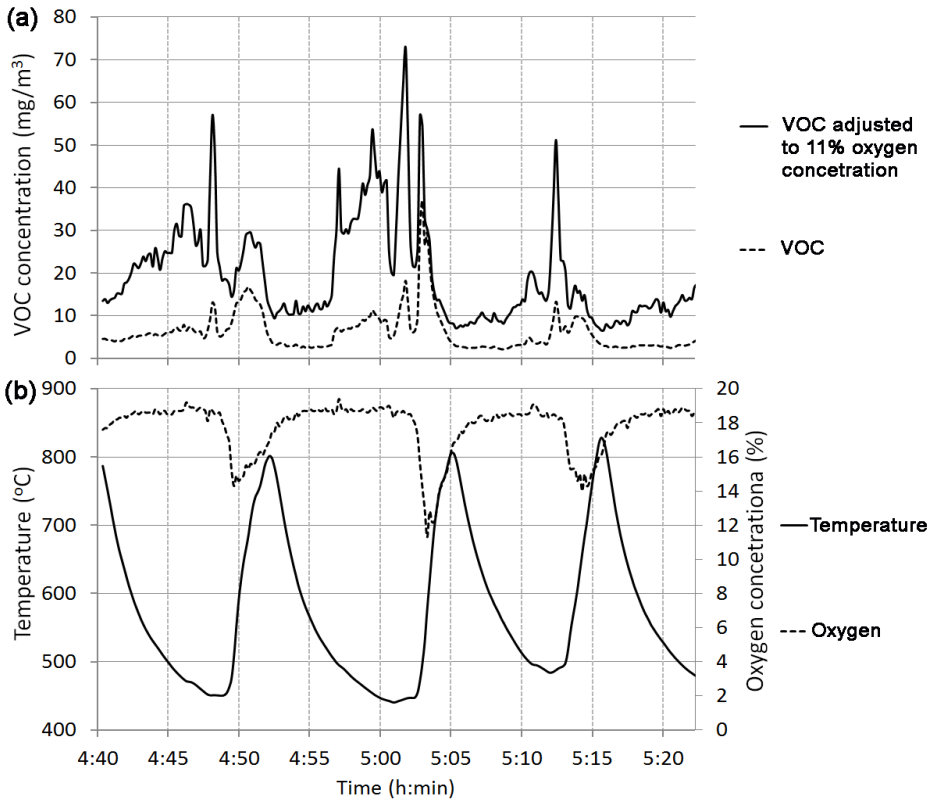

Fig. 4. (a) VOC concentration in flue gas and VOC concentration adjusted to 11 % oxygen concentration vs. time; (b) Temperature in the first section of the tunnel and oxygen concentration in flue gas vs. Time

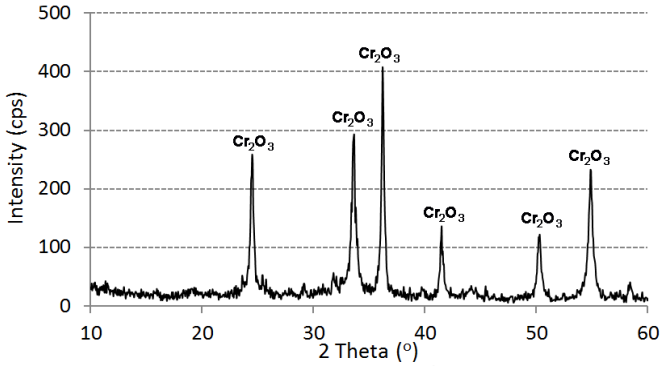

Fig. 5. XRD pattern of residue ash

6. CONCLUSION

The experiment proves that incineration of tanned wastes from the leather industry is feasible. An installation based on a tunnel furnace concept is suitable for such a process. It is possible to set process conditions such that combustion is complete and the obtained ash contains mostly chromium(III) oxide. Measurements of oxygen and VOC concentrations in the flue gas enabled an overview of volatilization process preceding ignition.

Further planned experiments include changing amounts and types of waste incinerated (including untanned waste), velocity of rollers, different temperature and air flow set, and additional analysis of the flue gas composition. Further on, the energy balance will be calculated so that the efficiency of the process could be estimated. It is expected that the experiments will allow us to choose the best parameters for the tannery waste incineration technology which could find wide application.

ACKNOWLEDGEMENT

The authors would like to thank Stanisław Kirsek and Zenon Woźny for their advice and cooperation in conducting research, and Mark Kozlowski, a Fulbright Fellow at the Faculty of Chemical Engineering and Technology, Cracow University of Technology, for English language editing and other linguistic contributions to this paper.

REFERENCES

1. Kowalski Z., Technologie związków chromu, Kraków, Wyd. Politechniki Krakowskiej 2002.
2. Pawłowa M., *Ekologiczne aspekty przetwórstwa skóry i odpadów skórzanych*, Radom, Wyd. ITeE 1995.
3. Reference Document on Best Available Techniques for the Tanning of Hides and Skins, European IPPC Bureau, July 2003, ch. 3.
4. Famielec S., Wieczorek-Ciurowa K., *Waste from leather industry – threats to the environment*, Kraków Czasopismo Techniczne PK (*Technical Transactions)*, 1-Ch (2011), 43-48.
5. Kanagaraj J., Velappen K.C., Chandra Babu N.K., Sadulla S., *Solid wastes generation in the leather industry and its utilization for cleaner environment – A review*, Journal of Scientific and Industrial Research, **65**, 7 (2006), 541-548.
6. Fela K., Wieczorek-Ciurowa K., Konopka M., Woźny Z., *Zagospodarowanie odpadów przemysłu garbarskiego – stan aktualny*

i perspektywy, in: Materiały Konferencyjne VII Konferencji nt. Technologie bezodpadowe i zagospodarowanie odpadów w przemyśle i rolnictwie, Międzyzdroje, 2010, 91-94.
7. Fela K., Wieczorek-Ciurowa K., Konopka M., Woźny Z., *Comprehensive thermal treatment as a way of utilization of industrial leather waste*, in: Abstracts of 14th Conference on Environment and Mineral Processing, Part I, Ostrava, 2010, 59-64.
8. Wieczorek-Ciurowa K., Famielec S., Fela K., Woźny Z., *Proces spalania odpadów przemysłu garbarskiego*, Chemik, 65, 10 (2011), 917-922.
9. Polish Patent Application P.39372.

SPALANIE ODPADÓW GARBARSKICH W PIECU TUNELOWYM

Streszczenie

Przemysł garbarski generuje znaczne ilości odpadów, dla których nie istnieje kompleksowa metoda unieszkodliwiania. Odpady te są głównie składowane, co wiąże się z zagrożeniami dla środowiska. Możliwe jest jednakże spalenie stałych odpadów garbarskich ze względu na znaczną zawartość materii organicznej. W artykule opisano badania dotyczące spalania odpadów garbarskich w doświadczalnej instalacji, której głównym komponentem jest piec tunelowy. Przedstawiono zwięzłą charakterystykę odpadów, opis instalacji doświadczalnej, jak również warunki prowadzenia eksperymentów oraz wyniki pomiarów i analiz pozostałości poprocesowych.

CIVIL AND ENVIRONMENTAL ENGINEERING REPORTS

No. 10 2013

EMISSION AND DISPERSION OF GASEOUS POLLUTION FROM EXHAUST SHAFTS OF COPPER MINE

Marzena JASIEWICZ*, Oryna SŁOBODZIAN-KSENICZ,
Sylwia GROMADECKA
University of Zielona Góra, Faculty of Civil and Environmental Engineering
Institute of Environmental Engineering
Szafrana st 15, 65-516 Zielona Góra, Poland

The primary objective of the study was to determine the volumes of emission and dispersion of gaseous pollution from 3 exhaust shafts of a copper mine P-VII, SW-3 and SG-2. To calculate the volumes of emission and dispersion of SO_2, NO_2 and CO the KOMIN and RWW computer programs were applied. The conducted analysis of the calculations and computer simulation showed that the extent of the impact of emisson on the rural residential area situated in the nearest vicinity of the shaft site is insignificant. The observed exceedance of reference values occurred on the premises of KGHM Polska Miedź S.A. The computer simulation proved that the nature reserve 'Buczyna Jakubowska' situated 1.6 kms north-west of the nearest emitters belonging to the mine is not exposed to above-standard concentrations of SO_2, NO_2 and CO.

Keywords: exhaust shafts, gaseous pollution, emission, dispersion

1. INTRODUCTION

Business entities conducting mining activity may exert a negative impact on the environment by emitting dust and gaseous pollution and by storing the post-floatation waste [3]. The gaseous pollution is emitted into the atmospheric air are on-ground and underground installations and facilities such as: exhaust shafts, heating installations, dust exhaust and extraction installations for salt transportation, ore and salt loading facilities.The underground exploitation makes it necessary to ventilate this part of the mine. The operating ventilation system is aimed to pump in the fresh air (downcast shafts) from the outside and remove the polluted air (exhaust shafts) [5].

* Corresponding author. E-mail: m.jasiewicz@iis.uz.zgora.pl

The environmental impact of such a big mining and minerals processing business entity as a copper mine, built in a densely-populated agricultural area, is unavoidable and includes the following: terrain deformation in the mining area, the discharge of mineralized water from mine drainage into surface water courses, the discharge of mill waste containing heavy metal compounds, the storage of slag, post-floatation and other industrial waste in large-format waste storage facilities, the emission of gaseous and dust pollution (containing heavy metal compounds) and its impact on the neighbouring area[6].

The impact of dust fall emission from mining sources (both current and forecast) is small. The emission does not exceed the standards of air quality outside the mine's premises [12].

The pollution emitted from the ventilation systems includes dust and gases, especially sulphur dioxide, nitrogen oxides and carbon oxides. They have a particularly negative impact on the environment as they undergo numerous transformations in the air and react with water vapour to form acid rain [13].
In compliance with *the Regulation of the Minister of the Environment of 2 July 2010 on the types of installations whose exploitation requires registration (Dz.U.10.130.880),* business entities utilizing the environment are obliged to prepare documentation on the kinds and volumes of pollution emitted into the environment.

The primary objective of this study was to determine the volumes of emission and dispersion of the gaseous pollution emitted from the exhaust shafts of the copper mine with special regard to its impact on the nature reserve 'Buczyna Jakubowska'.

2. MATERIAL AND METHODS

The installation for minerals exploration ore deposits is an underground copper ore mine.

The following exhaust shafts were evaluated: P-VII, SW-3 and SG-2 located respectively in the communes of Polkowice, Radwanice and at the border of Radwanice and Jerzmanowa communes:

– the P-VII shaft: located in the P-VII region, has an on-ground ventilation station equipped with 4 radial fans WPK-3.9. The air is removed from the ventilators by means of individual diffusers with the outlet dimensions of 3.9 m x 6.0 m (the equivalent diameter dz = 5.46 m) and the height of 12 m above ground level. During normal operation 3 of the 4 ventilators are in

operation and the fourth one is on standby as required by the law. - the SW-3 shaft: located in the SW-3 region, with an on-ground ventilation station equipped with 6 radial fans WPG-278/1.8 with the rated output of 850 m3/s each. The ventilators are connected in pairs to three diffusers with the height of 23.2 m AGL and the outlet dimensions of 11.5 m x 6.5 m (dz = 9.76 m). During normal operation 4 ventilators are in operation and the remaining two are on standby as required by the law. - the SG-2 shaft: located in the region of Sieroszowice Główne (SG), with an on-ground ventilation station equipped with 4 axial fans GAF38/24-1W with the rated output of 400 m3/s each. The ventilators are connected to individual diffusers with the outlet at the height of 36.3 m and the effective cross section of S = 46.6 m2 (dz = 7.7 m) (there are ceramic-coated silencers installed inside the diffusers). During normal operation 3 ventilators are in operation and the fourth one is on standby as required by the law. The volumes of the gaseous pollution emitted into the air was determined on the basis of measurements taken with automatic measuring systems.

The calculations of the volumes of emission from the ventilation shafts and the modelling of SO_2, NO_2 i CO dispersion in the atmospheric air was done in compliance with the referential methodology specified in the Regulation of the Minister of the Environment of 26 January 2010 on the reference values for certain substances in the air [11].

The reference values for

SO_2 350 μg/m^3 for one hour and 20 μg/m3 for a calendar year,
NO_2 200 μg/m^3 for one hour and 40 μg/m3 for a calendar year,
CO 30000 μg/m^3 for one hour.

The following assumptions were used for calculations:

– the aerodynamic terrain roughness – z 0 [m]

P-VII	SW-3	SG-2
0.53	0.63	1.09

– height of emitters

P-VII	SW-3	SG-2
12.0	23.3	36.3

– ambient temperature

The average annual temperature in Poland ranges between 7 and 9 °C. For the calculations 8 °C (281 K) was assumed.

– temperature of exhaust gases

As temperature of exhaust gases 25 °C (298 K) was assumed.

– parameters of exhaust shafts

Table 1. collates the calculation results obtained with the Komin program

Emission sources	Emitter symbol	Height of emitter [m]	Equivalent diameter [m]	Gas temperature [K]	Average annual ambient temp [K]
Exhaust shaft P-VII	P-VII/E1	12.0	5.46	298	281
	P-VII/E2	12.0	5.46	298	281
	P-VII/E3	12.0	5.46	298	281
	P-VII/E4	12.0	5.46	298	281
Exhaust shaft SW-3	SW-3/E1	23.3	9.76	298	281
	SW-3/E2	23.3	9.76	298	281
	SW-3/E3	23.3	9.76	298	281
Exhaust shaft SG-2	SG-2/E1	36.3	7.7	298	281
	SG-2/E2	36.3	7.7	298	281
	SG-2/E3	36.3	7.7	298	281
	SG-2/E4	36.3	7.7	298	281

The calculations of the volumes of emission of gaseous pollution into the air were done in 2012 on the basis of measurements of concentrations taken with automatic measuring systems in the collector ducts situated before the ventilation stations for each of the exhaust shafts.

The calculations of the volumes of emission from the ventilation shafts and the modelling of SO_2, NO_2 i CO dispersion in the atmospheric air was done in compliance with the referential methodology specified in the Regulation of the Minister of the Environment of 26 January 2010 on the reference values for certain substances in the air [11].

3. RESULTS AND DISCUSSION

Table 1. Emissions of SO2, NO2, CO from exhaust shaft.

Shaft name	Pollution type	Smm [µg/m3]	Maximum of average annual concentrations [µg/m3]	Maximum of 1-hour concentrations [µg/m3]	Maximum of percentile S99.8 [µg/m3]	Maximum of percentile S99.726 [µg/m3]
P	SO_2	0.225	0.045	1.125	-	0.784

	NO_2	13.507	2.701	67.511	47.053	-
	CO	16.884	3.376	84.388	58.817	-
SW-3	SO_2	1.668	0.089	8.383	-	4.153
	NO_2	24.602	1.309	123.644	61.250	-
	CO	14.178	0.755	71.253	35.296	-
SG-2	SO_2	2.111	1.656	323.029	-	45.925
	NO_2	40.820	32.010	6 245.229	887.889	-
	CO	17.595	17.595	2 691.909	382.711	-

The analysis of the above data shows that the lowest values of SO_2 concentrations calculated for Smm, of maximum average annual and 1-hour concentrations were for the shaft P-VII. The highest values of SO_2 concentrations calculated for Smm, of maximum average annual and 1-hour concentrations were for the shaft SG-2. The lowest values of NO_2 emission calculated for Smm, of maximum average annual and 1-hour concentrations were also for the shaft P-VII, and the highest for the shaft SG-2. The Smm values of maximum average annual and 1-hour concentrations of emitted CO were the lowest for the shaft SW-3, and the highest for the shaft SG-2.

3.1. The distribution of contour lines for the shaft P-VII

Figures 1-5 present the distribution of the contour lines illustrating the dispersion of the analyzed pollution from the ventilation shafts only when the reference values were exceeded.

The only pollution exceeding the threshold values within the area of the shaft P-VII is nitrogen dioxide.

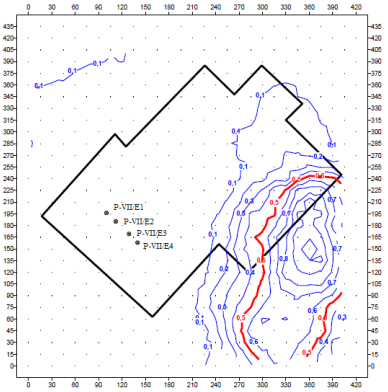

Source: author's calculations

Fig. 1. The incidence of reference value exceedance for NO_2 for a calendar year [%]

The distribution of the contour lines of NO_2 emittions into the atmospheric air shows that it disperses eastward of the four emitters P-VII/E1, P-VII/E2, P-VII/E3 and P-VII/E4. The contour lines cover the area of the shaft P-VII and go beyond that area. The red contour line represents the exceeded value. The threshold value is exceeded in the east part of the P-VII region and that exceedance disperses beyond its boundary in a southward direction (Fig.1). The exceeded levels of NO_2 pollution do not have a negative impact on the nearest residential area as it is situated approx. 400 metres north-west of the region.

The shaft SW-3

The only pollution exceeding the threshold values within the area of the shaft SW-3 is nitrogen dioxide.

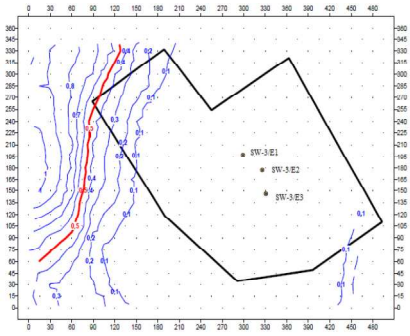

Source: author's calculations

Fig. 2. The incidence of reference value exceedance for NO_2 for a calendar year [%]

The distribution of the contour lines of NO_2 emissions into the atmospheric air shows that it disperses westward of the three emitters SW-3/E1, SW-3/E2 and SW-3/E3. The contour lines cover the area of the shaft SW-3 and go beyond it. The red contour line represents the exceeded value. The permissible value is exceeded in the west part of the region and has a minor impact on the shaft region (Fig. 2). However, it disperses over the whole of the west part, from north to south. The reference values are exceeded in the west part of the region and go 50 metres beyond that area, to which the copper mine holds a legal title. The nearest residential area is the village of Sieroszowice, situated 1.5 km south-west of the shaft site, so the excessive NO2 pollution will not have a negative impact on it.

The shaft SG-2

Within the area of the shaft SG-2 the threshold values of SO_2 and NO_2 pollution were exceeded.

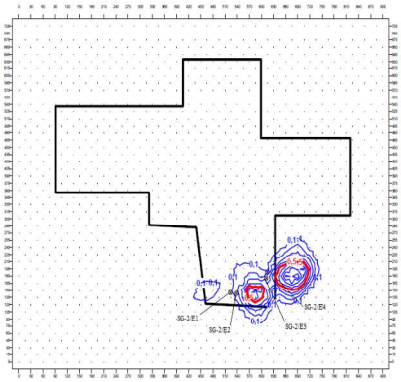

Source: author's calculations

Fig. 3. The incidence of reference value exceedance for SO_2 for a calendar year [%]

The distribution of the contour lines of sulphur dioxide emissions into the atmospheric air from the emitters SG-2/E1 and SG-2/E2, situated in the south of the SG region, disperses over a short distance in an eastward direction. The contour lines above the emitters SG-2/E3 and SG-2/E4, situated in the south-east of the region, show the same direction. The plumes cumulate tightly in the south-east. The reference values for SO_2 concentrations are exceeded in the south of the SG region and about 100 metres beyond its area (Fig. 3). North and north-east of the shaft site, beyond a belt of cultivated land, at a distance of approx. 1.5 km, lies a compact residential area of the villages Jakubów and Maniów Górny.

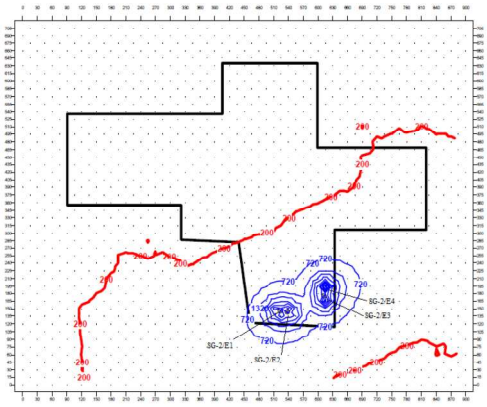

Source: author's calculations

Fig. 4. The distribution of the contour lines of NO2 dispersion for a maximum 1-hour concentration

The distribution of the contour lines of nitrogen dioxide emissions into the atmospheric air shows that it cumulates in the south of the region, reaching

about 60 metres beyond it. The red contour lines represent the exceeded maximum 1-hour concentrations of NO2. The exceedance occurred south-east of the SG area, where there is a large forest complex. The contour line representing the exceeded reference values shows that the plume disperses from south-west up to north-east. It covers part of the SG region, the adjacent cultivated land and the forest area in the south. The exceeded levels of the maximum 1-hour concentration should not have a negative impact on the rural residential area as it is situated 1.5 km north-east of the SG region.

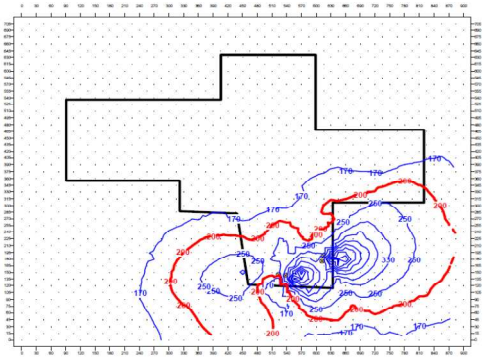

Source: author's calculations

Fig. 5. The maximum of percentile S99.8 for NO2

Fig. 5 presents the dispersion of the plume of the emitted nitrogen dioxide for the maximum of percentile S99.8. The red contour lines represent high incidence of the reference value exceedance. The pollution disperses in a southward and eastward direction. It covers the south part of the SG area so it may have a negative impact on the nearby forest complex.

4. SUMMARY AND CONCLUSIONS

The applied computer program KOMIN allowed for a precise and reliable calculations of the volumes of emission of gaseous pollution (sulphur dioxide, nitrogen dioxide and carbon monoxide) from the exhaust shafts of a copper mine. The extent of the impact of the analyzed pollution was determined with the sue of the Rww program, which generated readable and clear images of pollution dispersion. The conducted analysis of calculation results and computer simulations that mining complexes emit gaseous pollution that may be an environmental hazard.

The exhaust shafts are the source of organized emission of gaseous pollution (sulphur dioxides, nitrogen dioxides and carbon oxides) into the air,

which then react with other compounds present in the atmosphere. The products of these transformations may have a negative impact on the environment intensifying the acid rain effect or increasing the effect of ozonesphere destruction.

The few sources of unorganized emission present on the mining complex make a minor contribution to the environment pollution. The result analysis showed that the reference values were exceeded at the shaft SG-2, and the exceedance concerned the maximum 1-hour concentrations of NO2. For other analyzed pollutions (SO2 and CO) the permissible values were not exceeded.

The extent of dispersion of the emitted pollution is relatively small with the exception of the shaft SG-2, which exerts a limited impact on an area to which the mine does not holds a legal title. The emission of sulphur dioxide, nitrogen dioxide and carbon monoxide pollution is unavoidable resulting from the continuous operations of the mine. By implementing environmental measures the emission can be reduced, thus minimizing its negative impact on the natural environment.

The following conclusions can be drawn from the conducted analysis:

1. Every business entity that generates pollution should prepare an environmental impact assessment, a reliable document allowing one to determine the level of noxiousness.
2. The use of the computer programs KOMIN i Rww allowed for a precise determination of the volumes of the emitted gaseous pollution (SO2, NO2 and CO) and accurate imaging of the impact area.
3. The impact of the emission of sulphur dioxide, nitrogen dioxide and carbon monoxide pollution on the residential area situated in the nearest vicinity of the shaft site is insignificant. Whenever the standards of air quality are violated, it is only in an area being the property of the mine and in a limited bordering area.
4. The computer simulation proved that the nature reserve 'Buczyna Jakubowska' is not exposed to above-standard concentrations of SO_2, NO_2 and CO.

REFERENCES

1. Alloway B. J., Ayres D. C.: *Chemiczne podstawy zanieczyszczenia środowiska*, Warszawa, Wyd. Naukowe PWN, 1999.
2. BOK A.,: *Przewodnik Przyrodniczo-Turystyczny*, Polkowice, Związek Gmin Zagłębia Miedziowego, Wyd. Unigra.

3. Kraszewski A., Iwińska K.: - *Konflikty ekologiczne i negocjacje*. Materiały dydaktyczne, Politechnika Warszawska, 2008 (http://www.is.pw.edu.pl/zibjs).
4. Ostrowski J., red.: - *Ochrona środowiska na terenach górniczych*, Kraków, Wyd. IGSMiE PAN, 2001.
5. Pęczek D., Rosiek F., Sikora M., Urbański J.: *Rozwój wentylacji kopalń na przestrzeni dziejów.* Prace Naukowe Instytutu Górnictwa Politechniki Wrocławskiej Nr 117, 2006.
6. Pietraszek J.: *KGHM otrzymał tytuł "Lidera Polskiej Ekologii"* [Dokument elektroniczny]. Dostępny w World Wide Web: HYPERLINK http://www.kghm.pl/index.dhtml?module=articles&id=120.
7. Pyłka-Gutowska E.: *Ekologia z ochroną środowiska*, Warszawa, Wyd. Oświata, 2004.
8. Rozporządzenie Ministra Środowiska z dnia 24 sierpnia 2012 r. w sprawie poziomów niektórych substancji w powietrzu (Dz.U. 2012 nr 0 poz. 1031).
9. Rozporządzenie Ministra Środowiska z dnia 2 lipca 2010 w sprawie przypadków, w których wprowadzanie gazów lub pyłów do powietrza z instalacji nie wymaga pozwolenia (Dz.U.10.130.881).
10. Rozporządzenie Ministra Środowiska z dnia 2 lipca 2010 r. w sprawie rodzajów instalacji, których eksploatacja wymaga zgłoszenia (Dz.U.10.130.880).
11. Rozporządzenie Ministra Środowiska z dnia 26 stycznia 2010 r. w sprawie wartości odniesienia dla niektórych substancji w powietrzu (Dz.U. Nr 16/2010, poz. 87).
12. Sadurski A.,: *Stanowisko Zespołu Roboczego Krajowej Komisji do spraw ocen oddziaływania na środowisko, do rozpatrzenia sprawy związanej z realizacją przedsięwzięcia pn. wydobycie rudy miedzi ze złoża „POLKOWICE", „SIEROSZOWICE", "RADWANICE-WSCHÓD", „RUDNA" oraz „LUBIN-MAŁOMICE", polegające na kontynuacji eksploatacji złoża rudy miedzi w granicach obszarów górniczych: „POLKOWICE II", „SIEROSZOWICE I","RADWANICE-WSCHÓD", „RUDNA I", „RUDNA II" , „MAŁOMICE I", „LUBIN I.*, Wrocław, 2012.(http://www.gdos.gov.pl)
13. Szklarczyk M.: *Ochrona atmosfery*, Olsztyn Wyd. Uniwersytetu Warmińsko-Mazurskiego, 2001.

EMISJA I DYSPERSJA ZANIECZYSZCZEŃ GAZOWYCH Z SZYBÓW WYDECHOWYCH KOPALNI MIEDZI

S t r e s z c z e n i e

Podstawowym celem pracy jest określenie wielkości emisji i dyspersji zanieczyszczeń gazowych z 3. szybów wydechowych kopalni miedzi P-VII, SW-3 i SG-2. Do obliczeń wielkości emisji i dyspersji SO_2, NO_2 i CO wykorzystano program komputerowy KOMIN oraz Rww. Analiza wyników obliczeń i symulacji komputerowej pokazała, że zasięg oddziaływania emisji na zabudowę wiejską znajdującą się w najbliższych odległościach od rejonów szybów jest znikomy. Stwierdzone przekroczenia wartości dopuszczalnych znajdowały się na terenie należącym do KGHM Polska Miedź S.A. Symulacja komputerowa wykazała, że Rezerwat przyrody ,,Buczyna Jakubowska'' leżący 1,6 km na północny-zachód od najbliższych emitorów rejonu kopalni nie jest narażony na ponadnormatywne stężenia SO_2, NO_2 oraz CO.

CIVIL AND ENVIRONMENTAL ENGINEERING REPORTS

No. 10 2013

PREDICTING BENDING MOMENT IN CROWN OF SOIL-STEEL STRUCTURE BUILT AS ECOLOGICAL CROSSING FOR ANIMALS

Marcin MUMOT*
Politechnika Wrocławska
Instytut Inżynierii Lądowej

The paper concerns soil-metal structures made of a thin shell (usually - corrugated steel) and soil backfill. During backfilling significant deformations of the structure can be observed (the upper part of the shell buckles and its width narrows). This phenomenon results in a subsequent prestressing effect during placing the backfill material above the crown of the structure. In the paper the method of bending moment determination in the crown of the structure, which is the main component affecting stresses in the steel shell, is proposed. The results obtained using in-situ method were compared with the results obtained using FEM software. The conclusions were drawn and the diagrams presenting the curvatures necessary to estimate values of the bending moment in the crown of the structure were obtained from the studies. Relations that could help in development of the methodology for determining internal forces in the crown of the structure of different geometry were found. The studies will help in designing of that type of structures and will allow to prevent critical forces in the steel shells during the erection process.

Keywords: soil-steel structures, ecological crossing, corrugated steel, soil backfill, deformation, bending moment.

1. INTRODUCTION

Experiences in designing and fabrication of corrugated metal structures show that the largest bending moments can be observed during construction. Internal forces in the metal shell during backfilling, when the level of the backfill material is equal to the height of the crown of the structure, are ever ten times larger than during the entire lifetime of the structure. Therefore, an exact

* Corresponding author. E-mail: marcin.mumot@pwr.wroc.pl

determination of the internal forces in the shell is an important issue in the designing process of the soil-metal structures. It was observed that bending moments (which are the main component of stresses) can be determined based on the change of the curvature in the crown of the shell. This paper presents computer analysis carried out in order to verify the correctness of this method and to observe relations necessary to determine correctly the values of bending moments in soil-metal structures. There are three basic shapes of the lightweight shells: open bottom A, closed bottom B and frame C.

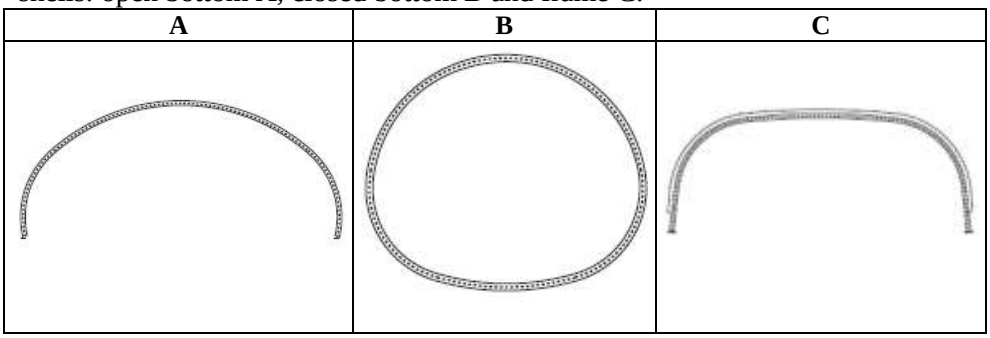

Fig. 1. Characteristic types of the shells

Structures A and B behave in the similar manner during backfilling, their deformations are similar to the drawing in Figure no. 2. This paper does not concern box structures –type C, because these are non-standard structures and their deformation is different than in traditional structures.

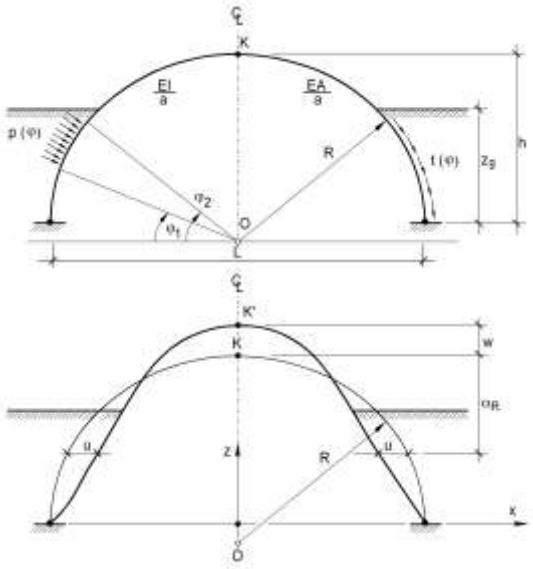

Fig. 2. Basic parameters of the shell and its deformation, typical for soil-steel arch structures

2. DEFORMATION OF SHELL DURING BACKFILLING

Two typical displacements can be distinguished in soil-metal structures. The basic displacements are: upward vertical displacement of the shell "w", measured in the highest point and horizontal displacement "u", where 2u is the shrinkage of the shell. As long as the level of the backfill is lower than the shell crown height we can observe an increase of the displacements A up to the height of the structure zg = h, when the value of the upward displacement attains its maximum – K. However when the backfill material level is above the crown of the shell, stresses are reduced E to the moment of loss of stability (Fig. 3)

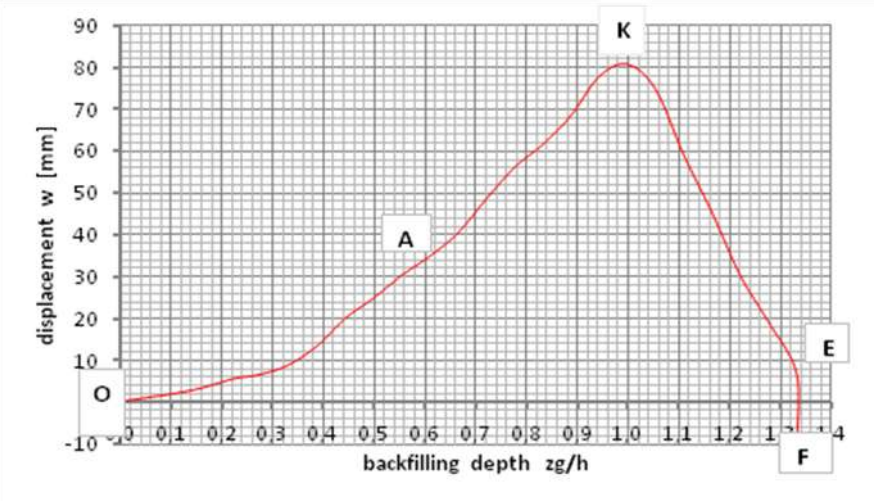

Fig. 3. Diagram of the displacements in the shell crown

The diagram show that the most dangerous stage of the soil-metal structure's construction is when the level of the backfill material is equal to the height of the crown of the structure. Current methods of determining bending moments in such structures do not guarantee obtaining exact values of the internal forces [2]. It was observed, however, that the bending moment can be calculated based on the change of the radius of the steel shell curvature (1) [1].

$$\Delta R = R - R_{uw} \tag{1}$$

R_{uw} – radius of curvature in the deformed steel shell,
R – design radius of curvature of the steel shell.

In order to determine a change of the radius of curvature it is necessary to interpret properly horizontal and vertical displacements of the shell. The vertical displacement in the crown should be reduced by subtracting the value of the vertical displacement in points of shrinkage measurement (2).

$$w_k = w - w_p \tag{2}$$

w – vertical displacement in the shell crown,
w_p – vertical displacement in point of shrinkage measurement.

For the calculations a value of the coefficient α is also required. The coefficient is calculated as follows (3):

$$\alpha = \frac{(h - z_g)}{R} \tag{3}$$

h – design height of the structure,
z_g – total thickness of the backfill layer,
R – design radius of curvature of the steel shell.

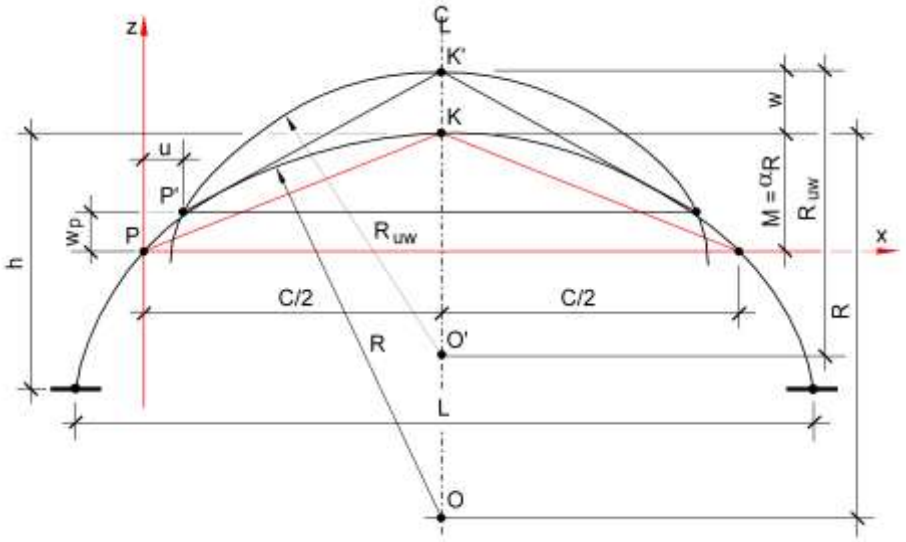

Fig. 4. Graphic scheme of the radius of curvature changes

Knowing the displacements of the shell, changes of the radius of curvature can be determined by transforming the formula for the radius of the circle (4):

$$R = \frac{4M^2 + C^2}{8M} \rightarrow dR_\alpha(z_g) = R - R_\alpha = \frac{R\left[w_k(1-\alpha) + u\sqrt{\alpha(2-\alpha)}\right]}{\alpha R + w_k} \tag{4}$$

Knowledge of the radius of curvature of an arc can be simply used to determine the maximum bending moment in a structure (5).

$$M = \frac{EI}{R} * \frac{dR}{R - dR} \tag{5}$$

In order to ensure the accuracy of the calculations, shrinkage measurement should be carried out at points situated at the level of backfill or above it. These are formulas for the loading scheme that does not include vertical earth pressure, because the radius of curvature is assumed constant and

vertical earth pressure would prevent that situation. In order to verify that method of determination of the internal forces in the steel shell, the field measurements of the assembled structure and the computer calculations by FEM software - Plaxis were carried out.

3. VERIFICATION OF THE BENDING MOMENT DETERMINATION METHOD IN THE SOIL-STEEL STRUCTURES

On the assembled structure (geometry presented in the Figure 5) some points were determined in order to determine bending moments.

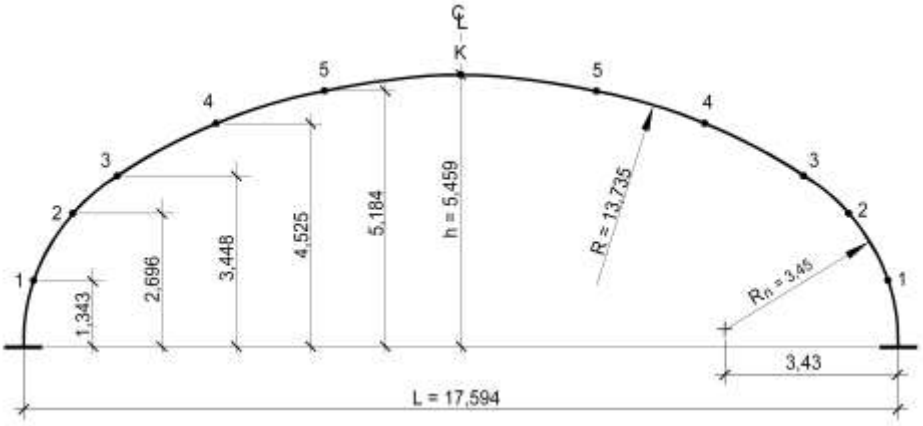

Fig. 5. Locations of the measurement points and shell geometry

6 measurement points were selected but because of the calculation method (measurement points should be located on the arc of the same curvature) points 1 and 2 have been omitted in considerations and points 3,4,5 and K were used to determine the bending moment. Procedures of calculation and internal forces determination is described in the paper [1]. The diagram presenting changes of the curvature depending on measurement point looks like in the presented diagram [diagram 1]. A significant influence of the vertical loads can be observed on this diagram. Up to the moment when the measurement points are above the backfill level, deformation diagrams are convergent, with additional layers of the backfill material the diagrams "move away" from each other. Therefore, to compare results the highest measurement point was selected, for which α=0.02. By selecting that point for further consideration the influence of vertical earth pressure can be minimized. A change of the radius of curvature for that measurement point when $z_g = z_\alpha$ ($z_g/h = 0.9497$) equals 9.890%, while the maximum value of the shell deformation equals about 11%.

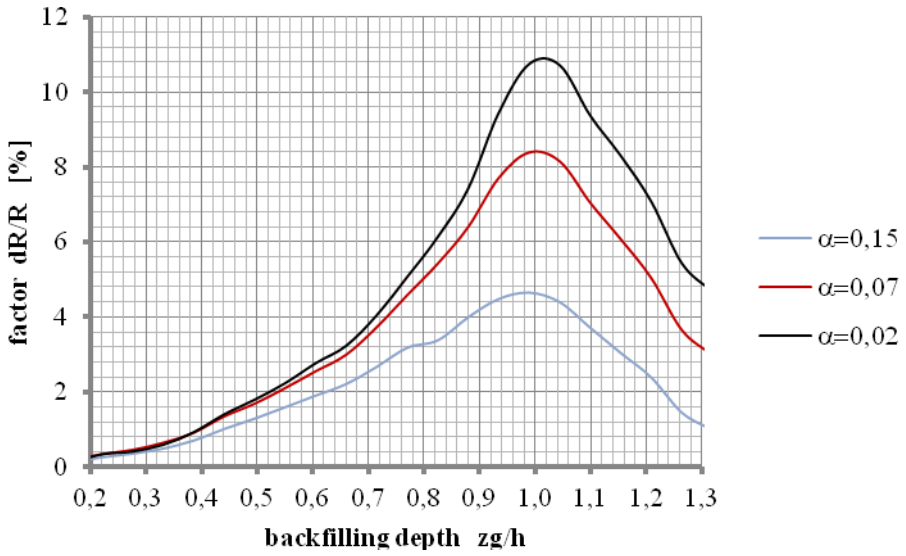

Diagram 1. Change of the radius of curvature depending on backfill height

In order to compare the obtained results a FEM model was created using Plaxis3D software. The modelled shell presents the actual geometry of the structure in the most accurate way and the soil parameters are assumed in accordance with the actual conditions. The following soil parameters were assumed E=40,0MPa, v=0,3; γ=20,0kN/m3. For modeling a shell made of the 7 mm thick SuperCor corrugated steel was assumed. Young's modulus of steel is 210 GPa, v=0,3.

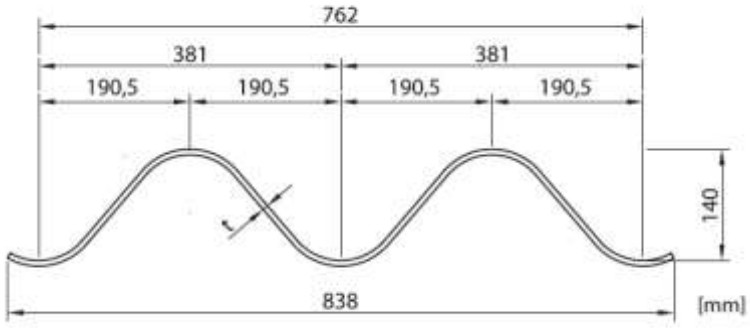

Fig. 6. Cross-section the SuperCor

24 stages of backfilling were modelled and non-linear behaviour of the structure was assumed. The support of the structure is linear, modelled as a concrete spread footing foundation of 0,5 m thickness.

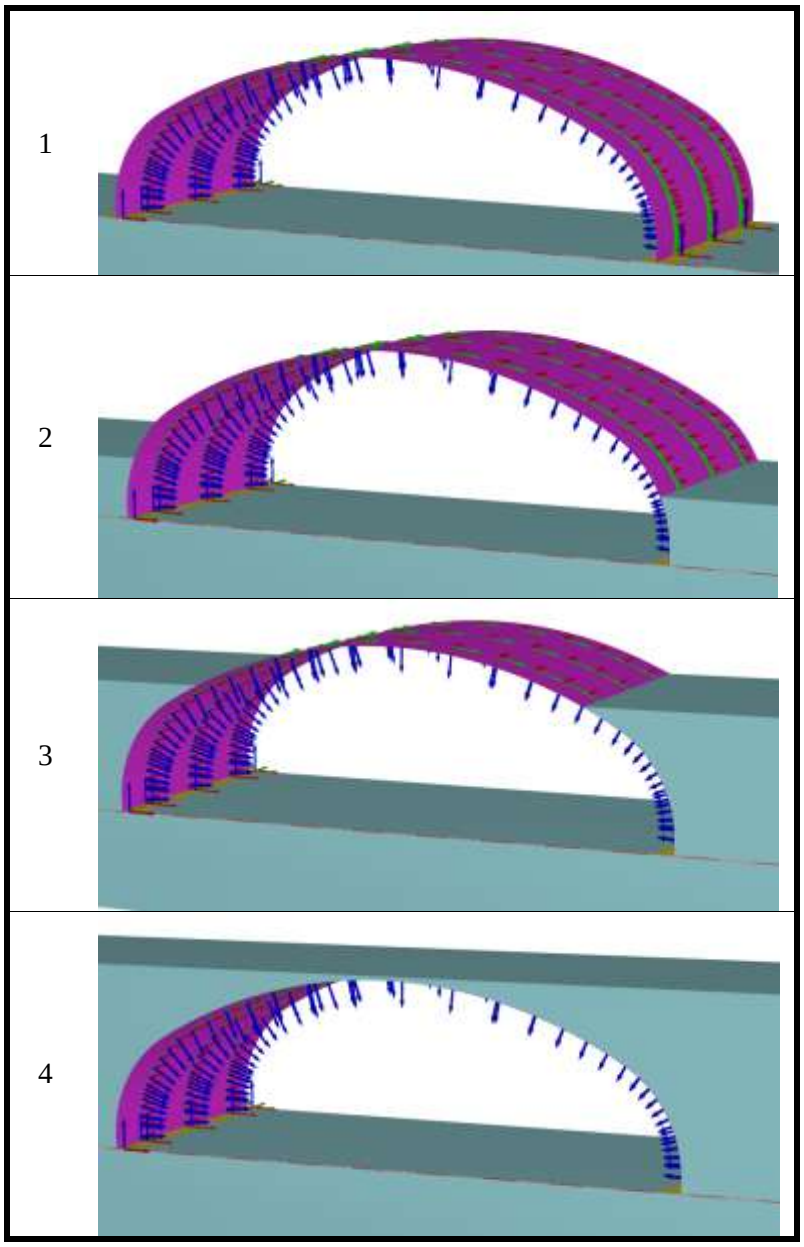

Fig. 7. Selected stages of backfilling

Values of the deformations and bending moments in the crown of the structure can be interpreted from the model. All the results were summarized in the table and the diagrams were drawn. Bending moments in the crown of the

shell in the middle of its width and the shrinkage value at the point for which α=0,002872 are presented.

Table 1. Data obtained by using FEM software

SC-27NA					
z_g [m]	α	M_{FEM} [kNm]	M_{displ} [kNm]	Δ_{FEM} [%]	Δ_{displ} [%]
0	0,378	0,000	0,000	0,00	0,00
0,3	0,357	-0,083	-0,102	-0,03	-0,03
0,6	0,335	-0,151	-0,180	-0,05	-0,05
0,9	0,314	-0,193	-0,230	-0,06	-0,07
1,2	0,292	-0,198	-0,239	-0,06	-0,07
1,5	0,271	-0,153	-0,197	-0,05	-0,06
1,8	0,249	-0,044	-0,085	-0,01	-0,03
2,1	0,228	0,159	0,119	0,05	0,04
2,4	0,206	0,543	0,506	0,16	0,15
2,7	0,185	1,225	1,200	0,37	0,36
3	0,163	2,331	2,318	0,71	0,71
3,3	0,142	3,982	3,918	1,22	1,20
3,6	0,120	6,352	6,164	1,96	1,90
3,9	0,099	9,664	9,385	3,02	2,93
4,2	0,077	13,864	13,505	4,38	4,27
4,5	0,055	19,048	18,714	6,12	6,01
4,8	0,034	25,102	24,797	8,23	8,12
5,1	0,012	31,485		10,54	
5,4	-0,009	32,742		11,01	
5,7	-0,031	29,777		9,91	
6	-0,052	26,930		8,88	
6,3	-0,074	24,332		7,96	
6,6	-0,095	21,880		7,10	
6,9	-0,117	19,572		6,30	
7,2	-0,138	17,463		5,59	

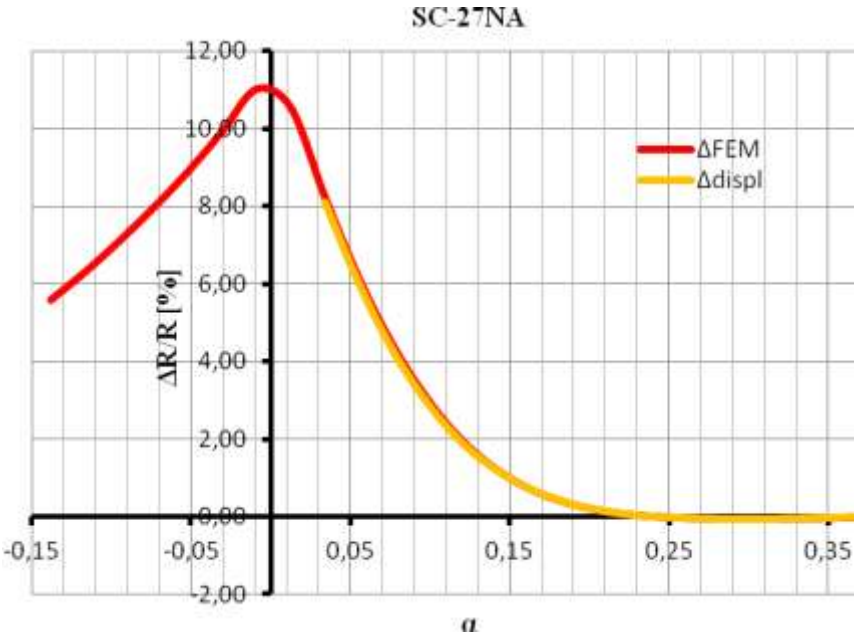

Diagram 2. Change of the radius of curvature depending on backfill height

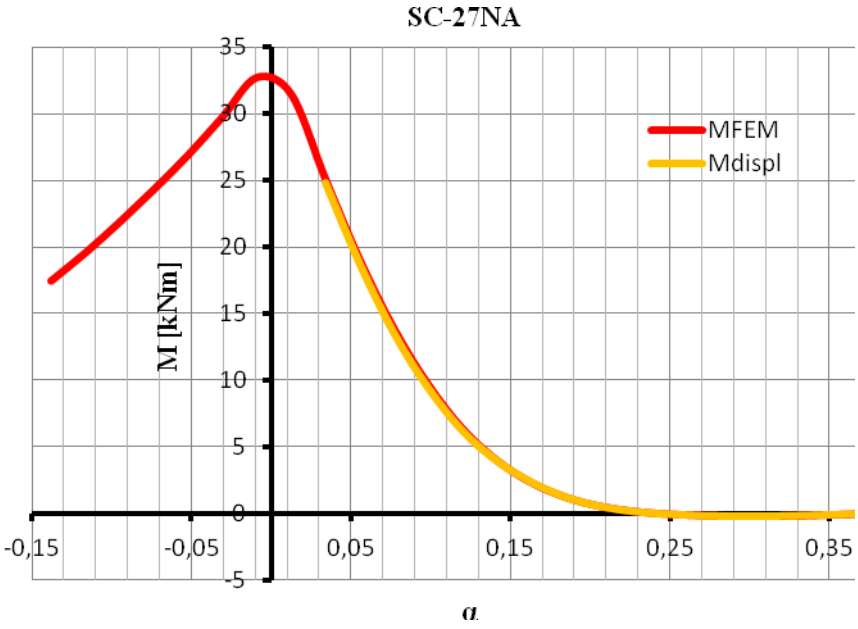

Diagram 3. Change of maximum bending moment depending on backfill height

It can be observed from the diagrams that the maximum value of the shell deformation in the crown of the structure equals about 11%. The exact value of the deformation could not be obtained, because the level of the last layer of the backfill material did not equal the shell height. Comparing the actual change of the radius of curvature with the results obtained from computer analysis it can be assumed that the presented method of bending moments determination is correct. In the paper [1] it was noticed that the curve describing the change of the curvature depending on the backfill height can be approximated (6). From these calculations results that the maximum deformation of the shell equals 12,16% and it was calculated using the formula:

$$dR_k^{max} = dR_\alpha \left(\frac{h}{h-\alpha R}\right)^4 \tag{6}$$

The formula can be applied in order to reduce the influence of the vertical earth pressure on the shell deformation. The value can be used as a design value in order to provide a safety margin for the designed structure. The diagrams (2 and 3) show that strain measurements during backfilling and determination of the radius of curvature changes allow calculating the maximum bending moment. That regularity can be applied also in the opposite direction. Knowing the maximum value of bending moment (shell's deformation) it can be verified if the permissible values of forces are not exceeded during erection process, allowing the contractor to reduce bending moments and upward displacements of the shell, for example by placing ballast.

4. OTHER CALCULATION MODELS

The test were also carried out for different shell shapes and for different shell stiffness. They have shown that the shell's stiffness has a great influence on its behaviour during construction. Soil-metal structures should be designed according to the guidelines described in the paper [3,4]. Following these guidelines should lead to an observation of radius of curvature deformation within the range 8-14 %. Designing of too thin or too stiff shell results in a risk that the vertical deformation in the crown will be too big and the plastic deformation will occur in the shell, in the latter case it leads to unnecessary oversizing of the structure. The diagrams (4,5) show changes of the radius of curvature depending on the backfill height (red line) and calculated displacements based on the deformations (yellow line). In spite of the different stiffness of the shells and their geometry, deformation curvatures have a similar shape.

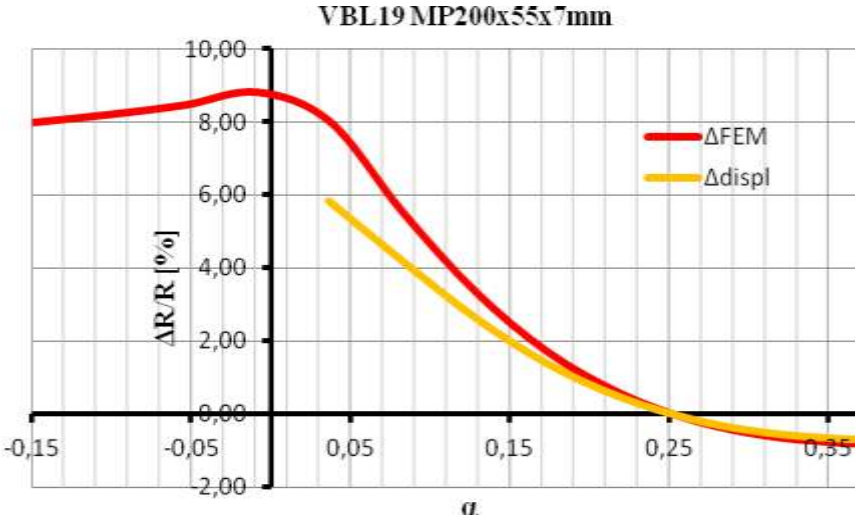

Diagram 4. Change of the radius of curvature depending on backfill height

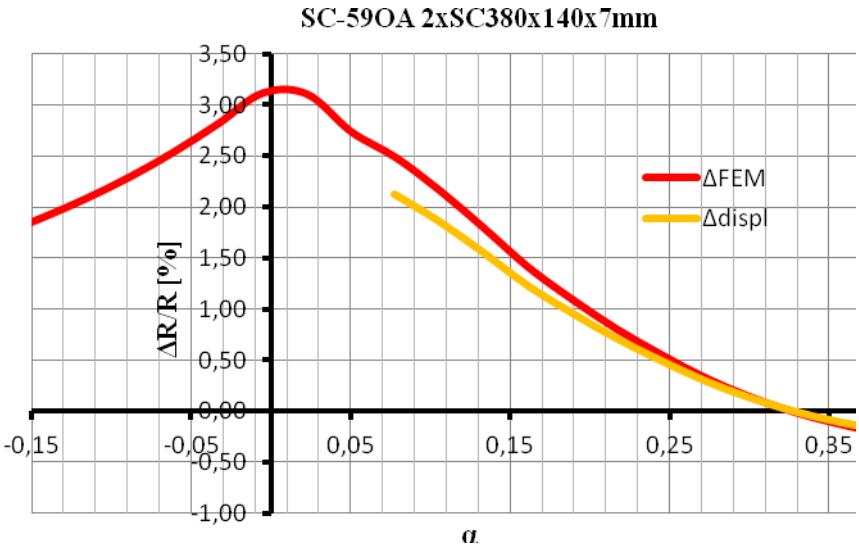

Diagram 5. Change of the radius of curvature depending on backfill height

However, graphs [6,7] show the change of deformation of similar shells [Fig. 8]. It can be observed that the change in stiffness does not cause the change of the deformation ratio between different shapes of shells. It can be noted that knowing the round-shape shell deformation we can assume deformation in other types of closed shells of similar dimensions. In both cases the difference between deformation of the shell VE 35 and VC 70 equals 45 % and between VE 35 rotated 90 degrees and VC 70 equal about 22 %.

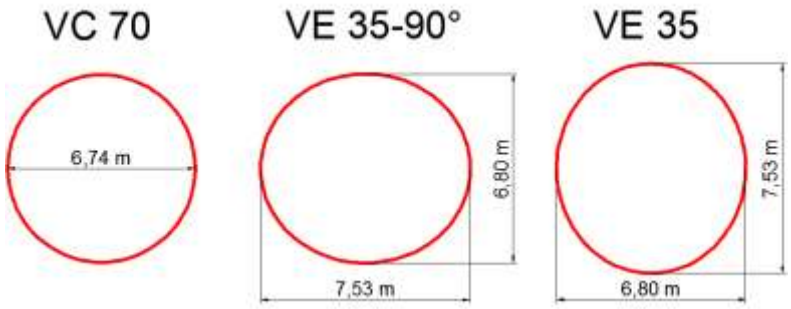

Fig. 8. Shapes and general dimensions of compared shells

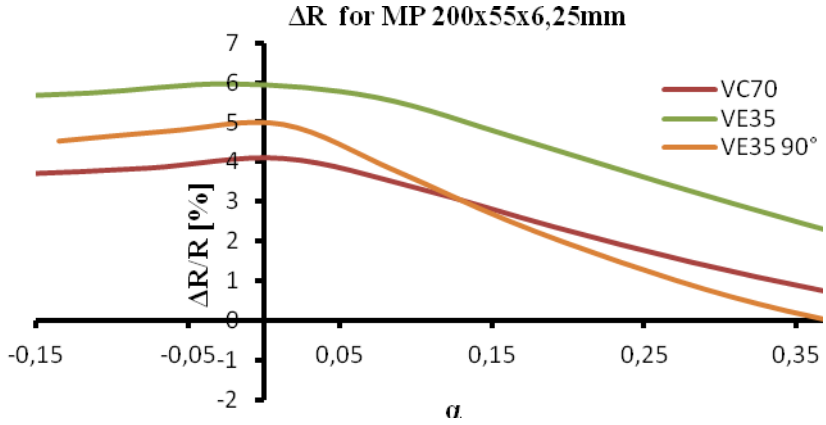

Diagram 6. Change of the radius of curvature depending on backfill height for a shell of 6,25 mm thickness

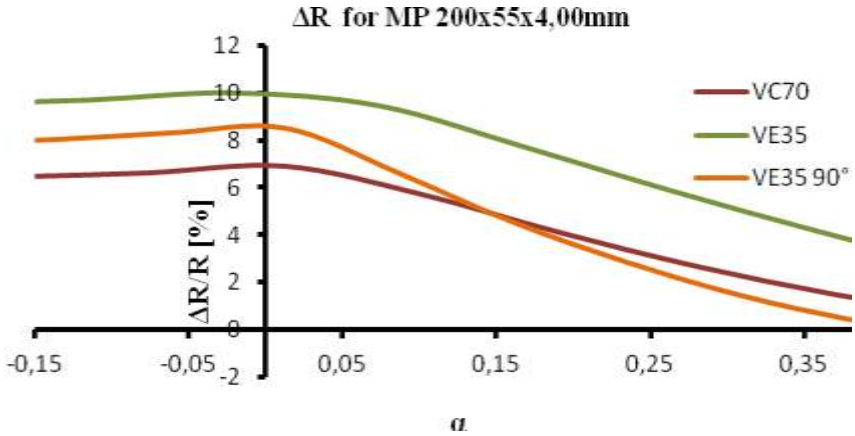

Diagram 7. Change of the radius of curvature depending on backfill height for a shell of 4,00 mm thickness

These examples show that there is a relation that could allow the correct determination of the radius of curvature in the crown of the structure for different shell shapes and for different spans. Unfortunately, it was noticed that change of the shell span results in changing of the determined proportions.

5. CONCLUSIONS

This paper draws attention to the occurrence of the maximum bending moment in the shell during backfilling. Presented calculations initiate the development of the methodology for determining internal forces in the crown of the shell. Insufficient accuracy of the current methods for determining internal forces was noted and a different method was proposed. In the paper a method for estimating of bending moments as a local effect of the global shell deformation was proposed. A procedure that allows correct determination of bending moments in the crown of the soil-metal structure was presented. The relations observed in results obtained from calculation models of that type of structures were presented and compared with the measurements performed on an actual structure. It is necessary to estimate correctly the deformation of the shell and to select a proper stiffness of the shell in relation to the span of the structure. A curvature shape was preliminary defined, according to which the maximum bending moment can be determined based on the measurements performed in the initial stage of construction. That method allows to predict exceeding of the critical force in the initial stage of construction and gives a possibility to reduce it (for example by ballasting shell).

REFERENCES

1. Machelski Cz. Janusz L.: *Estimation of bending moments acting in the crown of a soil-steel bridge structure during backfilling*, ECCS European Convention for Constructional Steelwork, (2011). s. 1365-1370.
2. Antoniszyn G.: *Mostowe konstrukcje gruntowo-powłokowe : siły wewnętrzne w powłokach mostów gruntowo-powłokowych typu SUPER-COR*, Geoinżynieria, Drogi, Mosty, Tunele. (2008), nr 3, s. 58-60.
3. Machelski Cz.: *Modelowanie mostowych konstrukcji gruntowo-powłokowych*, Dolnośląskie Wydawnictwo Edukacyjne, Wrocław 2008.
4. Pettersson L.: Full *Scale Tests and Structural Evaluation of Soil Steel Flexible Culverts with low Height of Cover*, Doctoral Thesis, KTH , Sweden 2007.

PROGNOZOWANIE MOMENTÓW ZGINAJĄCYCH W KLUCZU KONSTRUKCJI GRUNTOWO-POWŁOKOWYCH BUDOWANYCH JAKO PRZEJŚCIA EKOLOGICZNE DLA ZWIERZĄT

S t r e s z c z e n i e

Praca dotyczy konstrukcji gruntowo-powłokowych wykonanych z wiotkiej powłoki (przeważnie blacha falista) oraz zasypki gruntowej. Podczas zasypywania konstrukcja deformuje się w znacznym stopniu (wypiętrza się góra powłoki i zwęża na szerokości). Zjawisko to przekłada się na późniejszy efekt sprężenia, gdy grunt układamy nad kluczem powłoki. W artykule zaproponowano metodę wyznaczania momentu zginającego w kluczu powłoki, który jest głównym czynnikiem wpływającym na naprężenia w stalowej powłoce. Wyniki otrzymane metodą in-situ zostały porównane z wynikami otrzymanymi w programie MES. Z badań nad różnymi kształtami powłok wyciągnięto wnioski oraz otrzymano krzywe potrzebne do szacowania momentów zginających w kluczu powłoki. Znaleziono zależności które pomogą w opracowaniu metodyki wyznaczania sił wewnętrznych w kluczu powłok o różnej geometrii. Badania pomogą projektować tego typu konstrukcje oraz pozwolą na zapobieganie występowania krytycznych sił w powłoce w trakcie budowy.

CIVIL AND ENVIRONMENTAL ENGINEERING REPORTS

No. 10 2013

DETERMINATION OF RELIABLE CONCENTRATIONS OF POLLUTANTS IN RAW WASTEWATER BASED ON DIFFERENT SAMPLING METHODS

Sylwia MYSZOGRAJ[*1], Zofia SADECKA[1], Omar QTEISHAT[2], Monika SUCHOWSKA-KISIELEWICZ[1]

[1] University of Zielona Góra, Institute of Environmental Engineering
Szafrana st 15, 65-516 Zielona Góra, Poland

[2]Al-Balqua' Applied University, Zarka University College, Jordan

The aim of this study was to check the extent to which the sampling method and the volume of sewage (size of the wastewater treatment plant) influence the determined daily average concentrations of pollution components. Within three days of dry weather, the composition of two raw sewage wastewater treatment plants was continuously monitored. The WWTPs were designed for the flow of 820 m^3/d and 51000 m^3/d, respectively. The concentrations of pollutants were measured in samples taken both in time-proportional and flow-proportional ways. The obtained values show the possibility of taking the samples mixed at equal time intervals and in proportion to the flow as reliable sources for design values of concentrations. The size of WWTP, i.e. the amount of investigated raw sewage, was of no significant importance to the obtained results regarding concentrations of pollutants.

Keywords: sampling, raw sewage, pollution loads, desing of wastewater treatment plant

1. INTRODUCTION

Amendments and adaptation of legal regulations to the EU requirements forces operators of sewage treatment plants to carry out precise measurements of quantity and analysis of physical-chemical composition of sewage. Technical progress and abundant offer of devices allows to meet these requirements. Yet, usefulness of measurement results for further processing is determined by accuracy of measuring devices and skills of the analyst who performs the test, but also but whether the sample can be considered a representative sample. Lack

* Corresponding author. E-mail: S.Myszograj@iis.uz.zgora.pl

of „good measuring material" is the reason why, despite state-of-the-art devices and qualified staff, test results frequently can not be considered reliable. Devices which help meeting of the reliability criterion, and furthermore, significantly facilitate the laboratory technicians' work, are samplers.

In accordance with the Polish Norm PN – ISO 5667 – 10, 1997 „Water quality, Sampling, Guidelines for sewage sampling", there are:

- Random samples - indicating physical-chemical parameters of the sewage at the moment of sampling.
- Qualified random samples – consisting of at least 5 samples. Interval between individual sampling must be at least 2 minutes long, whereas the duration of such sampling cannot exceed 2 hours. A qualified random sample, taken and analysed regularly, provides somewhat more complete quality image of the measured utility. A definite drawback of this sort of sampling are its time and labour requirements.
- Time-proportional samples – are characterized by taking of a small sample volume, performed at specified and permanent intervals. Such form of sampling does not take into account changes in the flow rate. Yet for an accepted, possibly short, interval, the taken sample is relatively representative. This method is characterised by the following features: regular sampling, permanent volume of single samples and permanent frequency of sampling.
- Quantitative-proportional samples – are characterized by combination of sampler with a flow meter. The are characterized by permanent size of the taken sample, perfumed at intervals which result from flow of specified volume of sewage. In order to control the sampler operation, a quantitative measurement signal is required. This type of sampling provides good and representative results, because it considers the actual flow.

  A drawback of this solution is the fact that there is no correlation between the taken sample and the contamination load (especially with high flow fluctuation). This problem occurs often in small sewage treatment plants, where at nigh-time, the flow drops almost to zero. In such situation, the sampling is performed at relatively long intervals, which can prevent disturbances in the plat operation from being recorded. Quantitative-proportional sampling is currently becoming increasingly popular. This method is characterised by the following features: sampling after a specified quantity has flown, constant volume of single samples and changeable frequency of sampling.
- Flow-proportional samples – are taken by combining sampler with a flowmeter. Such mode of sampling is characterized by collection of variable volume of a single sample, depending on the current flow.

Moreover, the sample – as in the time-proportional mode – is taken at constant intervals.

This method of sampling provides very good, representative results, and the results are the best with fluctuating flow and variable contamination load. Unlike the quantitative-proportional sampling, here the sample is taken even if the flow is very low. In practice, this means a possibility of detecting all disturbances in the treatment plant operation. This method is characterised by the following features: changeable volume of single samples and permanent frequency of sampling.

– Event-proportional samples – make use of samplers cooperating with appropriate meter, e.g. pH. In this mode, the sampler waits for an „event" Only when this event occurs, the sampling is initiated. An impulse which triggers the sampling can be exceeding of a boundary value (e.g. liquid level, pH, conductivity, etc.) As long as the "event" lasts, the sampling is performed at specified intervals.

  This sort of sampling is particularly recommended for sewage quality control, as long as we are not interested in the very fact of exceeding some boundary values, but rather in the reason of such state of affairs. With the previously described modes of sampling, seizing a sample taken during the "event" is difficult. This method is characterised by the following features: sampling depending on the event, permanent volume of single samples and permanent frequency of sampling.

– Combined sampling programs, i.e. event-proportional sampling can be made parallel to other modes (e.g. with the quantitative-proportional method). Advances of the combined mode are the resultant of the employed, single modes of the sampler operation. This method is characterized by the following trait: combination of time-related, quantitative and event-based criteria of sampling.

Modernization works and optimization of sewage treatment technologies as well as treatment plant classification expressed with PE (equivalent of population) require determining of equivalent contamination loads, which shall be the basis for further calculations and studies. An optimal solution for measurement for quantity of sewage and determination of physical-chemical composition of the sewage, and, as a result, of contamination loads, is a permanent measurement (on-line) of flow and concentration of factors significant for operation of the treatment plant. As long as the flow measurement is not difficult, systems which measure concentrations are still rather unpopular, due to technical capabilities and costs.

In the case of an existing system of sewerage – treatment plant – receiver, an archival database, containing information about volume and composition of sewage which comes into the treatment plant, is used.

An order of the Minister of environment regarding requirements for introducing sewage into waters or ground, and regarding substances particularly harmful for water environment (Journal of Laws 2006, no. 137, item 984), as well as Directive 91/271/EEC regarding treatment of municipal sewage state that representative values of concentration are those indicated in medium samples resulting from mixed samples, taken manually or automatically within 24 hours, at intervals not longer than 2 hours, proportional to the sewage flow. Yet, automatic samplers in treatment plants usually take time-proportional samples, at regular intervals (as a rule every 2h), a constant volume of single raw sewage samples is taken, which are then merged.

The aim of this study was to check the extent to which the sampling method and the volume of sewage (size of the wastewater treatment plant) influence the determined daily average concentrations of pollution components.

2. MATERIAL AND METHODS

Monitoring of the quality and quantity of raw sewage carried out in two wastewater treatment plants: designed for flow of 820 m^3/d (WWTP1) and 51 000 m^3/d (WWTP2). Sampling and measurement was performed within three days (Monday, Tuesday, Wednesday) of dry weather.

Every two hours, starting from 7^{00} on the first day of research, a raw sewage sample was taken before the drum sieve, manually at WWTP1 and using automatic sampler at WWTP2. Physical-chemical parameters within the range of: total suspension, BOD_5, COD, TKN, $N\text{-}NH_4^+$, total phosphorus (P_{tot}) were marked in each of the 12 samples during subsequent days of monitoring.

3. RESULTS

3.1. Quantity of sewage

The volume of sewage influent into the WWTP1 within three days of permanent monitoring varied between 347 and 424 m^3/d, whereas the volume of sewage delivered via vacuum trucks within 24 hours was 10 to 28 m^3/d. The share of the delivered sewage in the general volume of sewage influent into the wastewater treatment plant within two hours did not exceed 12%.

Whereas WWTP2 received from 14287 m^3/d to 14720 m^3/d, and the share of the delivered sewage was 2,9 to 3,7%. Oscillations of raw sewage inflow to WWTP1 and WWTP2 within 24 hours are presented in Fig. 1.

Within three days of testing, the amount of sewage flowing into a WWTP1 varied from 3 m^3/h to 33 m^3/h, and for WWTP2 from 338 m^3/h to 784 m^3/h. In both wastewater treatment plant after 11PM the quantity of sewage decreased to about 25% of maximum flow. Hourly average of quantity of sewage was 16 m^3/h and 607 m^3/h, for WWTP1 and WWTP2 respectively.

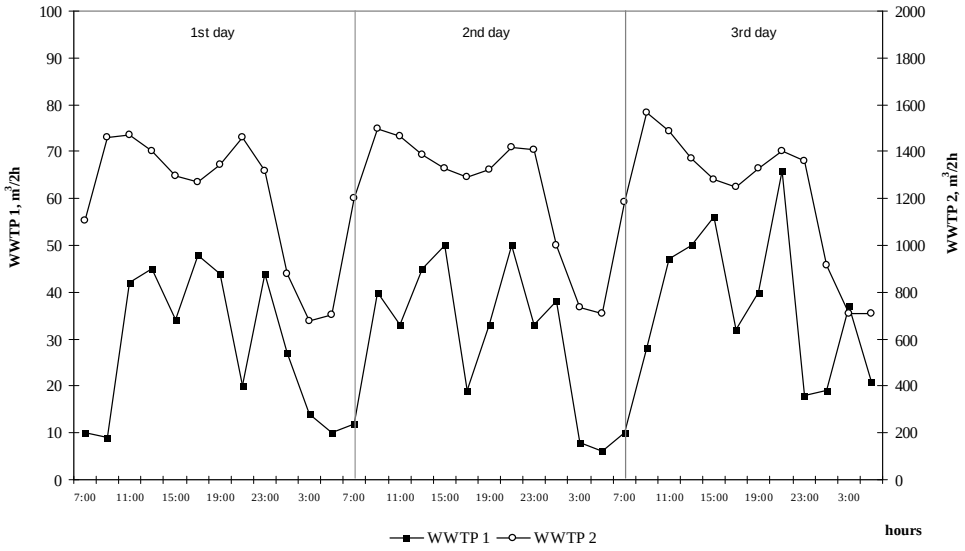

Fig. 1. Changes in raw sewage inflow to WWTP 1 and WWTP 2

3.2. Characteristic of raw sewage

Pollution concentration values, marked in raw sewage sampled in WWTP1 and WWTP2 are presented in Table 1.

Data analysis explicitly indicates high unevenness of volume and concentration of raw sewage for WWTP1, as well as values of pollution index concentration higher, than for WWTP2, which could be caused by significant share of delivered sewage. In particular, these differences were observed for concentration of TKN, ammonia nitrogen, and total phosphorus.

Were also found large changes in concentrations of pollutants in raw wastewater. For example, COD determined in instantaneous samples collected every 2 hours changed in the range from 640 mg/dm^3 to 1840 mg/dm^3 and from 240 mg/dm^3 to 1040 mg/dm^3, for WWTP1 and WWTP2 respectively.

On the basis of the obtained pollution concentrations in 12 samples for each day, average daily concentrations were calculated, which, in accordance with the Polish Norm PN-ISO 5667-10, reflect values marked in time-proportional and flow-proportional samples (table 2).

Table 1. Characteristic of raw sewage influent to WWTP 1 and WWTP 2

Time of sampling		WWTP1						WWTP2						
		Flow $m^3/2h$	COD	TKN	N-NH_4	P_{tot}	Total suspens.	Flow $m^3/2h$	COD	BOD_5	TKN	N-NH_4	P_{tot}	Total suspens.
			mg/dm^3						mg/dm^3					
1st day	7^{00}	10	960	175	90	45	630	1108	440	189	98	54	11	720
	9^{00}	9	640	140	78	44	822	1461	480	226	70	41	11	890
	11^{00}	42	1560	196	176	68	646	1470	520	152	70	42	9	360
	13^{00}	45	1560	154	123	42	730	1401	640	263	70	58	7	480
	15^{00}	34	1200	182	106	42	492	1298	520	226	70	46	7	160
	17^{00}	48	1560	280	238	41	588	1270	480	152	56	54	6	400
	19^{00}	44	1680	140	91	35	522	1346	840	374	70	56	21	680
	21^{00}	20	1840	126	86	41	992	1462	600	263	56	50	8	500
	23^{00}	44	1840	126	94	39	516	1317	440	189	56	51	6	800
	1^{00}	27	1440	126	89	49	894	878	400	115	56	53	3	920
	3^{00}	14	1480	112	97	35	1360	676	440	189	56	47	2	380
	5^{00}	10	1760	154	93	38	754	704	400	189	56	44	4	860
2nd day	7^{00}	12	1120	119	93	34	378	1201	560	115	112	63	7	780
	9^{00}	40	820	112	92	31	728	1496	680	152	70	52	7	240
	11^{00}	33	1080	147	144	51	976	1464	1040	152	56	51	8	1040
	13^{00}	45	1380	112	112	44	778	1385	320	189	98	54	5	1080
	15^{00}	50	1120	147	113	32	236	1328	680	152	70	57	5	580
	17^{00}	19	1260	105	88	27	324	1293	600	189	56	49	6	300
	19^{00}	33	1320	105	92	38	516	1323	800	263	56	53	6	300
	21^{00}	50	1340	105	82	42	520	1417	320	226	70	58	4	220
	23^{00}	33	1120	105	85	39	564	1408	800	78	56	45	3	600
	1^{00}	38	1320	105	95	36	356	999	320	26	70	48	3	400
	3^{00}	8	1120	112	84	43	448	733	240	152	56	48	2	880

	5^{00}	6	1040	105	85	44	214	707	240	189	70	54	3	200
3rd day	7^{00}	10	736	105	78	27	338	1185	880	203	84	42	16	860
	9^{00}	28	848	112	83	24	154	1568	840	203	98	44	5	880
	11^{00}	47	1088	140	132	33	618	1489	560	175	84	38	3	940
	13^{00}	50	688	119	97	28	298	1371	480	148	56	41	3	460
	15^{00}	56	896	140	103	22	300	1282	560	175	84	42	3	160
	17^{00}	32	928	119	94	35	622	1247	720	312	56	45	2	360
	19^{00}	40	880	112	78	19	444	1330	680	230	70	43	5	840
	21^{00}	66	928	105	77	26	414	1401	320	148	56	44	3	100
	23^{00}	18	1136	112	74	29	728	1359	240	203	56	43	4	400
	1^{00}	19	896	105	71	29	202	914	560	175	56	42	2	600
	3^{00}	37	864	140	80	37	220	710	560	120	42	36	2	600
	5^{00}	21	896	123	78	29	224	709	560	94	56	40	10	900

Table 2. Average daily values of pollution concentrations determined for flow-proportional samples and time-proportional samples

Parameter/test type		WWTP1			WWTP2		
		1st day	2nd day	3rd day	1st day	2nd day	3rd day
COD mg/dm^3	flow-proportional sample	1536	1189	899	532	585	580
	time-proportional sample	1460	1170	899	516	550	580
	difference between methods of sampling	4,9%	1,6%	0,0%	3,0%	6,0%	0,0%
BOD_5 mg/dm^3	flow-proportional sample	-	-	-	217	159	188
	time-proportional sample	-	-	-	210	157	182
	difference between methods of sampling	-	-	-	3,2%	1,3%	3,2%
TKN mg/dm^3	flow-proportional sample	169	117	122	66	70	69
	time-proportional sample	159	115	119	65	70	67
	difference between methods of sampling	5,9%	1,7%	2,5%	1,1%	0,0%	3,2%
$N\text{-}NH_4$ mg/dm^3	flow-proportional sample	127,0	100,0	91,0	49,8	52,9	41,9
	time-proportional sample	113,0	97,0	87,0	49,8	52,7	41,6
	difference between methods of sampling	11,0%	3,0%	4,4%	0,0%	0,4%	0,7%
P_{tot}	flow-proportional sample	43,9	38,4	28,1	8,3	5,2	4,7

mg/dm^3	time-proportional sample	43,1	38,4	27,8	7,7	5,0	4,7
	difference between methods of sampling	1,8%	0,0%	1,1%	7,2%	3,8%	0,0%
Total suspension mg/dm^3	flow-proportional sample	680	540	382	583	557	583
	time-proportional sample	745	503	380	596	552	592
	difference between methods of sampling	-9,6%	6,9%	0,5%	-2,2%	0,9%	-1,5%

Determined authoritative concentrations of pollutants in the wastewater influent to analyzed wastewater treatment plant were different in the subsequent days of measurement for both: time-proportional and flow-proportional samples.

For both WWTP the highest values concentration of pollutions were obtained in the first day of testing (on Monday), irrespective of the method of sampling.

4. CONCLUSIONS

The calculated differences between values calculated for flow-proportional and time-proportional samples are 0 to 11%, but for most samples they come to about 4%. This indicates good assessment of the reliable concentration values, both for sampling of permanent sewage volumes at regular intervals, and for volumes proportional to the flow.

There was also no evidence of any significant influence of the size of the treatment plant, and thus unevenness of raw sewage inflow, on the calculated pollution concentration values.

It is also obvious that pollution concentrations specified in random samples reflect the physical-chemical parameters of the sewage at the moment of sampling, and in no circumstances can they be a foundation for calculations which require reliable concentrations. For example, concentration of TKN marked within the first 24 hours of the monitoring for WWTP1 changed from 112 to 280 mg/dm^3. Such a large range of values indicates the possibility of making significant errors in the design, if you will be taken into account the instantaneous values. On the other hand, it is important to provide buffering capacity of the inequality of pollutants influent into wastewater treatment plant.

REFERENCES

1. Rozporządzenie Ministra Środowiska z dnia 24 lipca 2006r. w sprawie warunków, jakie należy spełnić przy wprowadzaniu ścieków do wód lub ziemi, oraz w sprawie substancji szczególnie szkodliwych dla środowiska wodnego, (Dz. U. 2006 nr 137 poz. 984) z póź. zm.
2. PN-ISO5667-10,1997 *Jakość wody. Pobieranie próbek. Wytyczne pobierania próbek ścieków.*

WYZNACZANIE MIARODAJNYCH STĘŻEŃ ZANIECZYSZCZEŃ W ŚCIEKACH SUROWYCH W OPARCIU O RÓŻNE METODY POBORU PRÓBEK

S t r e s z c z e n i e

Nowelizacja i dostosowywanie przepisów prawnych do wymagań UE wymusza na eksploatatorach oczyszczalni ścieków wykonywanie precyzyjnych pomiarów ilości i analiz składu fizyko-chemicznego ścieków. Postęp techniczny oraz bogata oferta producentów urządzeń umożliwia sprostanie tym wymaganiom. Jednak o przydatności wyników pomiarowych do projektowania oczyszczalni ścieków obok dokładności urządzeń pomiarowych decyduje fakt, czy próbkę ścieków można uznać za próbkę reprezentatywną. Często pomimo najnowocześniejszych urządzeń i wykwalifikowanego personelu wyniki badań nie mogą być traktowane wiarygodnie.

W artykule na podstawie pomiarów ilości i analiz składu ścieków surowych zweryfikowano w jakim stopniu metoda poboru próbek oraz ilość dopływających ścieków (wielkość oczyszczalni ścieków) wpływa na wartość wyznaczonych średniodobowych stężeń wskaźników zanieczyszczeń. W ciągu trzech dób w pogodzie suchej przeprowadzono ciągły monitoring składu ścieków surowych w oczyszczalniach zaprojektowanych na przepływ 820 m^3/d (OŚ1) i 51000 m^3/d (OŚ2). W próbkach zbieranych czasowo-proporcjonalnie i przepływowo-proporcjonalnie wyznaczono stężenia miarodajne wskaźników zanieczyszczeń. Uzyskane wartości wskazują na możliwości przyjmowania do projektowania stężeń miarodajnych wyznaczonych w próbkach zlewanych w jednakowych interwałach czasowych, jak i proporcjonalnie do przepływu. Nie stwierdzono również istotnego wpływu wielkości oczyszczalni, a tym samym nierównomierności dopływu ścieków surowych na obliczone wartości stężeń wskaźników zanieczyszczeń.

CIVIL AND ENVIRONMENTAL ENGINEERING REPORTS

No. 10 2013

APPLICATION OF FUNDAMENTAL SOLUTIONS TO THE STATIC ANALYSIS OF THIN PLATES SUBJECTED TO TRANSVERSE AND IN-PLANE LOADING

Zdzisław PAWLAK*
Institute of Structural Engineering
Poznan University of Technology, Piotrowo 5, 61-138 Poznań

In this paper static analysis of Kirchhoff plates is considered. A transverse and in-plane loading is taken into consideration. The Finite Strip Method is used and the suitable fundamental solutions are applied. According to the finite strip method a continuous structure is divided into a set of identical elements simply supported on opposite edges. The unknowns are deflections and transverse slope variables along the nodal lines. The finite difference formulation is applied to express the equilibrium conditions of the discrete system. This reduces the number of degrees of freedom. The solution of a difference equation of equilibrium yields the fundamental function of the considered plate strip. The fundamental solution derived in this way, can be used to solve the static problem of a finite plate in the analogous way as the boundary element method is applied for continuous systems.

Keywords: Fundamental solutions, finite strip method, Kirchhoff plates, initial stability and static analysis

1. INTRODUCTION

The Finite Strip Method (FSM) was created as a numerical tool to solve specific engineering problems [8, 9]. This method is the alternative to the most popular Finite Element Method. Application of FSM does not require high number of degrees of freedom. The choice of the FSM to analyse structures requires finding and applying some types of functions called fundamental functions or fundamental solutions. A fundamental solution describes the behaviour of an infinite structure in the sense of generalized displacements and forces caused by a specific type of external loading.

* Corresponding author. E-mail: zdzislaw.pawlak@put.poznan.pl

The Boundary Element Method (BEM) which is often used in the thin and thick plates theory [2, 7, 11], was used to establish the critical forces. For the initial stability problem, the modified approach to the thin plate analysis with an assumed physical boundary condition was proposed by Guminiak and Sygulski [5], and also Guminiak [4]. Modelling of the plate bending problem with in-plane loading requires a modification of the governing boundary integral equation. It is necessary to introduce a set of internal collocation points in which the plate curvature should be found. The analysis of plates with a wide range of arbitrary shapes by BEM was discussed by Katsikadelis [6]. The author used the Analog Equation Method combined with BEM to establish distribution of in-plane forces, calculate critical forces and solve static problem with known in-plane forces. He presented the classic formulation of thin plate bending with corner concentrated forces and equivalent shear forces.

In this paper the critical forces were derived using the boundary element method and the procedure described by Guminiak [4, 5]. Moreover, the critical forces were derived analytically using the formula given in [12]. The static analysis based on the finite strip method (FSM) of an infinite plate strip with transverse and normal loading leads to the fundamental functions for the considered structure. A plate structure infinite in one direction, simply supported on its opposite edges is considered. The plate strips with such boundary conditions are commonly applied as bridge structures, as box or plate elements.

2. STATIC ANALYSIS OF A PLATE

According to the finite strip method [8] the continuous body is approximated by the regular mesh of identical finite strips of arbitrary width b and length L (see Fig. 1).

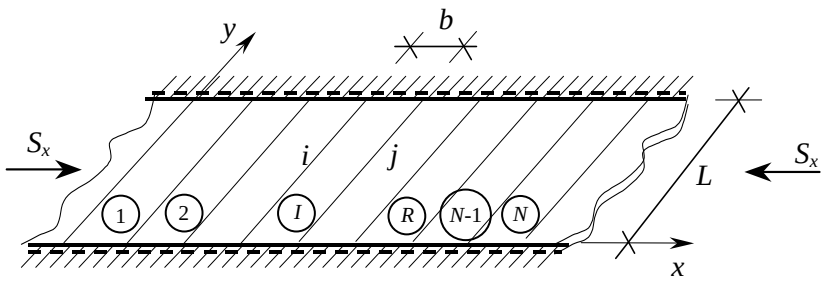

Fig. 1. An infinite plate strip discretization

The unknowns are deflections and transverse slope amplitudes along the nodal lines. Assuming a simply supported, four-degree-of-freedom finite strip for discretization (Fig. 2),

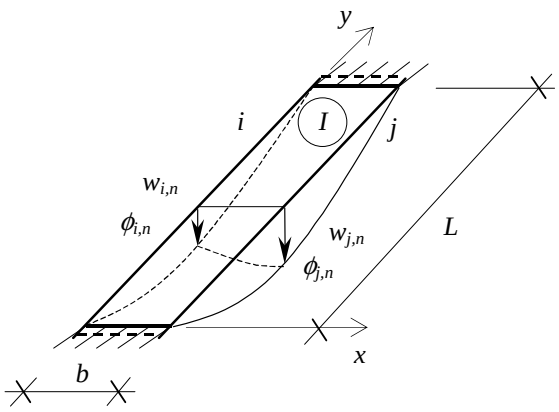

Fig. 2. A finite plate strip

the field of displacements for an arbitrary strip *I* is expressed in the combined form of harmonic series expansion:

$$w^I(x,y)=\sum_{n=1}^{\infty}\mathbf{N}\cdot\mathbf{q}_n^I\cdot\sin\frac{n\pi y}{L} \tag{1}$$

where: $\mathbf{q}_n^I=\left[w_{i,n}\ \ \phi_{i,n}\ \ w_{j,n}\ \ \phi_{j,n}\right]^T$ is the vector of displacement amplitudes for *n*–th harmonic, $\mathbf{N}=[N_1\ \ N_2\ \ N_3\ \ N_4]^T$ is the shape functions vector consisting of the well-known Hermite polynomials:

$$N_1=1-\frac{3x^2}{b^2}+\frac{2x^3}{b^3},\ \ N_2=x-\frac{2x^2}{b}+\frac{x^3}{b^2},$$
$$N_3=\frac{3x^2}{b^2}-\frac{2x^3}{b^3},\ N_4=-\frac{x^2}{b}+\frac{x^3}{b^2}. \tag{2}$$

For another boundary conditions of a finite strip one may use more complex trigonometrical functions in equation (1), i.e. for clamped edges $w^I(x,y)=\sum_{n=1}^{\infty}\mathbf{N}\cdot\mathbf{q}_n^I\cdot\frac{1}{2}\left(1-\cos\frac{2n\pi y}{L}\right)$. The total displacements at the *i*-th nodal line may be derived as the sum of amplitudes obtained for an arbitrary *n*-th element of the harmonic series:

$$w_i = \sum_{n=1}^{\infty} w_{i,n} \cdot \sin\frac{n\pi y}{L} \ , \ \ \phi_i = \sum_{n=1}^{\infty} \phi_{i,n} \cdot \sin\frac{n\pi y}{L} \ , \ \ \phi_i = \frac{\partial w_i}{\partial x}. \tag{3}$$

Using the displacement functions (1) in the minimization procedure for the potential energy formula:

$$U_p^I = \frac{1}{2}\int_0^L\int_0^b \left(- M_x(w)\frac{\partial^2 w}{\partial x^2} - M_y(w)\frac{\partial^2 w}{\partial y^2} + 2M_{xy}(w)\frac{\partial^2 w}{\partial x \partial y} + S_x(w)\frac{\partial w}{\partial x} \right) dxdy \,, \tag{4}$$

we obtain the set of infinite number of linear equations:

$$\sum_{I=-\infty}^{\infty} \mathbf{K}^I \cdot \mathbf{q}^I + \sum_{I=-\infty}^{\infty} \mathbf{G}^I \cdot \mathbf{q}^I = \mathbf{P}^I \,, \tag{5}$$

where: $M_x(w)$, $M_y(w)$, $M_{xy}(w)$ are appropriate bending moments, $S_x(w)$ is the axial force, $\mathbf{q}^I = \left[w_i \ \ \phi_i \ \ w_j \ \ \phi_j \right]^T$ and $\mathbf{P}^I = \left[T_i \ \ m_i \ \ T_j \ \ m_j \right]^T$ are the displacement and force vectors for *I*-th strip, respectively, $\mathbf{K}^I$ is the stiffness matrix and $\mathbf{G}^I$ is the geometrical matrix of the finite strip element.

2.1. The element geometrical matrix

The geometrical matrix **G** for the finite strip of width *b* (see Fig. 2) can be derived from the expression:

$$\mathbf{G}^I = \int_0^b\int_0^L \mathbf{B}^T \cdot \mathbf{S} \cdot \mathbf{B} \, dy \cdot dx \,, \tag{6}$$

where:

$$\mathbf{B} = \begin{bmatrix} \mathbf{N}_{,x} \\ \mathbf{N}_{,y} \end{bmatrix}, \ \ \mathbf{S} = \begin{bmatrix} \sigma_{xx} & \sigma_{xy} \\ \sigma_{xy} & \sigma_{yy} \end{bmatrix}, \tag{7}$$

σ_i are membrane stresses (constant across the plate thickness) produced by the in-plane forces acting at the finite strip borders. Using the equation (2) in the equation (6) leads to the geometrical matrix for any (*I*-th) finite element:

$$\mathbf{G}^I = \frac{S_x}{120hb} \begin{bmatrix} 72 & 6b & -72 & 6b \\ 6b & 8b^2 & -6b & -2b^2 \\ -72 & -6b & 72 & -6b \\ 6b & -2b^2 & -6b & 8b^2 \end{bmatrix}, \tag{8}$$

where *h* is the plate thickness.

2.2. The element stiffness matrix

The element stiffness matrix for a four-degree-of-freedom *I*-th strip can be derived from:

$$\mathbf{K}^I = \int_0^b \int_0^L \mathbf{B}^T \cdot \mathbf{D} \cdot \mathbf{B}\, dy \cdot dx\,, \tag{9}$$

where:

$$\mathbf{D} = \begin{bmatrix} D_x & D_1 & 0 \\ D_1 & D_y & 0 \\ 0 & 0 & D_{xy}/2 \end{bmatrix}.$$

The above mentioned flexural stiffness parameters for an orthotropic plate are:

$$\begin{gathered} D_x = \frac{E_x h^3}{12(1-\nu_{\mathrm{p}}^2)},\ D_y = \frac{E_y h^3}{12(1-\nu_{\mathrm{p}}^2)}, \\ D_1 = \frac{\nu_{\mathrm{p}}^2 \cdot (D_x + D_y)}{2},\ D_{xy} = \frac{(1-\nu_{\mathrm{p}}^2)\cdot (D_x + D_y)}{2}. \end{gathered} \tag{10}$$

In the case of an isotropic plate these coefficients (10) have simpler form:

$$D = D_x = D_y = \frac{Eh^3}{12(1-\nu_{\mathrm{p}}^2)},\ D_1 = \nu_{\mathrm{p}} \cdot D,\ D_{xy} = (1-\nu_{\mathrm{p}}^2)\cdot D, \tag{11}$$

where: E is the Young's modulus and ν_{p} is the Poisson's ratio.

After some operations the stiffness matrix takes the form:

$$\mathbf{K_n} = \alpha_1 \cdot \mathbf{K_1} + \alpha_2 \cdot \mathbf{K}_2 + \alpha_3 \cdot \mathbf{K}_3 + \alpha_4 \cdot \mathbf{K}_4 \tag{12}$$

where $\mathbf{K}_i$ are number matrices:

$$\mathbf{K}_1 = \begin{bmatrix} 156 & 22b & 54 & -13b \\ 22b & 4b^2 & 13b & -3b^2 \\ 54 & 13b & 156 & -22b \\ -13b & -3b^2 & -22b & 4b^2 \end{bmatrix} \quad \mathbf{K}_2 = \begin{bmatrix} 6 & 3b & -6 & 3b \\ 3b & 2b^2 & -3b & b^2 \\ -6 & -3b & 6 & -3b \\ 3b & b^2 & -3b & 2b^2 \end{bmatrix} \tag{13a}$$

$$\mathbf{K}_3 = \begin{bmatrix} 36 & 18b & -36 & 3b \\ 18b & 4b^2 & -3b & -b^2 \\ -36 & -3b & 36 & -18b \\ 3b & -b^2 & -18b & 4b^2 \end{bmatrix} \quad \mathbf{K}_4 = \begin{bmatrix} 36 & 3b & -36 & 3b \\ 3b & 4b^2 & -3b & -b^2 \\ -36 & -3b & 36 & -3b \\ 3b & -b^2 & -3b & 4b^2 \end{bmatrix} \tag{13b}$$

α_i are coefficients depending on physical and geometrical parameters of the considered structure:

$$\alpha_1 = \frac{\alpha_n^4 LbD_x}{840},\ \alpha_2 = \frac{LD_y}{b^3},\ \alpha_3 = \frac{\alpha_n^2 LD_1}{30b},\ \alpha_4 = \frac{\alpha_n^2 LD_{xy}}{30b},\ \alpha_n = \frac{n\pi}{L}. \tag{14}$$

2.3. The equilibrium equations

The equilibrium equations are derived applying the finite element methodology. Having derived the element geometrical (8) and stiffness (12) matrices the equilibrium equations for the *n*-th harmonic element, after assembling two adjacent elements *R*-th and (*R*+1)-th (Fig. 3) are of the form:

$$\begin{aligned} T_{r,r-1} + T_{r,r+1} &= P_r \\ m_{r,r-1} + m_{r,r+1} &= m_r \end{aligned} \tag{15}$$

where $T_{i,j}$ and $m_{i,j}$ are forces derived for each element using equation (5).

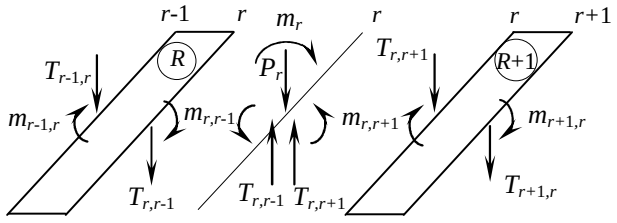

Fig. 3. Forces acting at a nodal line *r*

For a regular system the equilibrium conditions (15) can be written in the form of difference equations equivalent to the FEM matrix formulation [9]:

$$\begin{cases} \left[\beta_1 \Delta^2 + \beta_0\right] \cdot w_r - \beta_2 \left(E - E^{-1}\right) \cdot \phi_r = \beta_p \cdot P_r \\ \beta_2 \left(E - E^{-1}\right) \cdot w_r + \left[\beta_3 \Delta^2 + \beta_4\right] \cdot \phi_r = \beta_m \cdot m_r \end{cases} \tag{16}$$

where:

$\beta_p = \sin(y_p, \alpha_n)$, $\beta_m = \sin(y_m, \alpha_n)$, $\beta_0 = 420\alpha_1$, $\alpha_g = \dfrac{S_x}{120bhD_x}$,

$$\begin{aligned}
\beta_1 &= 6(9\alpha_1 - \alpha_2 - 6\alpha_3 - 6\alpha_4 - 12\alpha_g) , \\
\beta_2 &= b(13\alpha_1 - 3\alpha_2 - 3\alpha_3 - 3\alpha_4 - 6\alpha_g) , \\
\beta_3 &= b^2(-3\alpha_1 + \alpha_2 - \alpha_3 - \alpha_4 - 2\alpha_g) , \\
\beta_4 &= 2b^2(\alpha_1 + 3\alpha_2 + 3\alpha_3 + 3\alpha_4 + 6\alpha_g) ,
\end{aligned} \tag{17}$$

E^n is the shifting operator (see [1]):

$$\begin{aligned}
E^n(f_r) &= f_{r+n} , \\
\Delta_r^2 = \Delta^2 &= (E + E^{-1} - 2)
\end{aligned} \tag{18}$$

is the second-order difference operator

$$\Delta_r^2 f_r = (E + E^{-1} - 2) f_r = f_{r+1} + f_{r-1} - 2f_r , \tag{19}$$

α_i are the functions of harmonic number *n* given by (14), P_r and m_r are the forces and moments acting at the nodal line *r* (with co-ordinates y_p and y_m, respectively). After elimination of the slope function ϕ_r, the equilibrium conditions are transformed into one fourth-order difference equation with one unknown w_r (nodal transverse displacement amplitude for the *n*-th harmonic):

$$\left[B_4\Delta^4 + B_2\Delta^2 + B_0\right] w_r = \beta_p\left[\beta_3\Delta^2 + \beta_4\right] \cdot P_r + \beta_2\beta_m\left(E - E^{-1}\right) \cdot m_r \tag{20}$$

where:

$$B_0 = \beta_0\beta_4 \ , \ B_2 = \beta_0\beta_3 + \beta_1\beta_4 + 4\beta_2^2 \ , \ B_4 = \beta_1\beta_3 + \beta_2^2 \tag{21}$$

For the regular infinite plate strip, equation (20) is equivalent to the set of infinite number of equilibrium conditions derived using the finite strip methodology (FSM). The solution of this equation enables one to determine the state of deformation of the entire considered structure.

3. THE FUNDAMENTAL SOLUTION

Solution of the finite difference equilibrium equation (20) yields the fundamental functions for the considered system. In order to solve the static

problem of the structure loaded by the force $P_0 = P_r \delta_{r,0} = P \cdot \delta_{r,0}$ ($M_r = 0$, $\delta_{r,0}$ – Kronecker delta) we use the discrete Fourier transform in *x* direction [10]:

$$F\left[f_r\right] = \tilde{f}(\alpha) = \sum_{r=-\infty}^{\infty} f_r \; e^{ir\alpha} \;,$$
$$F^{-1}\left[\tilde{f}(\alpha)\right] = f_r = \frac{1}{2\pi}\int_{-\pi}^{\pi} \tilde{f}(\alpha)\, e^{-ir\alpha} \cdot d\alpha \;. \tag{22}$$

Applying both transforms (22) to the equilibrium equation (20) yields the formula:

$$w_r = \frac{P}{\pi}\int_0^{\pi} \frac{(S_1 \cos(\alpha) + S_2)\cos(r\alpha)}{\cos^2(\alpha) + B_m \cos(\alpha) + C_m} \cdot d\alpha \;, \tag{23}$$

where:

$$B_m = (B_2 - 4B_4)/(2B_4) \;,\; C_m = (4B_4 - 2B_2 + B_0)/(4B_4),$$
$$S_1 = \beta_3\beta_p/(2B_4) \;,\; S_2 = (\beta_4 - 2\beta_3)\beta_p/(4B_4) \;. \tag{24}$$

The solution, i.e. the nodal displacement amplitude may be expressed in the form of the following recurrent relation:

$$w_r = \frac{P}{\pi}\left[S_1 \cdot F_1(r) + S_2 \cdot F_2(r)\right] \tag{25}$$

where

$$F_1(r) = 2^{r-1} \cdot C(r+1) - \binom{r}{1} 2^{r-3} \cdot C(r-1) + \\ + \frac{r}{2}\binom{r-3}{1} 2^{r-5} \cdot C(r-3) - \frac{r}{3}\binom{r-4}{2} 2^{r-7} \cdot C(r-5) + \ldots \tag{26}$$

$$F_2(r) = 2^{r-1} \cdot C(r) - \binom{r}{1} 2^{r-3} \cdot C(r-2) + \\ + \frac{r}{2}\binom{r-3}{1} 2^{r-5} \cdot C(r-4) - \frac{r}{3}\binom{r-4}{2} 2^{r-7} \cdot C(r-6) + \ldots \tag{27}$$

The integrals occurring in the above formula:

$$C(n)=\int_0^{\pi}\frac{\cos^n(\alpha)}{\cos^2(\alpha)+B_m\cos(\alpha)+C_m}\,d\alpha \tag{28}$$

can be easily solved in an analytical way. The formula (25) expresses the deflection amplitude along the nodal line r for an arbitrary n-th element of the harmonic series in a closed analytical form. From the equilibrium equations (16) the following relations for the transverse slope amplitudes are obtained:

$$\begin{aligned}\theta_1 &= -\frac{\beta_p P_r}{2\beta_2}+\frac{\beta_1}{\beta_2}w_1-\frac{2\beta_1-\beta_0}{2\beta_2}w_0,\\ \theta_{r+1} &= \frac{2\beta_3-\beta_4}{\beta_3}\theta_r-\theta_{r-1}-\frac{\beta_2}{\beta_3}(w_{r+1}-w_{r-1}).\end{aligned} \tag{29}$$

The functions of displacements at the nodal line r are in the form of the sums:

$$w(r,y)=\sum_{n=1}^{N}w_r(n)\cdot\sin\frac{n\pi y}{L},\quad \theta(r,y)=\sum_{n=1}^{N}\theta_r(n)\cdot\sin\frac{n\pi y}{L}, \tag{30}$$

where N is the number of harmonic elements, $w_r(n)$ and $\theta_r(n)$ are amplitudes obtained from (25) and (29), respectively.

The fundamental functions (30) for the infinite strip enable one to solve the static problem of a rectangular plate with finite dimensions, according to the indirect BEM.

4. NUMERICAL EXAMPLES

A problem of the initial stability of rectangular plates subjected to uniformly distributed loading q and compressive forces N_x is considered. All types of boundary conditions are introduced in the analysis.

The plate properties are as follows: Young's modulus E = 205 GPa, Poisson's ratio ν = 0.3. The number of finite strips chosen for discretization was 6 and 12. Analytical solutions for the problem of initial stability of Kirchhoff plates were evaluated basing on the procedures given by Girkmann [3], Timoshenko and Woinowsky-Krieger [13] and Timoshenko and Gere [12].

4.1. The square simply-supported plate

The square plate, simply-supported on all edges and subjected to the uniformly distributed transverse loading and constant loading acting in plane is considered. The plate dimensions are $l = l_x = l_y$ = 1.0 m, the plate thickness h = 0.02 m, the uniformly distributed transverse loading p = 100 kN/m^2 and the constant loading acting in-plane N_x (Fig. 4).

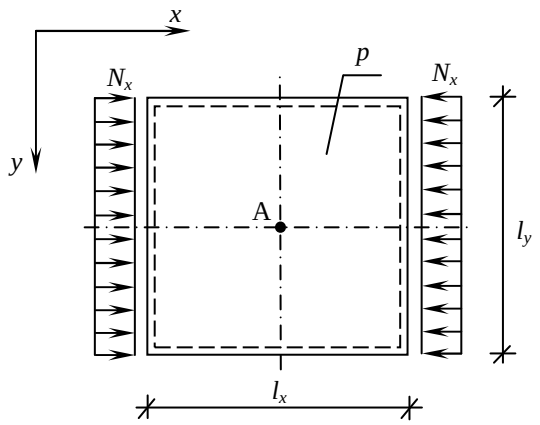

Fig. 4. Square, simply-supported plate subjected to the uniformly distributed loading p and constant loading in-plane N_x

The values of critical forces obtained using the analytical solution given in [12] and applying the BEM formulation presented in [5] are shown in Table 1. In the considered approach the plate boundary was divided into ten elements.

Table 1. The values of critical force

N_{cr} [kN/m]	Analytical solution	BEM solution
1	5928.993	5978.358
2	9264.052	9450.545
3	16.469.42	17102.466

The results obtained for the first critical force are presented in Table 2. The calculations were carried out for various values of in-plane loading. The constant loading N_x was assumed to be lower than the critical force.

Table 2. Deflection and bending moment at the point A

N_x	$w_A \cdot D/(pl^4)$	$M_x^A/(pl^2)$
0.0	0.004081	0.049700
$0.25 \cdot N_{cr}$	0.006903	0.070470
$0.50 \cdot N_{cr}$	0.012212	0.123610
$0.75 \cdot N_{cr}$	0.052933	0.533570

4.2. The square plate, simply-supported on two opposite edges with two clamped edges

In this example the square plate, simply-supported on two opposite edges with two clamped edges, subjected to the uniformly distributed transverse loading and constant loading acting in plane is considered. The plate dimensions are $l = l_x = l_y = 1.0$ m, the plate thickness $h = 0.02$ m, the uniformly distributed transverse loading $p = 100$ kN/m^2. The calculations were carried out for a few values of constant load N_x , which acts in plane (Fig. 5).

The value of the critical force for the considered plate obtained analytically [12] and derived applying BEM procedure [5] equals $N_{cr} = 10090$ kN/m and $N_{cr} = 11635$ kN/m, respectively. The values of deflection and bending moment at the middle point of the plate are shown in Table 3.

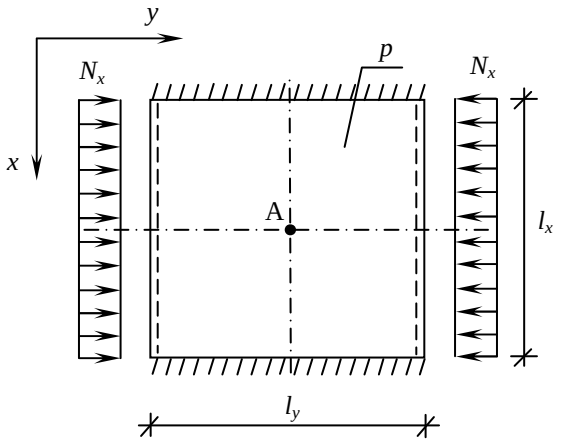

Fig. 5. Square plate, simply-supported on two opposite edges with two edges clamped, subjected to the uniformly distributed loading p and constant in plane loading N_x

Table 3. Deflection and bending moment at the point A

N_x	$w_A \cdot D/(pl^4)$	$M_x^A/(pl^2)$
0.0	0.002174	0.03430
$0.25 \cdot N_{cr}$	0.002792	0.04477
$0.50 \cdot N_{cr}$	0.003891	0.06335
$0.75 \cdot N_{cr}$	0.006397	0.10553

4.3. The rectangular plate, simply-supported on all edges

The rectangular plate, simply-supported on all edges subjected to the uniformly distributed transverse loading and constant loading acting in-plane is considered (Fig. 6).

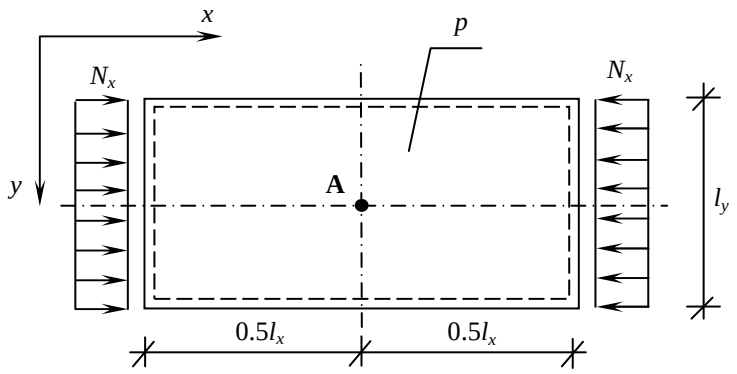

Fig. 6. Rectangular, simply-supported plate, subjected to the uniformly distributed loading p and constant in-plane loading N_x

The plate dimensions are l =0.5 l_x = l_y = 1.0 m, the plate thickness h = 0.02 m, the uniformly distributed transverse loading p = 100 kN/m^2. The value of constant loading N_x , which acts in-plane depends on the critical force (see Tab. 4).

Table 4. Deflection and bending moment at the point A

N_x	$w_A \cdot D/(pl^4)$	$M_x^A/(pl^2)$
0.0	0.01017	0.04434
$0.25 \cdot N_{cr}$	0.01358	0.05194
$0.50 \cdot N_{cr}$	0.01726	0.06208
$0.75 \cdot N_{cr}$	0.02340	0.07025

In this case the value of the critical force was derived applying BEM methodology [5]. For the considered plate the critical force equals N_{cr} = 5983 kN/m. The value of deflection and bending moment at the middle point of the plate are shown in Table 4.

4.4. The rectangular plate, simply-supported on two opposite edges and with two free edges

The rectangular plate, simply-supported on two opposite edges with two free edges is considered. Apart from the uniformly distributed transverse loading p = 100 kN/m^2 , the constant load N_x acts in-plane (Fig. 7). The plate dimensions are l_y = 2.0 m, l_x = 1.0 m, the plate thickness is h = 0.02 m.

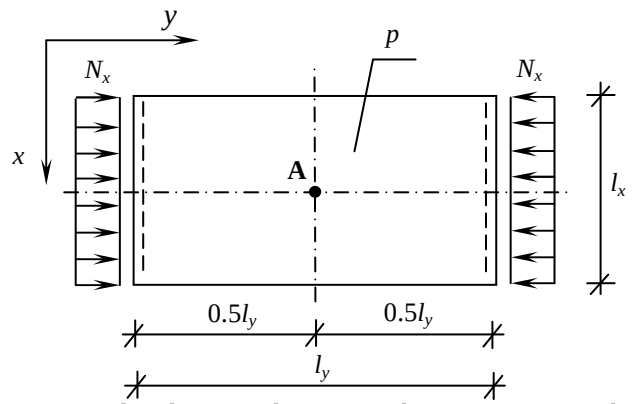

Fig. 7. Rectangular plate, simply-supported on two opposite edges and with two free edges, subjected to the uniformly distributed loading p and constant in-plane loading N_x

The results derived using the BEM procedure given in [5] yield the critical force value N_{cr} = 403 kN/m. The fundamental functions obtained using the FSM enable to derive the deflections and bending moments for the considered plate at the middle point A (Table 5).

Table 5. Deflection and bending moment at the point A

N_x	$w_A \cdot D/(pl^4)$	$M_x^A/(pl^2)$
0.0	0.19830	0.46548
$0.25 \cdot N_{cr}$	0.28101	0,70641
$0.50 \cdot N_{cr}$	0.48291	1,29549
$0.75 \cdot N_{cr}$	1.72861	4,93285

As it was expected the values of deflection and bending moment at the middle point for each example plate increase with the growth of the in-plane loading.

5. CONCLUDING REMARKS

In this paper the static analysis of thin plates with a transverse and in-plane loading was considered. The equilibrium conditions for an infinite strip were derived in the form of one difference equation. The solution of this equation, i.e. the fundamental function for an infinite plate strip, was derived basing on the finite strip method (FSM). This method is an important alternative to the most popular Finite Element Method, because it does not require a high number of degrees of freedom. The fundamental solution derived in this way, can be used to solve the static problem of a finite plate. Moreover, plates simply supported on their opposite edges and loaded in-plane are commonly applied as bridge

structures, as box or plate elements. The numerical results demonstrate the effectiveness and efficiency of the proposed method.

REFERENCES

1. Babuška I., *The Fourier Transform in the Theory of Differences Equation and Its Applications*. Arch. Mech. Stos. **4**, 11, 1959.
2. Brebbia C.A., Telles J.C.F. and Wrobel L.C.: *Boundary Element Techniques, Theory and Applications in Engineering*. Springer-Verlag, Berlin Heidelberg, New York, Tokyo, 1984.
3. Girkmann K.: *Plane Girders* (in Polish). Warszawa, Arkady Publishing House, 1957.
4. Guminiak M.: *Thin plates analysis by the boundary element method using new formulation of a boundary condition* (in Polish). PhD Thesis, Poznan University of Technology, Poznań, Poland, 2004.
5. Guminiak M., Sygulski R.: *Initial stability of thin plates by the boundary element method* (in Polish). Proc. of Stability of Structures Xth Symposium, Zakopane, 8-12 September, Technical University of Lodz, Poland, 173-180, 2003.
6. Katsikadelis J.T.: *Boundary elements. The second volume: plate analysis* (in Greek). 2010.
7. Katsikadelis J.T., Sapountzakis E.J., Zorba E.G.: *A BEM approach to static and dynamic analysis of plates*. Computational Mechanics, **7** (1), (1990), 31-42.
8. Loo Y. C., Cusens A. R.: *The Finite Strip Method in Bridge Engineering*, New York, Viewpoint Publications, 1978.
9. Pawlak Z., Rakowski J.: *Singular solutions for two-dimensional discrete systems by Difference Equation Method*. Proc. of the Second International Conference on Difference Equations and Applications, Veszprem (Hungary), 7-11 August, 1995.
10. Rakowski J., *A critical analysis of quadratic beam finite elements*, International Journal for Numerical Methods in Engineering, **31**, (1991) 949-966.
11. Shi G.: *Flexural vibration and buckling analysis of orthotropic plates by the boundary element method*. International Journal of Solids Structures, **12** (26), (1990), 1351-1370.
12. Timoshenko S., Gere J. M.: *Theory of elastic stability*. McGraw-Hill Book Company, Inc., New York, Toronto, London, 1961.
13. Timoshenko S., Woinowsky-Krieger S.: *Theory of plate and shells*. McGraw-Hill Book Company, Inc., New York, Toronto, London, 1959.

ZASTOSOWANIE FUNKCJI FUNDAMENTALNYCH W ANALIZIE STATYCZNEJ PŁYT CIŃKICH OBCIĄŻONYCH POPRZECZNIE I W PŁASZCZYŹNIE

S t r e s z c z e n i e

W pracy przedstawiono analizę statyczną płyt cienkich, obciążonych zarówno poprzecznie jak i w płaszczyźnie, z wykorzystaniem metody pasm skończonych. Zgodnie z zasadami metody pasm skończonych, ciągły i nieograniczony układ aproksymowany jest nieskończoną liczbą identycznych elementów, którymi są pasma skończone swobodnie podparte na przeciwległych bokach. Niewiadomymi są tzw. amplitudy ugięć i kątów obrotu na liniach węzłowych, czyli na brzegach swobodnych pasma skończonego. Po określeniu macierzy sztywności i macierzy geometrycznej elementu skończonego wyprowadzone zostało różnicowe równanie równowagi, które obowiązuje dla każdej linii węzłowej pomiędzy elementami. Główną zaletą tej metody jest możliwość przedstawienia warunków równowagi dla całego rozważanego układu w postaci jednego równania rekurencyjnego. Rozwiązanie wpomnianego równania dla regularnego, dyskretnego pasma płytowego nazywane jest funkcją fundamentalną. Rozwiązanie fundamentalne otrzymane w ten sposób zostało wykorzystane do rozwiązania problemu statyki płyty o skończonych wymiarach, w sposób analogiczny jak metoda elementów brzegowych w statyce układów ciągłych. Podstawową korzyścią wynikającą ze stosowania metody elementów brzegowych (BEM) oraz metody pasm skończonych (FSM) jest mniejszy nakład obliczeniowy w porównaniu z innymi, podobnymi metodami.

CIVIL AND ENVIRONMENTAL ENGINEERING REPORTS

No. 10 2013

HYDRAULIC RESEARCH FOR SUCCESSFUL FISH MIGRATION IMPROVEMENT – ”NATURE-LIKE” FISHWAYS

Angelika TEPPEL, Tomasz TYMIŃSKI*
Uniwersytet Przyrodniczy we Wrocławiu
Instytut Inżynierii Środowiska

This article presents an overview of the design solutions for fishways which are locates nearby hydrotechnical constructions. Currently fashionable and recommended hydraulic design of fishways are moving towards "close to nature" solutions. Their characteristic feature is applicable to the construction a natural building materials (tree trunks, stones, gravel, vegetation) in such a way that its appearance resembled a small natural water courses. Design of hydraulic fishways based solely on the criteria of maximum speed v_{max} and *parameter of unitary energy of water E*, it does not give complete information about the effectiveness of these devices. In order to produce the optimal flow conditions for ichthyofauna, very useful are spatial structure research of hydraulic parameters, such as disorders of velocity field or the degree distributions of turbulence *Tu*. The article presents an example of such a study, which the authors carried out on the model seminatural fishway in the water laboratory in Institute of Environmental Engineering in Wrocław. The results were used to assess the accuracy of the functioning of the fishway.

Keywords: fish ladders, hydraulic conditions of water flow, model test

1. INTRODUCTION

The loss of ecological permeability of the rivers, very often is associated with hydrotechnical constrictions of riverbeds. On the other hand, an artificial barriers like the dams, weirs, thresholds, etc. are in many cases necessary for the regulation of rivers, flood protection, retention, water balance and management in the catchment, agriculture and environmental needs in adjacent areas. Hydroelectric power plants also contribute in ecological production of electricity.

* Corresponding author. E-mail: tomasz.tyminski@up.wroc.pl

Polish accession to the European Union, forced ecological operations in the widely understood water management. For instance, in order to allow the fish to overcome damming, free migration and reduce their mortality in hydroelectric turbines, the law requires a special structures in the vicinity of hydrotechnical obstacles, so-called fishways. Taking into account the structure, the type of materials which they are made and the hydraulic flow conditions prevailing inside the construction of fishpassages, they can be divided into: technical and "close to nature"/seminatural/ [3, 5, 12, 15, 18].

Fig. 1. Baffle fishway in Schleusingen/Gernany (photo Tymiński)

Fig. 2. Vertical slot fish pass by Villach/Austria [9]

Technical fishways are the oldest known structure to allow fish upstream migration. We can distinguish the following types of devices: baffle fishways (Fig. 1), fish ladder of the reverse current (Denil fishway), vertical slot fishways (Fig. 2), eel's gutters, locks and fish elevators. Technical ladders are well described in the professional literature [1-2, 5-7, 9-13, 15-16] and therefore will

not be a theme of certain research. Most of them are not difficult to hydraulic dimensioned and until recently a designers willingly chose technical solutions of fishways. Technical ladders are built mostly of concrete. This fact makes that they are compared to nature and local foreign prosthesis. Currently fashionable and recommended hydraulic design of fishways are moving towards solutions "close to nature" - a fishways with biological build-up.

2. THE NATURE-LIKE FISHWAYS

Close to nature fishways are more modern than solutions of technical ladders type. Long research and analysis of hydraulic fishways design and better understanding of the environmental determinants of ecosystems, led to emergence of solutions that will enable aquatic organisms to overcoming obstacles in conditions similar to natural way. At the same time, these ladders should allow for the proper functioning of the hydrotechnical object and harmoniously interact with the surroundings. Hallmark of "close to nature" fishways is applied to their design natural materials such as wood, vegetation, stone, gravel and river bed load - molded in a specific way for each type of structure. To nature-like fishways we can include:

- rock-ramp fishways (rapids, ramps),
- chain of reservoirs,
- by-pass channels (seminatural bypass fishways).

2.1. Rock-ramp fishways

Rock-ramp fishways otherwise artificial rapids or ramps are the constructions, that reflect the steep drop in the river bottom slope equivalent 1: 20-1: 30. They are made of stones with a diameter from 30 to 80 cm. The size of the material should be precisely selected to ensure a suitable water velocity and the amount of flowing water. The material used for the construction of the ramp should be the stones from the nearby surroundings. There is a division of the ramp due to their location. We can distinguish:

- ramps arranged over the whole width of the riverbed,
- ramps arranged in part of the riverbed (built in additional narrow overflow hole of hydrotechnical object, separated by a partition structure from the rest),
- ramps such a stream, which revolve around a hydraulic obstacle (for instance: a weir).

Thesecond group of these fish-passes are:

- ramps pool,
- erratic-ramps – irregular heap up stones.

Cascades

The cascades are small collections of pools connected with each other with a little ramps angle or a number of steps with a low gradient (Fig. 3).

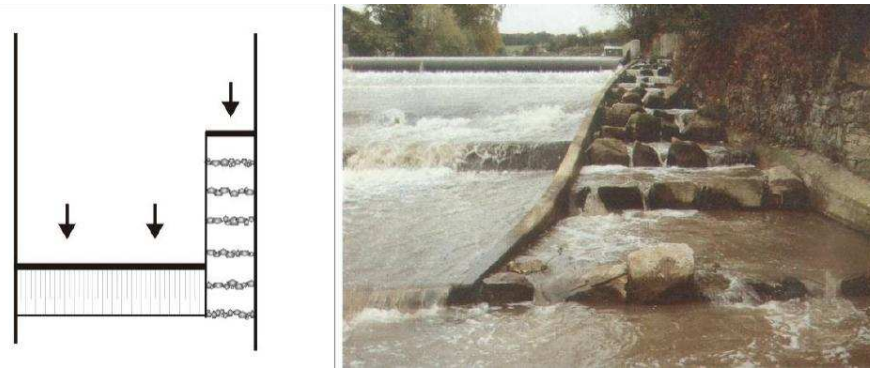

Fig. 3. Rock-ramp fishway [6]

Ramps

Resemble stone ramps, but their shape is more regular. They are built with stones and boulders reinforced by concrete. Here you can highlight the ramp boulders made of layers pour off rocks and boulders, also with deck-mounted ramps - edgewise embedded boulders. Sometimes the ramps can be spread across the entire width of the watercourse, however, are more likely to meet the ramp on one side of the shore.

2.2. Chains of basins

In this case, the crossing for fish are connected to each other with small basins, ponds, which are located on the ladders (Fig. 4). Following basins are connected by short overflows. Another variation of this type of ladder is step-pool fishway.

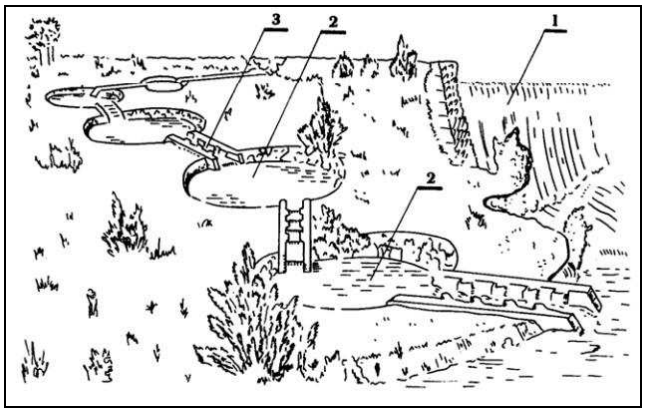

Fig. 4. Chains of basins: 1-artificial barrier , 2-basin, 3-ramp [20]

Ponds are places where fish can rest during the journey. They also have the role of speed reduction on the ladders. In this type of system, the arrangement of intermediate pools are usually irregular and varied, the main cause of this type of asymmetry are off-road conditions [15].

2.3. By-pass channels

By-pass channels (circulation channels) are constructions resemble a rivulet or mountain stream (Fig. 5). This type of ladder has a dual function - it is a temporary way to fish as well as a permanent habitat for other organisms. The first such ladders originated in countries highly urbanized, where as a result of the river adjustment many natural habitats were destroyed.

To build a popular by-pass channel we must use natural materials as stones, gravel, tree stumps, boulders, fascines, etc. The bottom of the ladder is also composed of similar elements. Its slope varies in the range of 1:75 to 1:20. It is formed by natural depressions and pools, which automatically reduces too high velocity of water. By-pass channel must be leaded a winding route, resulting in minimizing the velocity and to reduce the difference between the downstream and upstream level. If the designers have at their disposal a relatively much space to build, there is possible to reduce the impoundments even up to 10 m. Under these conditions, the circumvent is more diverse and has sections characterized by large and small declines [5, 8].

The disadvantage of this kind of transition is that to function properly there must be a large flow of water. Unfortunately, may occur such hydrological and hydraulic conditions, that this requirement will not be fulfilled.

Fig. 5. Semi-natural bypass fishway in the old river bed of the Rhone/France [10]

3. RECOMMENDATIONS FOR FISHWAY DESIGNERS

In Poland, the design guidelines for fishway drawn up by a German interdisciplinary expert team [2, 6, 7, 13, 14] are popular and commonly used. A summary of its key assumptions is given in the Table 1.

Table 1. Ichthyofauna Requirements and Guidelines for Fishway Design [2, 6, 7, 13]

Type of fish	*Permissible water flow velocities in fishways*
Small fishes and juveniles	$v < 1.0$ m/s
Medium-size fishes like cyprinids (chub, barbel)	$v < 1.5$ m/s
Big-size fishes like salmonids (salmon, trout)	$v < 2.0$ m/s
Flow parameter	*Size*
Mean velocity	$v = 0.4–0.6$ m/s
Velocities at the fishway mouth	$v < 1.9$ m/s
Velocities at the inlet of the upper water	$v < 1.2$ m/s
Specific discharge	$q > 0.1$ m^2/s
Unitary energy of water	$E < 200$ W/m^3
Geometric parameter of fishway	*Size*
Diameter of used stones	$d = 0.4–0.7$ m
Width of stone baffle	$w = 0.9–1.2$ m
Bottom slope	1:75–1:20
Difference in water levels between chambers	$\Delta h = 0.05–0.15$ m
Width of fishway	$b > 0.8$ m
Length of chamber	$L_{min} = 3 \times L$
	$L > 4.0$ m
Water depth in chamber	$t_{min} = 2.5 \times H$
	$t = 0.2–1.5$ m
Width of slots	$s_{min} = 2 \times D$
	$s = 0.1–0.5$ m
where: D – width, H – high and L – length of fish *[m]* [13]	

Fishways dimensioning based on the above design recommendations should be at the same time, related to the need to adapt them to local conditions

prevailing at the construction site of fishway (species composition of fish, terrain, hydrological conditions).

4. ASSESSING THE EFFICIENCY OF FISHWAY

It is important during designing a "close to nature" passage for fish provide a suitable for hydraulic conditions of fish fauna. Mostly, to assess the effectiveness of the functioning of those structures, designers using the data about the maximum velocities of the flow (Tab. 1) and analyzing a stream of water turbulence inside the ladders. Turbulence in a fishway is often estimated by means of the so called *parameter of unitary energy of water E.* This value can be calculated from:

$$E = \frac{\rho \cdot g \cdot \Delta h \cdot Q}{A \cdot t} \quad , \quad [\mathrm{W/m^3}] \tag{1}$$

where:
Δh – difference in water levels between chambers [m],
Q – water flow rate in the fishway [m^3/s],
A – chamber (pool) surface area [m^2],
ρ_w – density of water [kg/m^3],
t – filling of the chamber (depth) [m].

For strong fish species which are good swimmers this parameter’s value should not exceed *200 W/m^3*, whereas for small fish species, juvenile fish and fry the limit is *E = 100 W/m^3*.

Unfortunately, often a built of fish-passages is limited only to the directory selection of ladders type. Even in the case when its hydraulic dimensioning is compatible with the required engineering standards, it happens that the effectiveness of fishway is limited. About such cases, alerts inter alia a professional literature in Germany [1, 2, 13, 14], where amount of fishways is disproportionately higher than in Poland. Therefore, in the authors opinion of the publication, to assess the effectiveness of fishway is necessarily needed a spatial analysis of speed distribution inside the ladders and especially stream turbulence. Study of turbulence in fishways are possible on objects in nature (for example to optimize them), using 2D-numerical simulation or physical models in the laboratory. A quantitative measure of the intensity of turbulence is the degree of turbulence *Tu*, which can be set separately for each direction of flow [17]. This value can be calculated from:

$$Tu = \frac{\sqrt{\frac{1}{3}(v_x^2 + v_y^2 + v_z^2)}}{v_{sr,x}^2 + v_{sr,y}^2 + v_{sr,z}^2} \quad , \quad [\,-\,] \tag{2}$$

where:
v_x , v_y , v_z – fluctuation velocity components [m/s],
$v_{śr,x}$,$v_{śr,y}$, $v_{śr,z}$ – average velocity components [m/s].

5. LABORATORY INVESTIGATION

At the Institute of Environmental Engineering at the Wrocław University of Environmental and Life Sciences was made a hydraulic model research of the flow conditions for a part of seminatural fishway. 3 m-long fishway (scale 1:3) with elements of biotechnical build-up was built in the linear trapezoidal flume with bottom roughness n = 0.012 $m^{-1/3}s$, longitudinal bottom slope J = 12 ‰, width of the bottom b = 0.90 m and 1:1 bank slopes. Adopted fishway configuration shown in Figs. 6 and 9.

In our experiments we used the common reed (*Phragmites communis TRIN.*). Density of the vegetation zones was 577 stems/m^2, representative diameter of the reed was d_P = 5.6 mm and the representative dimensions of the used stones (*B*-width, *H*-height, *L*-length in the direction of flow) were: a) horizontal projection *B* x *L* = 176.5 x 97.2 mm; b) vertical cross-section *B* x *H* = 176.5 x 66.1 mm.

Fig. 6. Laboratory model of fishway with biotechnical build-up

Tested in the laboratory fishway model with biotechnical building elements is modular construction. Building "close to nature" fishway in the form of a bypass channel, we use modules, which you can duplicate and expand structure at length, depending on your needs.

5.1. Methods and scope of research

Experiments in the laboratory has mainly focused on the measurement of depth and velocity of water flow at the inflicted flow *Q*. Multidirectional instantaneous velocity measurements carried out using electromagnetic probe PEMS type (Fig. 7) 360 points with dimensions of mesh 0.10 x 0.15 m and characteristic points of movement disorders, especially in apertures of fishway.

Depth was measured by water level indicator with a micrometric screw and a cathetometer. Laboratory measurements have been carried out within the following limits of hydraulic parameters:

- stream flow intensity Q = 30-50 dm^3/s
- momentary speeds v = 0-1,00 m/s
- depth of flow h = 0,15-0,22 m

During the conversion the corresponding values from the model to the nature conditions was used an appropriate criterion of hydrodynamic Froude similarity [17].

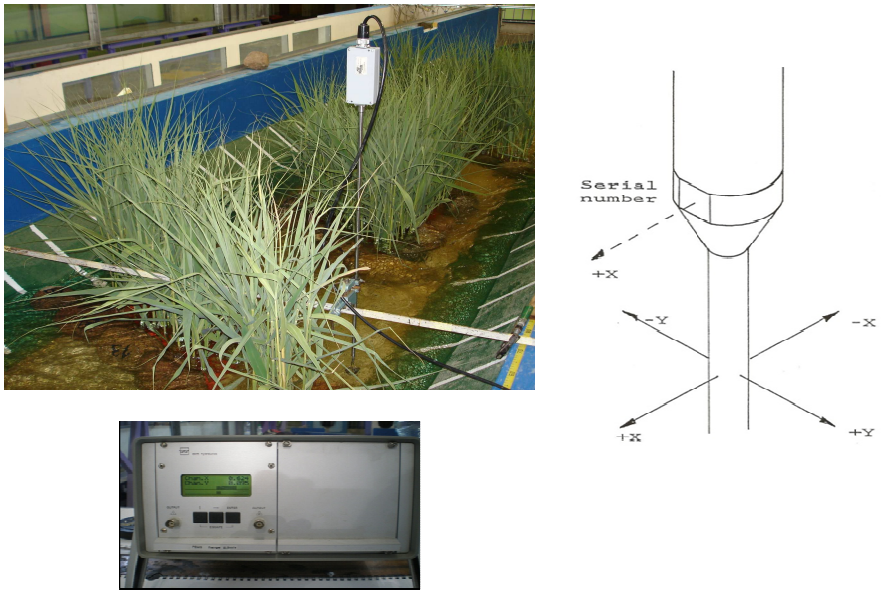

Fig. 7. Measuring instruments (probe PEMS)

5.2. Results and discussion

An example of the results of measurements for discharge Q = 780 dm^3/s (Q_{LAB} = 50 dm^3/s) is shown in Figs. 8-9 and Tab. 2. These data are developed and converted according to the scale (1:3). From the formula (1) set *the unit parameter of water energy E*. You can see that E = 67.80 W/m^3 does not exceed

the limit values, even for the young and the weak fish. The same applies to the average flow velocity in fishway (Tabs. 1-2).

Table 2. Example of research results

Lp.	Coordinates of measuring point (Fig.9)		v_i	t_i	t	A	Δh	v_m	E
-	x [m]	y [m]	[m/s]	[m]	[m]	[m^2]	[m]	[m/s]	[W/m^3]
1.	3.60	0.6	1.31	0.630	0.579	20.25	0.104	0.41	67.8
2.	4.20	0.7	0.41	0.585					
3.	5.60	1.0	0.44	0.578					
4.	6.60	1.0	1.36	0.522					

where:
t, A, Δh, E – by formula (1);
v_m - average flow velocity;
v_i - average local measurement points of depth;
x – distance in the direction of the flow;
y - distance perpendicular to the flow (Fig. 9).

However, a full assessment of the effectiveness of fishway is only possible in case of the analysis of the spatial distribution of hydraulic parameters. Laboratory measurements of the velocity field allowed to determine the formula (2) the degree of turbulence *Tu*. Graphic illustration of the turbulence distribution in tested fishway and inside the empty riverbed (for comparison) is shown in Figs. 8-9.

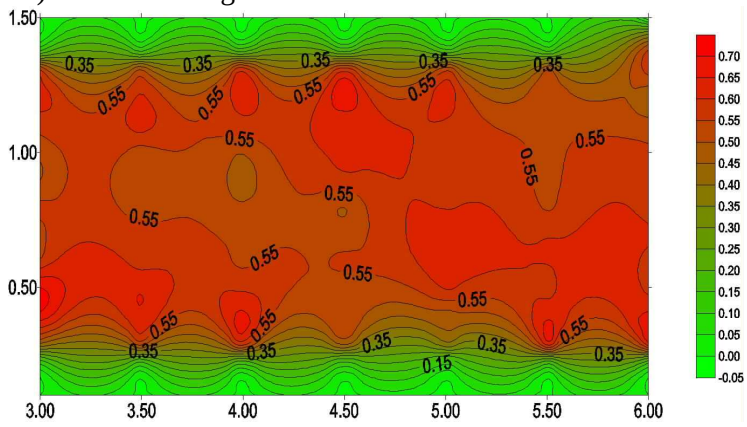

Fig. 8. Distribution of turbulence degree „*Tu*" for empty laboratory flume

Biotechnical build-up affects significantly on the distribution of turbulence in the water stream of fishway (cf. Fig. 8 and Fig. 9). So, it is possible to create a different hydraulic flow conditions inside the fishway e.g. areas of increased turbulence (*Tu* = 0.5-0.7) and so-called resting areas for

upstream fish migration ("the island" on Fig. 9, where *Tu* = 0.3). This is especially valuable because of the ichthyological requirements [1, 3, 4, 15, 19].

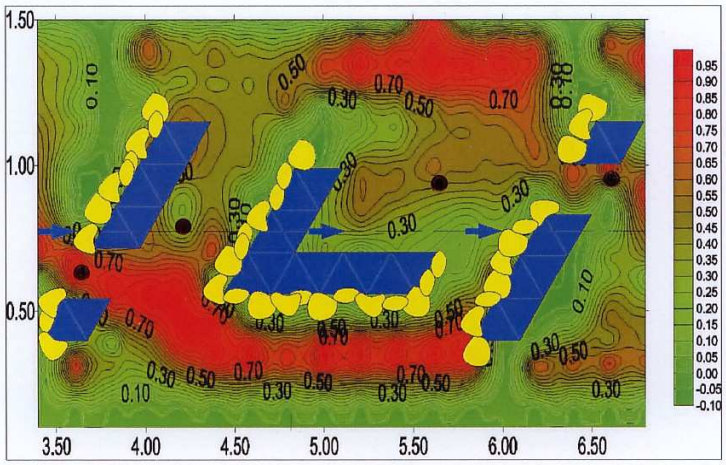

Fig. 9. Distribution of turbulence degree *„Tu"* in fishway with biotechnical build-up (• points of depth measurements)

6. CONCLUSIONS

Biotechnical arrangement (vegetation + boulders) in seminatural fishway is a disorder (obstacle) input to the flow, which results in a reduction of the local velocity and dissipation energy (cf. Fig. 8 and Fig. 9).

Appropriate use of biotechnical arrangement enables to create stable hydraulic conditions for fishway in established parameters, e.g. clear, constant current (Fig. 9) the fish-friendly navigation system in fishways, but also make a rest areas for migratory fish, where the water speed is reduced (Fig. 9).

In order to find for ichthyofauna the optimal deployment configuration of plants and boulders inside the fishway and to evaluation of its efficiency - particularly useful are the spatial structure of hydraulic parameters tests for example. the velocity field or distributions the degree of turbulence *Tu*. Fishways design only on the basis of the average and generalized parameter values *v* or *E* (Tab. 1) does not give complete information about the efficiency of the fish ladders.

The article points out an example of the results obtained for hydraulic research made on the artificial model of fishway in the water laboratory. They represent the output base for further analysis and research. While at the fishways design stage worth recommendations are computer simulations of hydraulic flow conditions e.g. on two-dimensional numerical models.

REFERENCES

1. Adam B., Lehmann B.: *Allgemeine Anforderungen an Fisch-aufstiegsanlagen*. Konferenzmaterialien: "Oekologische Durchgängigkeit in Fließgewässern", LUA Brandenburg, Lebus 2009.
2. Adam B. et al.: *Fischschutz- und Fischabstiegsanlagen – Bemessung, Gestaltung, Funktionskontrolle*. DWA, 2. Auflage, Hennel 2005.
3. Bartnik W. i in.: *Gospodarka rybacka w aspekcie udrażniania cieków dorzecza Małej i Górnej Wisły*. Infrastruktura i ekologia terenów wiejskich. Wydawnictwo PAN Oddz. w Krakowie, Zeszyt nr 13, Kraków 2011.
4. Bojarski A., Jeleński J., Jelonek M., Litewka T., Wyżga B., Zalewski J.: *Zasady dobrej praktyki w utrzymaniu rzek i potoków górskich*. Ministerstwo Środowiska, Departament Zasobów Wodnych, Warszawa 2005.
5. Bosmou M., Teppel A., Tymiński T.: *Assessing the functionality of fishways as the essential element of rivers continuity*. [W:] Szczęśniak E. (red.), Tymiński T. (red.): Środowisko Dolnego Śląska oczami przyrodników. Uniwersytet Wrocławski, Monografia, Nr 4, Wrocław 2012.
6. DVWK: *Fischaufstieganlagen: Bemessung, Gestaltung, Funktions-kontrolle*. Merklblaetter zur Wasserwirtschaft, Nr. 232, Bonn 1996.
7. DWA: *Durchgängigkeit und Habitatmodellierung von Fließgewässern.* Verlag der Bauhaus-Universität Weimar 2010.
8. Grobelny M., Nowicki M., Tymiński T., Zhou Yinting: *Hydrauliczne warunki przepływu w przepławkach „bliskich naturze"*. Materiały konferencyjne, Ogólnopolska Sesja Naukowo - Techniczna: „Przepływy wody i zanieczyszczeń w ośrodkach porowatych i korytach otwartych", KIWiS, Uniwersytet Przyrodniczy w Poznaniu, Poznań 30 marca 2012.
9. Hassinger R.: *Components for Ecological Improvements at Water Power Sites*. Materiały konferencyjne, Międzynarodowe Seminarium Naukowe: „State of the Art of Building Fish Passes in Germany", PAN Komitet Gospodarki Wodnej, Sekcja Ochrony Środowiska Wodnego, Warszawa 2009.
10. Jelonek M., Wierzbicki M.: *Prezentacja technicznych możliwości przywrócenia wędrówek ryb w rzekach na podstawie wybranych przykładów inwestycji zrealizowanych we Francji i Niemczech oraz USA*. Materiały Ministerstwa Rolnictwa i Rozwoju Obszarów Wiejskich, Kraków-Poznań 2008.
11. Jens G.: *Der Bau von Fischwegen*. Verlag Paul Parey, Hamburg und Berlin 1982.
12. Jędryka E. *Metody zapewnienia ekologicznej drożności cieków*. Wiadomości melioracyjne i łąkarskie, Nr 1/2011.
13. Krüger F.: *Anforderungen an Fischaufstiegsanlagen, Beispiele aus der Praxis*. Konferenzmaterialien: Vortrag zum Wasserbaulichen Kolloquium

"Oekologische Durchgängigkeit von Fließgewässern", Universität Hannover 2008.
14. Lehmann B.: *Ethohydraulische Untersuchungen, Veranlassung – Methode – Einsatzmöglichkeiten*. Konferenzmaterialien: "Oekologische Durchgängigkeit von Fließgewässern", Universität Hannover 2008.
15. Lubieniecki B.: *Przepławki i drożność rzek*. Wydawnictwo Instytutu Rybactwa Śródlądowego, Olsztyn 2003.
16. Mokwa M. (red.) i Wiśniewolski W. (red.).: *Ochrona ichtiofauny przed szkodliwym działaniem budowli hydrotechnicznych*. Monografia. Dolnośląskie Wyd. Edukacyjne, Wrocław 2008.
17. Puzyrewski R., Sawicki J.: *Podstawy mechaniki płynów i hydrauliki*. Wydawnictwo Naukowe PWN, Warszawa 2000.
18. Szczerbowski J. A. (red.).: *Encyklopedia rybacko-wędkarska*. IRS Olsztyn 1998.
19. Zgrabczyński J.: *Identyfikacja i ocena sprawności przepławek dla ryb w regionie wodnym Warty*. Nauka Przyroda Technologie, Tom 1, Zeszyt 2 (wyd. elektroniczne #35), Poznań 2007.
20. Żbikowski A., Żelazo J.: *Ochrona środowiska w budownictwie wodnym*. Ministerstwo Ochrony Środowiska, Zasobów Naturalnych i Leśnictwa, materiały informacyjne, Warszawa 1993.

BADANIA HYDRAULICZNE DLA POPRAWY WARUNKÓW MIGRACJI RYB - PRZEPŁAWKI „BLISKIE NATURZE"

S t r e s z c z e n i e

W pracy przedstawiono przegląd rozwiązań konstrukcyjnych przejść dla ryb (przepławek) przy obiektach hydrotechnicznych. Modne obecnie i zalecane konstrukcje zmierzają w kierunku rozwiązań „bliskich naturze". Ich cechą charakterystyczną jest zastosowanie do budowy przepławek naturalnego budulca (kamienie, pnie drzew, żwir, roślinność) w taki sposób, by swoim wyglądem przypominały małe cieki naturalne. Projektowanie hydrauliczne przepławek oparte wyłącznie na kryteriach prędkości dopuszczalnych v_{max} oraz parametru jednostkowej energii wody E, nie daje pełnej informacji o skuteczności działania tych urządzeń. W celu wytworzenia w przepławce optymalnych dla ichtiofauny warunków przepływu przydatne są badania struktury przestrzennej parametrów hydraulicznych np. zaburzeń pola prędkości lub rozkładów stopnia turbulencji Tu. W pracy zaprezentowano przykład takich badań, które autorzy przeprowadzili na modelu przepławki seminaturalnej w laboratorium wodnym IIŚ UP we Wrocławiu. Otrzymane wyniki posłużyły do oceny poprawności funkcjonowania przepławki.

CIVIL AND ENVIRONMENTAL ENGINEERING REPORTS

No. 10 2013

REMOVAL OF PRIORITY PAHS FROM COKING WASTEWATER

Agnieszka TUREK, Maria WŁODARCZYK-MAKUŁA*
Water and Wastewater Technology Czestochowa University of Technology,
Department of Chemistry, 42-200, Częstochowa, Poland

The purpose of these tests described in this study was to determine the effectiveness of removing eight aromatic compounds from the list of priority. Tests were carried out using coke produced during wastewater treatment of coke oven gas. The technology research was consisted in introducing into wastewater samples taken with 30% solution of hydrogen dioxide (50 mg/dm^3, 100 mg/dm^3, 300 mg/dm^3, 600 mg/dm^3, 900 mg/dm^3, 1000 mg/dm^3, 2000 mg/dm^3). The PAHs analysis included: sample preparation, quantitative and qualitative chromatographic determination, it was also carried out using gas chromatography coupled with mass spectrometer. Total concentration of PAHs in the effluent eight coke before oxidation was 23 µg/dm^3. The largest loss of hydrocarbons examined, reaching 62%, was noted at the dose of 50 mg/dm^3 of the oxidant.

Keywords: oxidation, H_2O_2, PAHs, GC-MS, industrial wastewater

1. INTRODUCTION

Studies, reported in the literature has shown, that the wastewater from processing fuels like coke or petroleum is the most loaded organic micropollutants [2,16].

The presence of PAHs in coking wastewater were confirmed in literature reports and earlier research [9,11,12,13,15]. Bartkiewicz says that the content of organic compounds expressed as oxygen consumption may reach 1,000 mg/L. The concentration of total nitrogen and volatile phenols may be suitably in the range from 980 to 6500 and 260 to 3000 mg/dm^3 [1].

The Directive of the European Parliament and the Council 2008/105/EC from the 16th of December 2008, provides environmental quality standards for priority substances and certain other pollutants [4]. In Polish legislation it is the

* Corresponding author. E-mail: mwm@is.pcz.czest.pl

ordinance of the Minister of the Environment from the 9th of November, 2011 [7]. Lists of priority substances on 8 PAH: naphthalene, anthracene, fluoranthene, benzo(a)pyrene, benzo(b)fluoranthene, benzo(k)fluoranthene, benzo(g,h,i)perylene, indeno(1,2,3-cd)pyrene.

With the above hydrocarbons, five exhibit carcinogenic, mutagenic or teratogenic effects that depend on the strutury and environmental conditions.

Toxicological studies have shown that PAHs themselves are not carcinogenic, but only derivatives which occur in the environment, or in organisms as a result of metabolism [3]. PAH derivatives may be formed by reaction with other components of the matrix (halogenation, nitration, sulfonation, alkylation, acylation). [8]. Hydrocarbons are also oxidation reactions and photochemical degradation. The oxidation of hydrocarbons can give products such as diols, quinones and aldehydes, for example, benzo(a)pyrene can be in the form of derivatives such as benzo(a)pyrene-1 ,6-dione and benzo(a)pyrene-3,6-dione [3,6].

An advanced oxidation methods of organic pollutants – AOP are increasingly being used for a treatment of industrial wastewater. These methods rely from the generation of hydroxyl radical, which allows the decomposition of organic compounds to CO_2 and H_2O. The most common agents that cause the generation of hydroxyl radicals are hydrogen dioxide, permanganate, ozone, UV radiation and ultrasound [14].

The total degradation of organic contaminants, without using chemicals, can process photocatalysis (TiO_2 + UV) [5]. According to the IUPAC nomenclature, the process is referred as a photocatalytic reaction of chemical change, or initiation by radiation in the presence of a catalyst, which absorbs light and cause chemical conversion of the compounds present in the sample. In addition to chemical oxidation and ozone above, dihydrogen dioxide can be used in Fenton's reagent and permanganate. It has been shown, that in the Fenton reaction (Fe^{2+}/H_2O_2) efficiency of the process depends from the dose of Fe^{2+} and H_2O_2, pH, reaction time and temperature, but also from the type of oxidized substances and the presence of other inorganic and organic compounds [10].

The purpose of these tests described in this study was to: determine the effectiveness of removing eight aromatic hydrocarbons from the coke wastewater.

2. MATERIALS AND METHODS

The tests were carried out using coke, produced during wastewater treatment of coke oven gas. In practice, the sewage is directed to a biological treatment works. Samples of water were taken as a temporary and pre-characterized, by

determining key indicators such as COD, TOC. Wastewater sample taken initially characterized by following the determination of such indicators as: COD with the American summary, TOC and N general - analyzer Multi N / C 2100, according to PN-EN 1484:1999. Concentrations of 16 PAHs compounds, including eight (Naf, Antr, Fl, BaP, BbF, BkF, BghiP, IP) were recognized as the original.

The technology research consisted introducing into water samples taken with 30% solution of hydrogen dioxide. The dose of the reagent was: 50 mg/dm^3, 100 mg/dm^3, 300 mg/dm^3, 600 mg/dm^3, 900 mg/dm^3, 1000 mg/dm^3, 2000 mg/dm^3. The samples were mixed and left in the laboratory conditions a period of 60 minutes. After this time the PAHs were determined and the analysis of physico-chemical indicators in the effluent was repeated.

2.1. Analytical Methods of PAHs

PAH analysis included initial sample preparation and chromatographic quantitative determination. Initial stage was the extraction of organic matter from wastewater. To 500 ml of water were added solvents: methanol, cyclohexane, dichloromethane, at a volume ratio of 20:5:1. Then subjected of shaking for 60 minutes, where a constant amplitude was maintaind. The extracts were separated from the water sample by centrifugation. Then the extracts were purified under vacuum (SPE) for the small columns filled with silica gel (fill conditioning was performed with a mixture of dichloromethane and cyclohexane, v/v 1:5, three times with 3 ml). Received extract was concentrated to a volume of 2 ml under a nitrogen stream. The final step was to determine the quantitative and qualitative indication, which was carried out using gas chromatography coupled with mass spectrometer (GC-MS-QP2010 Plus SHIMADZU). The analysis was performed on a ZB-5 ms length of 30 m and a diameter of 0.25 mm used as carrier gas helium, which was set at flow 1.08 ml/min. Injection volume was 1μl, split 1:5. Initial oven temperature was set at 140°C and maintained for 1 min. Then the temperature increased to 240°C at a rate of 15^oC/min, at 4^oC/min. to 275^oC and it was ultimately increasing from 10^oC/min. to 320^oC. The final temperature was maintained for 5 min. Received chromatograms were analyzed using the SIM card. Qualitative and quantitative indications were based on external standard PAH 16 each at a concentration of 200 ng/cm^3 The changes in the concentration of PAHs were determined on the basis of wastewater before and after oxidation. Samples were performed in duplicate.

3. RESULTS AND DISCUSSION

3.1 Preliminary studies

The initial stage of the study was to perform the basic signs of chemical indicators for coke plant before and after the oxidation process. Table 1 shows the values of the results.

Table 1. Characteristics of coke wastewater

Index	unit	Oxidant concentration (H_2O_2) [mg/dm^3]							
		0	50	100	300	600	900	1000	2000
COD	mg/dm^3	770	676	732	878	846	786	808	846
TOC	mg/dm^3	119	113	129	150	112	109	114	128

With regard to the indicators of organic pollutants such as COD and TOC before and after the oxidation process, we can conclude that their values have been slightly altered. During the process of oxidation defects observed concentrations of the hydrocarbons, but they can create other compounds, because general indicators of organic pollutants (COD, TOC) may remain at a similar level.

3.2 Quantitative changes of PAHs

Initial concentration of 16 PAHs in coking wastewater was 38 mg /dm^3. The concentration of eight main hydrocarbon was on average 23 µg/dm^3, which composed 60% of the total amount of 16 PAHs. The concentration of benzo(a)pyrene was 14% of the total concentration of 16 PAHs, and 24% of the total amount of hydrocarbons on the of priority compounds list. As can be seen in the force of the Directive of the European Parliament on environmental quality standards for priority substances, downloaded coke wastewater does not meet the conditions for entry into the water and require a clean [4].

Introduction of the oxidant into the wastewater in an amount of 50 mg/dm^3 caused significant changes in the removal of the analyzed hydrocarbons (8 PAH - 62%). If, however, the amount of hydrogen dioxide was 100, 900, 1000 mg/dm^3 the 16 PAH removal was recorded at a level from 21% to 24%, and eight hydrocarbons at - 22%. Larger percentage reductions were achieved by adding an oxidant PAHs in an amount of 300 mg/dm^3 and 2000 mg/dm^3. Then the percentage removal of 16 PAHs and 8PAHs were respectively 60% and 57% , 47% and 43%. Analyzed changes in the concentration of hydrocarbons in coking wastewater depending on the dose of oxidant is shown in Figure 1.

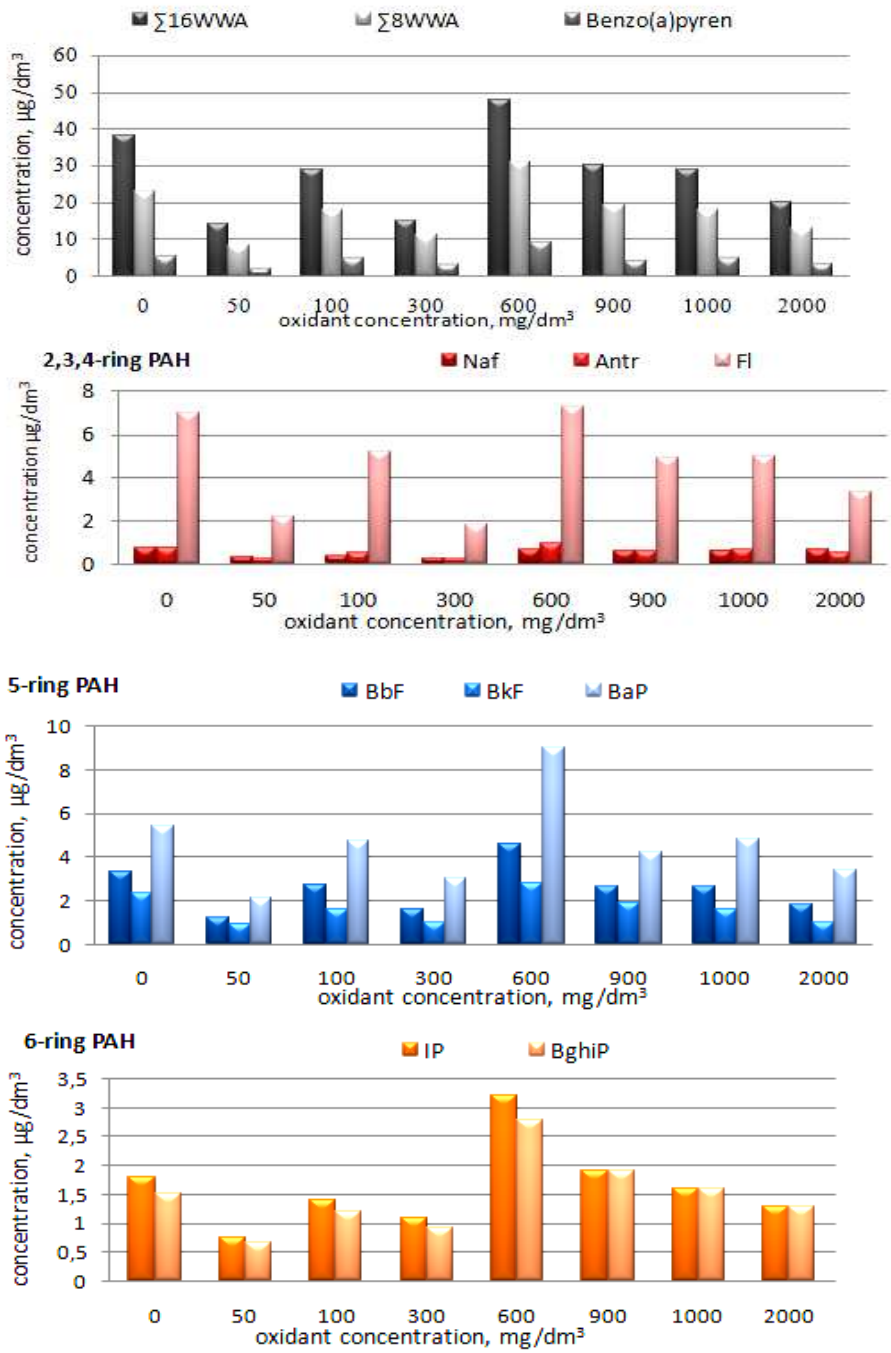

Fig. 1. Changes in the concentrations of PAHs in coking wastewater

In the process of oxidation, the wastewater prior to the parent compounds in the hydrocarbon group of eight, were: fluoranthene accounted for 31% (7.0 µg/dm^3) ,benzo(a)pyrene constituting 24% (5.4 µg/dm^3). Using suitable amounts of oxidant, the first one (Fig l) remained at 18% -29%, and benzo(a)pyrene was vairy from 23% to 30%. During the research process, the percentage of the remaining compounds in the mixture did not go under significant changes . The percentage of specific hydrocarbons are shown in Table 2, assuming Σ 8 PAH as 100%.

The highest tested concentration of PAHs losses to the sum of eight hydrocarbons were obtained using hydrogen dioxide in an amount of 50 mg/dm^3. Then, the efficiency of removal benzo(a)pyrene was respectively of 61% and the final concentration of the hydrocarbon did not exceed 2.1 µg/dm^3, The highest 68% reduction was observed in the case of fluoranthene (table 2).

Table 2. The percentage and the percentage of removal of PAHs

Concentration of H_2O_2 [mg/dm^3]									
	PAHs	**0**	**50**	**100**	**300**	**600**	**900**	**1000**	**2000**
Percentage %	Naf	3.0	4.0	2.2	3.0	2.0	3.2	3.4	4.8
	Antr	3.0	3.0	3.2	2.3	3.0	3.2	3.8	3.8
	Fl	31	26	29	18	23	26	27	25
	B(a)P	24	25	26	30	29	23	26	26,7
	B(b)F	14	14	15	16	15	14	14	13.6
	B(k)F	10	11	9.2	10	9.0	10.2	8.6	7.5
	I(1,2,3,c,d)P	8.0	9.0	8.2	11	10	10.2	8.6	9.8
	B(g,h,i)P	7.0	8.0	7.2	9.7	9.0	10.2	8.6	9.8
Percent removal %	Naf	0	**57**	51	65	8.0	20	16	14
	Antr	0	**67**	33	72	-	24	10	32
	Fl	0	**68**	26	74	-	30	29	53
	B(a)P	0	**61**	13	44	-	22	11	37
	B(b)F	0	**64**	18	52	-	21	21	45
	B(k)F	0	**59**	30	56	-	17	30	56
	I(1,2,3,c,d)P	0	**58**	22	39	-	-	11	28
	B(g,h,i)P	0	**55**	20	38	-	-	-	13

Amount of the eight PAHs, five of them have either carcinogenic, mutagenic or teratogenic (BaP, BbF, BkF, B(g,h,i)P, IP) properties. The content of these compounds in the wastewater before oxidation was 14 µg/dm^3 representing 61% of 8 PAHs. Introduction of the oxidant into the wastewater in an amount of 600 mg/dm^3 did not result in any changes of the removal these compounds. If, however, the amount of hydrogen dioxide was 100 mg/dm^3, 900 mg/dm^3 or 1000 mg/dm^3 five PAHs removal was recorded in the range from 7% to 14%. A greater percentage reduction was achieved by adding an oxidant in an amount of 300 mg/dm^3 and 2000 mg/dm^3. Then the final concentration was 7.6 µg/dm^3 and 8.8 µg/dm^3, however the percentge PAHs removal rates reached

46% and 37%. The highest (59%) loss of the compounds was achieved at a dose of 50 mgH_2O_2/dm^3, where the final concentration was 5.7 µg/dm^3.

The use of an oxidant in doses 600, 900, 1000 mg/dm^3 is not significantly reduced concentrations of the individual PAHs. Coking wastewater is rich organic material. In addition to the 8 analyzed polycyclic aromatic hydrocarbons during oxidation derivatives may be formed. The use of an oxidant in an amount of 50 mg/dm^3 resulted in a reduction of 8 PAH in 62%. As the amount to be donated dihydrogen dioxide process to go with a smaller loss. This may be due to the transformation of complex aromatic hydrocarbons, compounds of the complex structure. Preliminary identification of water indicated the presence of coke indeno(2,1-c)pyridine, and dibenzopyrolu, indeno(1,2-b)pyridine. Unequivocal evidence of their presence requires further research and detailed interpretation received chromatograpm.

4. CONCLUSIONS

Based on the study, the following conclusions can be drawn:

- High values of COD and TOC confirmed, that coke wastewater was highly loaded with organic compounds.
- The combined concentration of 8 PAHs in wastewater coke was 23 µg/dm^3, with carcinogenic compounds accounted for 61% (14 µg/dm^3).
- The percentage of the compounds in the mixture, did not go under significant changes during the testing process.
- The total amount of the eight PAHs removal efficiency was the highest (62%) when hydrogen dioxide was used at dose of 50 mgH_2O_2/dm^3
- The effectiveness of removal PAHs from wastewater after the 50 mg/dm^3 dihydrogen dioxide was: naphthalene - 57%, anthracene - 67%, fluoranthene - 68%, benzo(a)pyrene - 61%, benzo(b)fluoranthene - 64%; benzo(k)fluoranthene - 59%, indeno(1,2,3,c,d)pyrene - 58%, benzo(g,h,i)perylene - 55%.

The research was funded by the project No. BS/MN-402-303/12, BS/PB-402-301/11

REFERENCE

1. Bartkiewicz B.: *Treatment of industrial wastewater*, Warsaw, PWN 2006.
2. Bartulewicz E., Bartulewicz J., Gawłowski J.: *Determination of PAHs in water and wastewater; Materials Conference Problems of analytical determination of carcinogenic substances in the waters*, Warsaw, PZH 1997, 95-109.

3. Brown G.S., Barton L.L., Thomson B.M.:*Permanganate oxidation of sorbed polycyclic aromatic hydrocarbons*, Waste Management, **23** (2003) 737-740.
4. Directive of the European Parliament and of the Council 2008/105/EC.
5. Grzechulska-Damszel J., Orecki A., Mozik S., Tomaszewska M., Morawski A.W.: *Opportunities and prospects for water and wastewater treatment in the system photocatalysis/membrane processes,* Chemical Industry, **85** (2006) 1011-1014.
6. Jamróz T., Ledakowicz S., Miller J., Sencio B.:*Toxicity of polycyclic aromatic hydrocarbons and their decomposition products,* Engineering and Chemical Apparatus, **3** (2002) 45-46.
7. OJ No. 257, pos. 1545, 2011, Minister of Environment on the classification of surface waters and environmental quality standards for priority substances.
8. Kupryszewski G.:*Introduction to Organic Chemistry*, Warsaw, PWN 1997.
9. Mielczarek K., Bohdziewicz J., Kwarciak-Kozłowska A.:*Comparison of the effectiveness of water treatment processes using coke coagulation and advanced oxidation*, Environmental Engineering, **4** (2011) 184-194.
10. Mielczarek K., Bohdziewicz J., Kwarciak-Kozłowska A.: *Treatment of coke wastewater in the system combines integrated process of coagulation of the pressure membrane techniques,* Annual Set The Environment Protection, **13** (2011) 1965-1984.
11. Smol M., Włodarczyk-Makuła M.:*The initial removal of PAH from coke plants,* LAB Research Laboratory Apparatus, **17**, 1 (2012) 28-31.
12. Turek A., Włodarczyk-Makuła M.: *Oxidation of low molecular weight PAHs in industrial wastewater*, LAB Research Laboratory Apparatus, **17**, 3 (2012) 14-17.
13. Turek A., Włodarczyk-Makuła M.: *Removal of PAHs (C13-C16) from the coke wastewater using dihydrogen dioxide*, in: Scientific Papers, series of Environmental Engineering, Uniwersity of Zielona Góra, **25** (2012) 56-64.
14. Wąsowski J., Piotrowska A.:*The distribution of organic pollutants in water depth of oxidation processes*, Environmental Protection, **2**, 85 (2002) 27-32.
15. Włodarczyk-Makuła M.: *Quantitative changes of PAHs in treated sewage during oxidation,* Annual Set The Environment Protection, **13**, 2 (2011) 1093-1104.
16. Zhao X., Wang Y., Ye Z., Borthwick A.G.L., NI J.: *Oil field wastewater treatment in Biological Aerated Filter by immobilized microorganisms,* Process Biochemistry, **41** (2006) 1475-1483.

USUWANIE PRIORYTETOWYCH WWA ZE ŚCIEKÓW KOKSOWNICZYCH

S t r e s z c z e n i e

Celem badań opisanych w pracy było określenie skuteczności usuwania ze ścieków koksowniczych ośmiu węglowodorów aromatycznych z listy związków priorytetowych. Badania technologiczne polegały na wprowadzeniu do pobranych próbek ścieków przyjętych ilości 30% roztworu ditlenku wodoru (50 mg/dm^3, 100 mg/dm^3, 300 mg/dm^3, 600 mg/dm^3, 900 mg/dm^3, 1000 mg/dm^3, 2000 mg/dm^3). Analiza WWA obejmowała przygotowanie próbek oraz ilościowe i jakościowe oznaczenie chromatograficzne, które prowadzono z wykorzystaniem chromatografu gazowego sprzężonego ze spektrometrem masowym. Sumaryczne stężenie ośmiu WWA w ściekach koksowniczych przed procesem utleniania wynosiło 23 µg/dm^3. Największy ubytek badanych węglowodorów, sięgający 62%, odnotowano przy dawce utleniacza wynoszącej 50 mg/dm^3.

CONTENTS